Establishing the role of Cholesteryl Ester Transfer Protein (CETP) in Breast Cancer

by

Liang Gu

(683077)

Thesis

Submitted in fulfilment of Research by Thesis for the requirements for the degree

Philosophiae Doctor

in

Molecular and Cell Biology

in the Faculty of Science, University of the Witwatersrand, Johannesburg, South Africa

Supervisor: Prof. Mandeep Kaur

May 2022

Declaration

I, Liang Gu (683077), am a student registered for the degree of Doctor of Philosophy in Science (Molecular and Cell Biology) the academic year 2018.

I hereby declare the following:

- I am aware that plagiarism (the use of someone else's work without their permission and/or without acknowledging the original source) is wrong.
- I confirm that the research proposal submitted for assessment for the above degree is my own unaided work except where explicitly indicated otherwise and acknowledged.
- I have followed the required conventions in referencing the thoughts and ideas of others.
- I understand that the University of the Witwatersrand may take disciplinary action against me if there is a belief that this is not my own unaided work or that I have failed to acknowledge the source of the ideas or words in my writing.

NRF Declaration

The financial assistance of the National Research Foundation (NRF) towards this research is hereby acknowledged.

Opinions expressed and conclusions arrived at, are those of the author and are not necessarily to be contributed to the NRF.

signature____  _ 13th May 2022

1. Abstract

Hormone responsive breast cancer (BC) is the most common sub-type of BC and relies on steroid hormones for cell proliferation and survival, therefore endocrine therapy, Tamoxifen (TAM), serves as the main therapeutic strategy in treating and preventing the recurrences of hormone receptor positive BC. Despite the use of TAM for over four decades, overcoming drug resistance remains challenging. In our previous research, we investigated the effect of reducing intracellular cholesterol as a possible alternative method to induce cell death in BC cells, due to the fact that steroid hormones are derived from cholesterol and evidently, an increased level of cholesterol is associated with cancer progression. An important protein involved in cholesterol homeostasis is the Cholesteryl Ester Transfer Protein (CETP). CETP maintains cholesterol homeostasis by storing cholesteryl esters (CEs) in lipid droplets. The intracellular accumulation of CEs leads to aggressive cancer development and drug resistance. Therefore, we aimed to investigate whether *CETP* can possibly be used as a drug-resistance marker in BC. The preliminary results showed that knocking-down *CETP* resulted in increased apoptosis in MCF-7 cells when treated with TAM (by 10-40%) and various other drugs. Furthermore, *CETP* knock-down with the addition of a cholesterol-depleting agent increased apoptosis by 10-fold when compared to the non-transfected MCF-7 cells, possibly due to a decrease in CEs content. Similar results were observed in MDA-MB 231 cells. Therefore, it was concluded that *CETP* could thus serve as a potential drug-resistance marker in cancer cells, more specifically BC. However, the molecular mechanisms of CETP in the involvement of this resistance have not yet been explored. Therefore, we further looked at several genes that were affected from knocking down *CETP* in both cell lines using the RT² Profiler™ PCR arrays (Qiagen, Germany; Whitehead Scientific, SA), where each array identifies the expression of 84 genes involved in the human lipoprotein signalling and cholesterol metabolism pathway and 84 genes involved in the human cancer resistance pathway. From the arrays it was found that *CETP* knock-down, in MCF-7 cells, lowered the expression profiles of genes involved in the cholesterol synthesis and cholesterol uptake pathways, thereby lowering internal cholesterol levels. In addition, there was a shift of gene expression from high levels to low levels in hormone receptors and drug efflux pumps, thus reducing resistance. While in MDA-MB 231 cells, *CETP* knock-down increased the expression of genes involved in cholesterol efflux and interestingly, there was an increase in estrogen receptor genes, which possibly sensitized these triple negative BC (TNBC) cells to TAM. In addition to the *in vitro* study, we performed a mice xenograft study, and it was found that the mice injected with *CETP* knocked down cells had an 86.45% decrease in tumour growth compared to the mice injected with non-transfected cells. Therefore, *CETP* is a promising drug resistance marker in predicting the effectiveness of cancer treatments and possibly a good target in reducing drug resistance through a decrease in excess cholesterol.

2. Acknowledgements

I wish to thank my supervisor, Prof. Kaur, for all the help, advice and insight into the project as well as all the encouraging words, motivation and (not to forget) all the coffee meetings and our amazing end of year event throughout the years. 😊 I joined prof. Kaur's lab in 2016 for my Master's degree and I have enjoyed working in the lab ever since. I have learnt a lot from her and appreciate all that have been taught to me so that I can become a better researcher.

I would also like to thank all my colleagues in GH527 for all their help and company throughout the years. Every person that has come and left or still here working hard, trying to finish their degrees have really made the atmosphere in the lab a great environment to work in and I thoroughly enjoyed all the chats, lunch breaks and quizzes we've done together! You guys have been awesome!

A special thanks to the Department of Chemistry at the University of Witwatersrand for synthesizing Amplex red and Acetyl plumbagin for us.

I would like to give a special thanks to my mom and brother who have been very supportive of my studies. It hasn't been the easiest of journeys, but it was a rewarding one.

A special thanks to Tyrone Otgaar who has been very helpful throughout my studies. All the knowledge and suggestions have been of great help and I truly appreciate that. I have probably not been the greatest person to deal with at times, especially during stressful times during COVID-19 pandemic so I am grateful for your patience and support!

I'd also like to thank the University of Witwatersrand postgraduate merit award (PMA; 2016-2020) and the National Research Foundation (NRF; 2016-2020) for all the financial support during my study period. This has been a great relieve from tuition fees and without the funding I could have not furthered my studies.

A very big thank you to all the staff members at Wits Animal Research facility (WRAF) with all the help with the mice study during the pandemic. It was not easy and therefore all the help was appreciated to make this project a success.

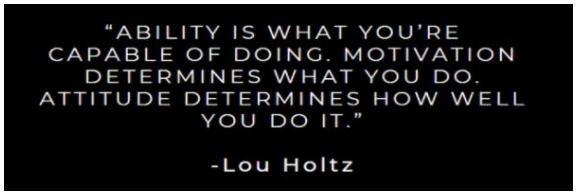

3. Table of Contents

4. List of Figures

5. List of Tables

6. List of Equations

7. List of Symbols

®	Registered trademark
µ	Micro
℃	Degree Celsius
nM	Nanomolar
™	Trademark
α	Alpha
β	Beta
Δ	Delta
κ	Kappa

8. List of abbreviations

5-FU	5-Fluorouracil
ABC	ATP-binding cassette
ABCB1	ABC subfamily B member 1
ABCC1	ABC subfamily C member 1
ABCC5	ABC subfamily C member 5
ABCG2	ABC subfamily G member 2
Abl	Abelson
ACAT	Acyl-CoA: cholesterol acyltransferase
AMPK	Adenosine monophosphate-activated protein kinase
AP	Acetyl plumbagin
AP-1	activator protein 1
Apaf-1	Apoptotic protease activating factor 1
APO%	APOPercentage
ApoA-1	Apolipoprotein A-1
APS	Ammonium persulphate
ATCC	American Type Culture Collection

BAK	BCl2 antagonist/killer-1
BAX	BCl-2-associated X protein
BC	Breast cancer
BCA	Bicinchoninic acid
BCl-2	B-cell lymphoma 2
BCR	Break point cluster gene
BCRP	Breast cancer resistance protein
BODIPY	Boron-dipyrromethene
BRCA1/2	Breast cancer type 1/2 susceptibility gene
BSA	Bovine serum albumin
Caspases	Cysteine-aspartic proteases
CD95	Cluster of differentiation 95/ Fas receptor
CE	Cholesteryl ester
CETP	Cholesteryl ester transfer protein
CO_2	Carbon dioxide
Ct	Cycle threshold
CT-B	Cholera toxin subunit B
Cu^{2+}	Copper sulphate
CYP	Cytochrome P450
DDR	DNA damage response
dH_2O	Distilled water
DME	Drug metabolising enzymes
DMEM	Dulbecco's Modified Eagle's Medium
DNA	Deoxyribonucleic acid
ECACC	The European Collection of Authenticated Cell Cultures
ECL	Enhanced Chemiluminescence

ECM	Extracellular matrix
EDTA	Ethylenediaminetetraacetic acid
EGF	Epidermal growth factor
EGFR/HER2	Human epidermal growth factor receptor
ER-	Estrogen receptor negative
ER+	Estrogen receptor positive
ERBB	Receptor tyrosine-protein kinase erbB
ERK1/2	Extracellular signal-related kinases 1/2
ESR1	ER gene
FADD	Fas-associated death domain
FBS	Foetal bovine serum
FGFR	Fibroblast growth factor receptor
GEPIA	Gene expression profiling interactive analysis
GM1	Glucosphingolipid ganglioside
GSH	Glutathione
GST	Glutathione S-transferase
GTEx	Genotype-Tissue Expression
GTPases	Guanosine triphosphate enzyme
H_2O_2	Hydrogen peroxide
HCl	Hydrochloric acid
HDL	High-density lipoprotein
HIF1α	Hypoxia-inducible factor 1-alpha
HMG-CoA	3-Hydroxy-3-methylglutaryl coenzyme-A
HMGCR	HMG-CoA reductase
HPCD	2-Hydroxypropyl-β-cyclodextrin
HR	Hazard ratio

HRP	Horseradish peroxidase
hr/s	hour/s
IAP	Inhibitors of apoptotic proteins
IGF1R	Insulin-like growth factor 1 receptor
INSIG	Insulin induced gene 1
IκBα	Inhibitory subunit of NF-κB
JC-1	5,5′,6,6′-Tetrachloro-1,1′,3,3′-tetraethylbenzimi-dazolylcarbocyanine iodide
JNK1	c-Jun N-terminal kinase 1
kDa	Kilodaltons
KPO_4	Potassium phosphate buffer
LCAT	Lecithin: cholesterol acyltransferase
LDL	Low-density lipoprotein
LDLRs	Low-density lipoprotein receptor
LXR	Liver X receptor
MCF-7	Michigan Cancer Foundation-7
MDA-MB 231	M.D. Anderson metastatic breast 231
MDM2	E3 ubiquitin-protein ligase
MDR	Multidrug resistance
min	Minutes
MOMP	Mitochondrial outer membrane permeabilization
MRP1	MDR-associated protein 1
mTOR	Mammalian target of rapamycin
MTT	3-(4,5-Dimethylthiazol- 2-yl)-2,5-diphenyl tetrazolium bromide
MVD	Mevalonate pyrophosphate decarboxylase
MVK	Mevalonate kinase
MβCD	Methyl-β-cyclodextrin

NaCl	Sodium chloride
NCEH	Neutral cholesteryl ester hydrolase
NF-κB	Nuclear factor kappa-light-chain-enhancer of activated B cells
ns	Not significant
OD	Optical density
OHT	4-hydroxytamoxifen
p53	Tumour suppressor protein 53
PBS	Phosphate buffered saline
PCSK9	Proprotein convertase subtilisin-like kexin type 9
PGE_2	Prostaglandin E_2
P-gp	p-glycoprotein
PI3K-AKT	phosphatidylinositol 3-kinase – protein kinase B
PKM2	pyruvate kinase M2
PL	Plumbagin
PR+	Progesterone receptor positive
PRKAA2	Protein Kinase AMP-Activated Catalytic Subunit Alpha 2
PS	Penicillin Streptomycin
PVDF	Polyvinylidene difluoride
RCT	Reverse cholesterol transport
RISC	RNA-inducing silencing complex
RNA	Ribonucleic acid
RNAi	RNA interference
ROS	Reactive oxygen species
RT-qPCR	Reverse transcription - quantitative polymerase chain reaction
s	second/s
SCAP	SREBP cleavage-activating protein

SDS	Sodium dodecyl sulphate
SDS-PAGE	SDS-polyacrylamide gel electrophoresis
SERM	Selective estrogen receptor modulator
siRNA	Small interfering RNA
smac	Second mitochondria-derived activator of caspase
SR-B1	Scavenger receptor class B type 1
SREBF	SREBP gene
SREBP	Sterol regulatory element-binding proteins
TAM	Tamoxifen
TCGA	The Cancer Genome Atlas
TEMED	Tetramethylethylenediamine
TNBC	Triple negative breast cancer
TNFR	Tumour necrosis factor receptor
TP53	Tumour suppressor protein 53 gene
TRAILR	TNF-related apoptosis-inducing ligand receptor

9. Introduction

9.1 Prevalence of cancer and BC

Cancer is the second leading cause of death globally with an estimated 19.3 million new cases reported, of which, 2.3 million cases were attributed to BC making it the most prevalent or commonly diagnosed cancer since 2020 (Sung et al., 2021). Shockingly, nearly 70% of BC cases and BC-related deaths occur in developing countries (WHO, 2018). According to the most recent statistics by GLOBOCAN 2020, BC is the most commonly diagnosed cancer in South African females (27.1% of all cancer types) and it is the leading cause of cancer deaths in women (CANSA, 2014). These statistics are expected to increase by 47% by the year 2040 and therefore highlights the importance of improving the current therapeutic strategies to treat cancer.

9.2 Cancer hallmarks

Cancer is a highly complex group of transformed cells that proliferate in an uncontrolled manner that forms benign or malignant neoplasms (Hanahan, 2014). Cancer is characterized by various hallmarks: over-proliferation, metastasis or invasion, and apoptosis (Hanahan and Weinberg, 2011). BC is a malignant tumour developed in or around the various tissues in the breast (American Cancer Society, 2016). One key hallmark of BC is the increase in apoptotic resistance. Apoptosis is the process of programmed cell death, which involves several physiological and morphological changes to the cells (Hanahan and Weinberg, 2011). There are two pathways to the activation of apoptosis namely, the extrinsic and intrinsic pathway. Both pathways initiate apoptosis through the activation of different cysteine-aspartic proteases (caspases). The extrinsic pathway or otherwise known as the death receptor pathway, is activated via the interaction of Fas receptor (cluster of differentiation 95 (CD95)), tumour necrosis factor receptor (TNFR) and TNF-related apoptosis-inducing ligand receptor (TRAILR) to its respective ligands or drugs (Fig 9.1) (Fulda and Debatin, 2006). Consequently, Fas-associated death domain (FADD) and caspase-8 are recruited and further promotes the activation of downstream caspase (caspase-3) to initiate cell death (Fulda and Debatin, 2006). On the contrary, the intrinsic pathway is activated through mitochondrial outer membrane permeabilization (MOMP). This occurs when cell stress signals activates B-cell lymphoma 2 (BCl-2), situated on the mitochondrial membrane, and stimulates the activation of the BCl-2-associated X protein (BAX) or BCl-2 antagonist/killer-1 (BAK) proteins (Brunelle and Letai,

2009; Suhaili et al., 2017). This results in MOMP and thus the release of pro-apoptotic molecules, such as second mitochondria-derived activator of caspase (smac), and blocks inhibitors of apoptotic proteins (IAP) leading to the activation of caspase-3 for cell death through DNA fragmentation (Fig 9.1) (Brunelle and Letai, 2009; Fulda and Debatin, 2006; Suhaili et al., 2017). Additionally, cytochrome *c* is also released from the mitochondria during permeabilization and interacts with apoptotic protease activating factor 1 (Apaf-1) inducing caspase-3 cleavage through caspase-9 causing apoptosis (Fig 9.1) (Brunelle and Letai, 2009; Fulda and Debatin, 2006; Suhaili et al., 2017). These pathways are often suppressed in cancer cells thus leading to uncontrolled cell proliferation.

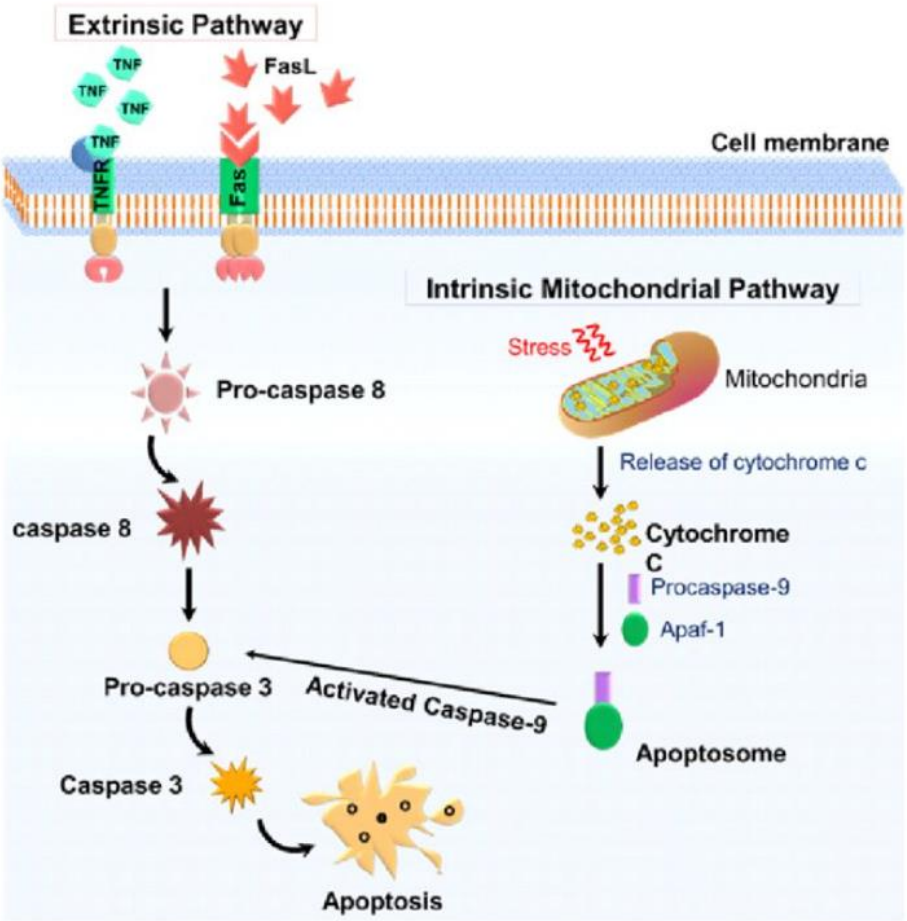

Figure 9.1: Intrinsic and extrinsic apoptotic pathways

[Adopted from:(Bhosale et al., 2020)]

Apoptosis occurs through two pathways namely: the extrinsic and intrinsic apoptotic pathways. Extrinsic pathway involves the binding of proapoptotic proteins or targeting drugs to TNFR and TRAILR and causes downstream activation of caspase-3 leading to cell death. Intrinsic

pathway involves MOMP activation through cell stress signals or damage and results in the release of proapoptotic molecules such as Smac and cytochrome c to induce the cleavage or activation of caspase-3.

Another key hallmark of cancer is the self-sustained proliferative signals as well as the ability to adapt and function in hypoxic conditions referred to as the Warburg effect (Bubici and Papa, 2019; Hanahan and Weinberg, 2011). In normal cells, the oxygen supply is adequate for normal metabolic needs for proliferation. However, in cancer cells the oxygen requirement far exceeds the supply rate due to rapid proliferation (Ward et al., 2013). As the tumours enlarge, the core of the tumours receives limited levels of oxygen, thereby causing necrosis from lactate accumulation (Ward et al., 2013). Therefore, it is critical for these cancer cells to adapt to this change in the tumour microenvironment. The Warburg effect explains the mechanism in which cancer cells acclimatise to this change in conditions by utilising the glycolytic pathway for energy production, independent of oxygen levels, and thus proliferation is sustained in both aerobic and anaerobic conditions (Bubici and Papa, 2019; Vaupel et al., 2019). This shift in energy metabolism from oxidative phosphorylation to anaerobic glycolysis for hypoxic adaptation is mediated by the transcription factor; hypoxia-inducible factor 1-alpha (HIF1α) (Galbraith et al., 2013). HIF1α induces the glycolytic energy production through the activation of genes involved in glucose import and enzymes that uses or breaks down the glucose for energy (Denko, 2008). Although HIF1α is activated in hypoxic conditions, it can also be activated independently through pyruvate kinase M2 (PKM2; involved in the control of energy production and therefore proliferation), insulin-like or epidermal growth factors, activation of certain pathways such as Ras-MAPK and PI3K/mTOR pathways, thereby increasing HIF1α expression, which further results in angiogenesis, metastasis, resistance and proliferation (Fig 9.2) (Ward et al., 2013).

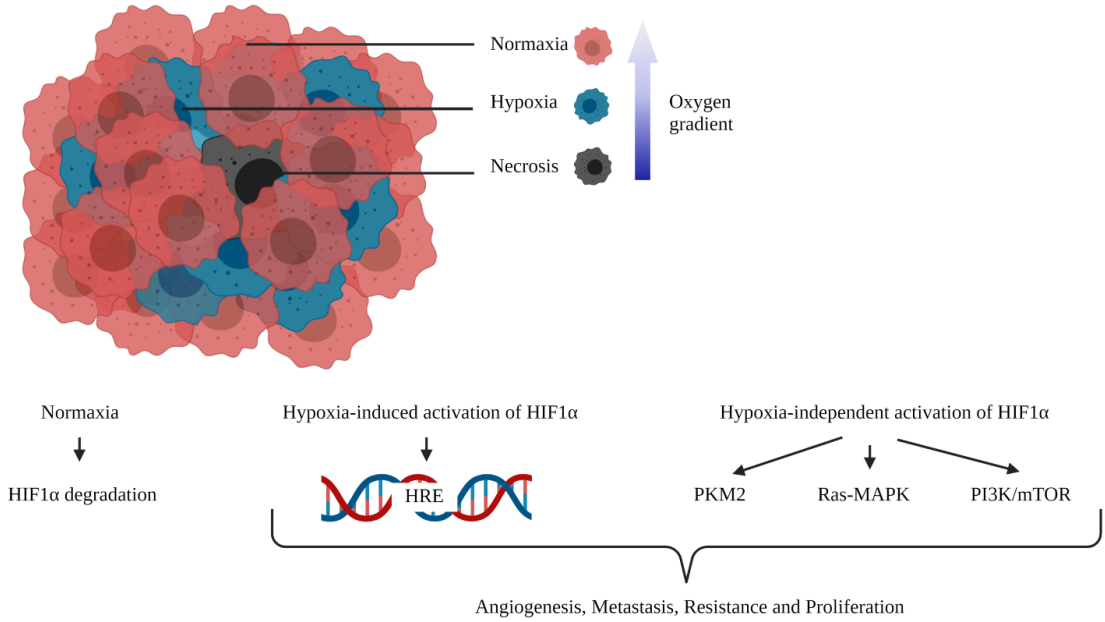

Figure 9.2: Hypoxia adaptation of cancer cells

The figure above represents the different pathways (including HRE (hypoxia-induced element, PKM2, Ras-MAPK and PI3K/mTOR pathways, which will be discussed further in the study) cancer cells overcome hypoxia/ adapt to the hypoxic conditions for metastasis, resistance and continuous proliferation in the absence of oxygen. [Image created with BioRender.com]

9.3 Hormone Induced BC

BC, being the most prevalent cancer as well as being the leading cause of cancer deaths in women currently, therefore warrants further improvements in understanding and the treatment of the disease. Endogenous steroid hormones, such as estrogen and progesterone, are the cause of majority of BC incidences. BC cells are categorized according to the presence or absence of surface receptors (Breastcancer.org, 2017a). Therefore, BC can be either estrogen receptor positive (ER+) or estrogen receptor negative (ER-), progesterone receptor positive (PR+) and triple negative cancerous cells (Fig 9.3) (Breastcancer.org, 2017a). Hormone positive BC cells have surface receptors that bind to their respective steroid hormones to promote cell proliferation (Breastcancer.org, 2017a). ER- and PR- BC cells do not have these surface receptors and thus are dependent on epidermal growth factor receptors (EGFR) or HER2 for cell growth. Triple negative BC (TNBC) cells lack the expression of the hormone receptors as well as HER2 and it is a highly aggressive form of BC (Cleator et al., 2007; Yu et al., 2017).

Due to the absence of these receptors, TNBC has poor prognosis and makes targeted therapies for TNBC ineffective (Cleator et al., 2007; Yu et al., 2017). Estrogen and progesterone hormones play important roles in vital processes such as the menstrual cycle, sexual development, pregnancy and childbirth (Breastcancer.org, 2017a). Since estrogen is involved in cell division of breast cells, an increase in expression of estrogen results in a higher risk of BC development (Clemons and Goss, 2001). Furthermore, research showed that risk for BC development can also be associated with obesity, age of first menstruation and the use of hormone regulating pills (contraceptives) (Althuis et al., 2004; Hankinson et al., 1998; Potischman et al., 1996). Approximately 80% of all BC are ER+ (NIH, 2017). ERs are part of the nuclear receptor superfamily of ligand-activated transcription factors that regulate gene transcription (Frasor et al., 2003). In cancer, estrogen promotes proliferative effects through both direct and indirect tumour initiation (Clemons and Goss, 2001). Direct tumour initiation involves the activation of oncogenes and several proteins that aid in nucleic acid synthesis. Whereas, in indirect tumour initiation, estrogen stimulates the secretion of prolactin and a number of transcription factors (Clemons and Goss, 2001). The ER- BC growth is independent of estrogen and it accounts for 25% of all BC cases (Breastcancer.org, 2017b). It has been found that epidermal growth factors (EGFs) are overproduced in ER- BC cells and EGF-induced mitogen signals activate several downstream proteins involved in the cell cycle resulting in enhanced proliferation of ER- BC cells (Biswas et al., 2000). In contrast, EGF levels are reasonably low in ER+ BC cells.

9.4 BC Treatments

Treatment varies depending on the type of BC cells (Fig 9.3), however benign BC tumours can often be surgically removed before it turns metastatic. Chemotherapy is recommended to patients who have early and late-stage invasive BC to reduce size and to insure the complete removal of the BC cells that could have metastasized before and after surgery (Breastcancer.org, 2017a). As mentioned previously, most BC cases are hormone induced. Therefore, hormone therapy or endocrine therapy has been successful, and involves the use of selective ER modulators (SERMs), such as TAM, which is the first-line treatment to hormone induced BC (Maughan et al., 2010). TAM has been used for over forty years to treat hormone-responsive BC, as it has anti-estrogen properties, playing an antagonistic role to hormone estrogen (Hodges et al., 2003; Mourits et al., 2001). The National Surgical Adjuvant Breast and Bowel Project proposed that using TAM reduces or slows down ER+ BC recurrences by

45% (Mourits et al., 2001). The molecular action of TAM involves the active metabolites, 4-hydroxytamoxifen (OHT) and endoxifen, formed by a family of cytochrome P450 enzymes (Cronin-Fenton et al., 2014; Lu et al., 2012). These metabolites directly compete for the estrogen-binding site on the ERs of ER+ BC cells and are then internalised. The metabolites initiate the recruitment of corepressors and consequently prevents the activity of various transcription factors involved in cell proliferation and thus halts cell growth (Hodges et al., 2003). Interestingly, TAM has also been found to have agonist properties, in which it promotes transcription by initiating the activator protein 1 (AP-1) pathway in uterine endometrium, bone and cardiovascular system (Hodges et al., 2003; Webb et al., 1995). However, following long term therapy of TAM has been found to cause adverse side effects such as: early onset of menopausal symptoms, blood clots, endometrial cancer (Acconcia et al., 2006) and relapses (Breastcancer.org, 2017a; Mourits et al., 2001). Moreover, naturally, BC cells may build-up resistance against TAM and as a result TAM becomes ineffective in treating BC (Ring and Dowsett, 2004). It was found that at least 40% of patients eventually relapse after TAM use despite its therapeutic activities (Ring and Dowsett, 2004). Therefore, further research is warranted to reduce the toxicity and resistance to TAM. One other drug type often used to treat ER+ BC patients involves the aromatase inhibitors, which blocks the function of aromatase enzymes that regulates the production of hormone estrogen (Fig 9.3) and thereby reducing the proliferation of ER+ cells (Breastcancer.org, 2017a). Other chemotherapeutic drugs include: 5-Fluorouracil (5-FU) and Paclitaxel. However, despite the use of these drugs, drug resistance remains a significant problem in the clinical field. Therefore, further research is needed to improve the response to currently available therapeutic strategies.

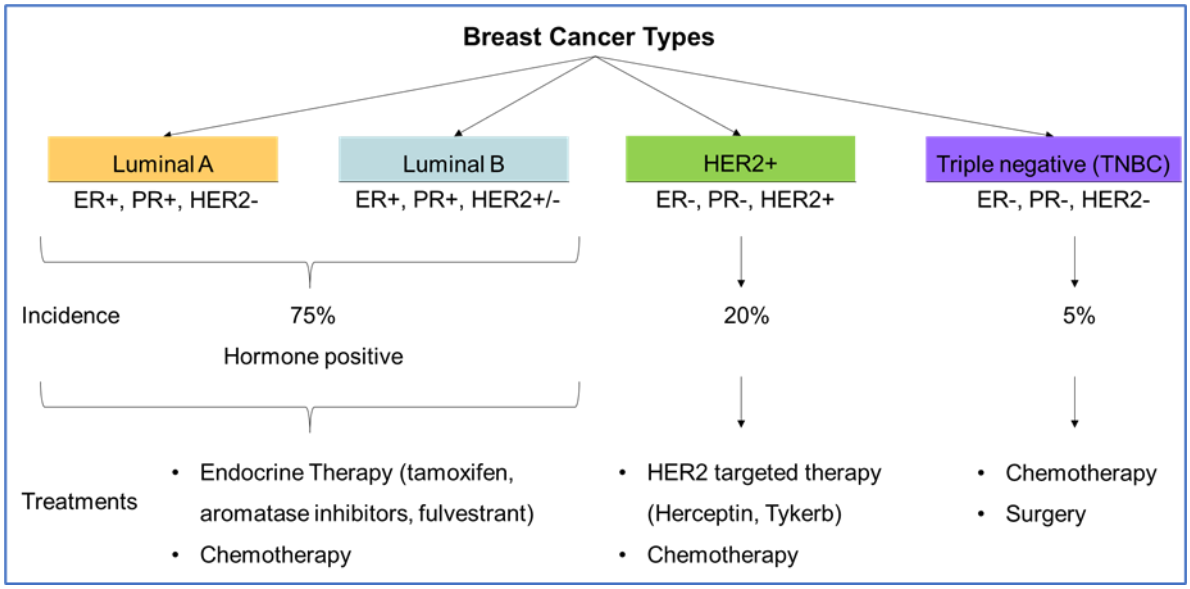

Figure 9.3: Hormone induced BC cell types and current treatment options

The above summarises the various treatments available for type-dependent BC. [Adapted from (Sharp and Harper-Wynne, 2014)].

9.5 Cancer Drug Resistance

Drug resistance is one of the main reasons for failures in the treatment of cancer. Multidrug resistance (MDR) can be categorised into two main groups; *de novo* and acquired drug resistance. *De novo* drug resistance is referred to as the pre-existing resistance of certain cancer cells towards certain drugs/ anticancer treatments (Holohan et al., 2013). The tumour microenvironment has been identified as one of the key mechanisms of *de novo* cancer drug resistance (Hazlehurst and Dalton, 2006; Nefedova et al., 2003). This includes cytokines, hormones, growth factors, cell to cell interactions and cell to extracellular matrix (ECM) interactions (Nefedova et al., 2003; Shain et al., 2000). In contrast, acquired drug resistance is the resistance that is developed over time post drug treatments (Holohan et al., 2013). This may include alterations in genes involved in various pathways, epigenetics, epithelial-mesenchymal transition, as well as drug metabolism (Housman et al., 2014). It has also been suggested that the tumour microenvironments may also trigger cancer cells to develop acquired resistance after the initial treatment and therefore the understanding of these two resistance types may also assist in the prevention or to subside the development of acquired resistance. As mentioned previously that despite the success of treating BC with TAM since the 1970s, at least 40% of patients show *de novo* TAM resistance or acquired resistance (a few years post TAM treatment) (Ali et al., 2016; Ring and Dowsett, 2004). The heterogeneity of tumours greatly contributes

to drug resistance, where a sub-population of the tumour may be non-responsive to various drug treatments. This heterogeneity is caused from various genomic, transcriptomic and proteomic alterations at a cellular level and thus certain drugs may be ineffective to a particular population or types of cells (Mansoori et al., 2017). These alterations or mutations often increase molecular mechanisms involved in drug efflux, drug inactivation, drug target changes, DNA damage repair, survival and proliferative pathways such as the phosphatidylinositol 3-kinase – protein kinase B (PI3K-AKT) and mitogen-activated protein kinase (MAPK) signalling pathways (Holohan et al., 2013). In addition, the highly adaptive nature of cancer cells often inactivate death signalling pathways (Ali et al., 2016; Holohan et al., 2013; Ring and Dowsett, 2004).

9.5.1 DNA damage repair

Mammalian cells are highly susceptible to DNA damage from various genotoxic agents. This damage could lead to numerous mutations promoting cancer development (Kastan and Bartek, 2004) and therefore, cells have developed various DNA damage response (DDR) factors to initiate DNA repair (Bouwman and Jonkers, 2012). DDR mechanisms can lead to different outcomes, depending on the severity of the damage ie. mild DNA damage can be restored, and cells continue in the cell cycle, arrest of cell cycle checkpoint progression to prevent further mutations and lastly, if DNA damage is irreparable apoptosis prevents the proliferation of these damaged cells (Sancar et al., 2004). An important transcription factor that regulates this response to damage is the tumour suppressor protein; p53 (Fig 9.4). The activity of p53 is tightly regulated by the E3 ubiquitin-protein ligase (MDM2), in which the interaction between MDM2 and p300 (transcriptional coactivator) initiates proteasomal degradation of p53 under normal circumstances (Meek, 2004). In addition, the binding of MDM2 to p53 prevents the interaction of p53 to the transcriptional site. In response to DNA damage, this interaction is interrupted through a series of phosphorylation to activate downstream cell cycle arrest or the mitochondrial apoptotic pathway (BAX and Apaf-1) and death receptor pathways (FADD) (Hientz et al., 2017; Meek, 2004). In cancer cells, the tumour suppressor gene *TP53* is often mutated, causing a loss of function in the p53 protein, and thereby causes it to lose its tumour suppressing ability (Hientz et al., 2017). These mutations usually occur in the DNA binding sites and thereby prevent the initiation of cell cycle arrest or apoptosis upon exposure to chemotherapeutic agents, thus contributing to drug resistance (Cao et al., 2020). Another well-known pair of tumour suppressor genes; involved in BC development and drug resistance are the BC type 1/2 susceptibility protein encoding genes (*BRCA1* and *BRCA2*). The BRCA1/2

proteins are involved in homologous recombinant repair upon double stranded DNA damage caused by chemotherapeutic drugs (Foulkes and Shuen, 2013). However, like p53, it is highly prone to mutations and women with the mutated BRCA1/2 are susceptible to cancer predisposition (Helleday, 2010). Interestingly, it was found that reversion of the BRCA1/2 mutation has been implicated in drug resistance (Fig 9.4) (Helleday, 2010; Schlacher, 2018). In addition, it was found that drug efflux was increased in BRCA-mutated cancer cells thereby conferring to drug resistance (Schlacher, 2018).

9.5.2 Drug Efflux, inactivation and drug target changes

Drug efflux is controlled by a group of transmembrane proteins known as the ATP-binding cassette (ABC) transporters, which prevent the build-up of toxins within healthy cells (Fig 9.4) (Housman et al., 2014). There are three main transporters namely: MDR1 (also known as p-glycoprotein (P-gp)), MDR-associated protein 1 (MRP1 or ABCC1) and BC resistant protein (BCRP, ABCG2) (Holohan et al., 2013; Housman et al., 2014). These proteins are highly overexpressed in cancer cells and therefore the drugs are not metabolised by the cells before it is transported out of the cells and excreted by the liver (Housman et al., 2014). In addition to drug efflux, drug inactivation is also implicated in cancer drug resistance. A group of detoxification enzymes, glutathione S-transferases (GST) initiates a direct detoxification through the conjugation between glutathione (GSH) and electrophilic compounds and protects cells from reactive oxygen species (ROS) that causes DNA damage (Longley and Johnston, 2005; Townsend and Tew, 2003). In addition, this prevents the binding of the compound to the respective receptors, thus preventing downstream signalling (Di Pietro et al., 2010). Furthermore, it was found that GSTs inhibit the activities of c-Jun N-terminal kinase 1 (JNK1), which is involved in the MAPK pathway in regulating stress response, apoptosis and cell proliferation (Townsend and Tew, 2003). Therefore, elevated levels of GSTs in cancer cells would greatly impact drug resistance. In contrast, the lack of drug activation could also impact on drug resistance as many drugs have to be converted to its active form before exerting an effect (such as TAM, which is activated through cytochrome P450 as explained previously) (Longley and Johnston, 2005). Lastly, cancer cells are able to overcome drug toxicity through various mutations or modifications of drug target sites. These target sites may include DNA transcriptional enzymes, surface receptors, various kinases such as Ras (which is involved in downstream signalling for cell growth and proliferation) (Housman et al., 2014) and cell cycle checkpoints that monitors DNA damage and repair (Kartal-Yandim et al., 2016). These

mutations would prevent the drugs from binding to its target sites and thereby blocking downstream apoptotic signalling pathways resulting in resistance.

9.5.3 MAPK and PI3K-AKT signalling pathways

As introduced earlier, MAPK signalling pathway is activated through a myriad of receptor tyrosine kinases (some examples include; extracellular signal-related kinases 1/2 (ERK1/2), JNK, p38-MAPK and ERK5) that results in the phosphorylation of various downstream proteins and transcription factors that controls cellular proliferation, cell growth, differentiation and apoptosis (Fig 9.4) (Pritchard and Hayward, 2013; Santarpia et al., 2012). External growth factors activate Ras, which is an important guanosine triphosphate enzyme (GTPases), initiating phosphorylation of numerous downstream cytoplasmic proteins, cytoskeletal proteins and transcription factors for signalling of cell proliferation, differentiation, adhesion, migration and apoptosis (Pritchard and Hayward, 2013; Santarpia et al., 2012). It has been found that Ras and other proteins within the ERK pathway is commonly mutated, with increased activation of Ras leading to resistance (Pritchard and Hayward, 2013; Santarpia et al., 2012). As briefly mentioned, JNK is activated in response to stress for DNA repair. In addition, it has also been found to be activated through Ras (Pritchard and Hayward, 2013). Therefore, deletion or epigenetic gene silencing of JNK or JNK-related proteins have been implicated in drug resistance (Pritchard and Hayward, 2013). Correspondingly, mutations in the p53-MAPK and ERK5 disrupts the proper response to stress and inflammatory cytokines for correct downstream signalling (Pritchard and Hayward, 2013). Similarly, like the MAPK pathway, PI3K-AKT pathway is also a series of cascades that is initiated through growth factors, cytokines and hormones. This, in turn, activates the PI3K-AKT pathway that activates the mammalian target of rapamycin (mTOR; also referred to as the mechanistic target of rapamycin), which is involved in the regulation of cell proliferation, cell cycle and apoptosis (Fig. 9.4) (Rascio et al., 2021). Therefore, the various mutations that occur within the PI3K-AKT pathway, including downstream and upstream targets, play a vital role in cancer resistance (Rascio et al., 2021).

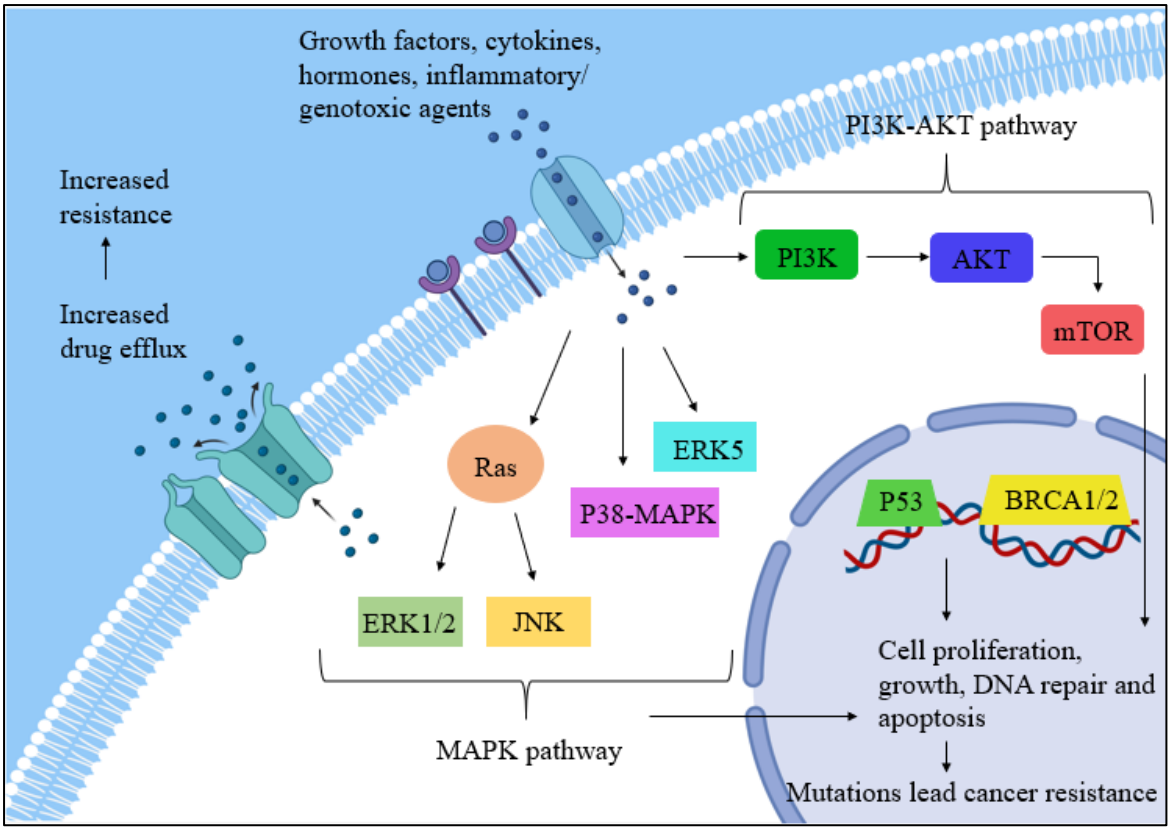

Figure 9.4: Cancer drug resistance through various mechanisms and pathways

The figure above summarizes the various mechanisms or pathways cancer cells adopt for resistance against chemotherapeutic agents. Increased drug efflux by drug efflux pumps greatly increases resistance against chemotherapeutic agents thus becomes ineffective when there is no interaction between the drug and the target. While the activation of the MAPK and PI3K-AKT pathways through growth factors, hormones, cytokines and inflammatory agents promotes proliferation, cell growth and apoptosis under normal circumstances. When it is mutated, it leads to cancer resistance. [Image created with BioRender.com]

Previous studies have identified cholesterol as one of the factors contributing to cancer resistance. Therefore, in this study, we focused on targeting cholesterol, specifically to reduce excess cholesterol to reduce resistance to TAM and possibly other chemotherapeutic drugs or to increase drug efficacy.

9.6 Steroid Hormone Synthesis

Steroid hormones are derivatives of cholesterol and are produced by the endocrine glands. These glands include: the adrenal cortex, testes, ovaries and peripheral tissues, such as the adipose tissues and the brain (Ghayee and Auchus, 2007). Steroid hormone production is a highly complex process that involves several different pathways and enzymes (Fig 9.5). It is known that estrogen and various other hormones such as progesterone, testosterone and cortisol are derivatives of cholesterol (Evans, 1988). Testosterone is further converted to estradiol by aromatase enzymes and interacts with ER on cell surfaces to induce cell proliferation.

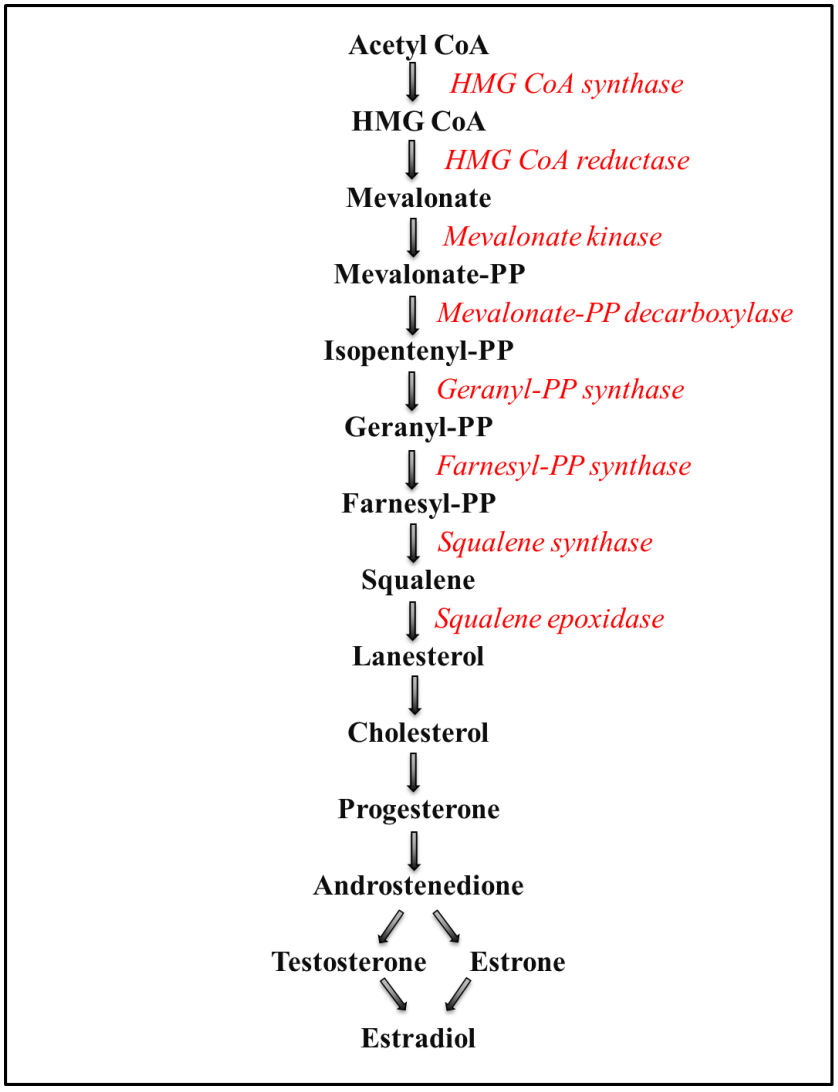

Figure 9.5: The production of steroid hormones from cholesterol

*The above figure illustrates the synthesis of cholesterol from acetyl-CoA through the mevalonate pathway. Acetyl-CoA is synthesized to 3-hydroxy-3-methylglutaryl coenzyme-*A *(HMG-CoA) by HMG-CoA synthase. It is then further converted into mevalonate through the*

HMG-CoA reductase. The mevalonate kinases then initiate the phosphorylation of mevalonate into phosphomevalonate (mevalonate-PP). Thereafter, a series of phosphorylation results in the synthesis of isopentenyl-PP, geranyl-PP, farnesyl-PP, squalene and lanesterol, which is then converted to cholesterol. Cholesterol is then the precursor for downstream synthesis of various hormones such as progesterone, testosterone and estradiol [Adapted from: (Buhaescu and Izzedine, 2007; Gu et al., 2019; Payne and Hales, 2004)].

9.7 Cholesterol and Cancer

It is known that cancer cells are 6 - 8 times higher in cholesterol level as compared to non-cancerous cells (Buchwald, 1992; dos Santos et al., 2014; Li et al., 2006a; Scientific American and Moyo, 2014). Cholesterol is a lipid molecule that is exclusively biosynthesized by all animals, through the mevalonate pathway (Isaacsohn, 1992) and poses three main functions. Firstly, as aforementioned, cholesterol is involved in the synthesis of various steroids, sex hormones (estrogen, progesterone and testosterone), and cortisone-like hormones in response to stress (Isaacsohn, 1992). In addition, it is involved in the production of bile in the liver for the digestion of fats (Isaacsohn, 1992). Most importantly, cholesterol is found in all animal cell membranes and maintains cell stability and shape (Isaacsohn, 1992). Due to these functions, cancer cells require more cholesterol for the rapid proliferation compared to non-cancerous cells. Cancer cells accumulate cholesterol either through biosynthesis or uptake through low-density lipoprotein receptors (LDLRs) (Mayengbam et al., 2021). Cholesterol is an amphipathic molecule meaning that it possesses both a hydrophilic and hydrophobic component (Masterjohn, 2005). Due to this nature, cholesterol is encapsulated in a water-soluble coat, also known as lipoproteins, that aids in the transportation of cholesterol through the circulatory system (Isaacsohn, 1992; Masterjohn, 2005).

9.8 Intracellular and Extracellular Cholesterol Homeostasis

There are two principal lipoproteins that aid in the distribution of cholesterol namely: low-density lipoproteins (LDL) and high-density lipoproteins (HDL) (Isaacsohn, 1992). Cholesterol is delivered to cells via LDLs and binds to the cell surface receptor, LDLRs (Fig 9.5) (Cruz et al., 2013). The LDL/LDLR are then internalised and forms lysosomes that dissociates the interaction between LDL and LDLR (Fig 9.5). The free cholesterol is then incorporated into cell membrane for stability and the LDLRs are recycled back to the surface

(Chang et al., 1997). Conversely, intracellular free cholesterol is converted to cholesteryl esters (CEs) by acyl-CoA: cholesterol acyltransferase (ACAT) (as intracellular free cholesterol is toxic) in the endoplasmic reticulum for storage or regulation of cholesterol synthesis through sterol regulatory element-binding proteins (SREBP) (Fig 9.6) (Chang et al., 1997; Ikonen, 2008; Nelson et al., 2014). In the presence of Proprotein convertase subtilisin-like kexin type 9 (PCSK9) bound to LDLR, it triggers LDLR degradation and thus reduces surface LDLR (Fig 9.6) and could possibly lead to an increased level of cholesterol in the plasma resulting in possible disease progression such as coronary heart disease and hypercholesterolemia (Horton et al., 2007; Wang et al., 2018). In contrast, HDLs are often referred to as the 'good cholesterol'. This is due to the fact that HDLs are involved in the reverse cholesterol transport (RCT), which is the removal process of cholesterol from plasma to the liver to be excreted (Fig 9.6) (Fielding and Fielding, 1995). This is achieved through two pathways; 1) Upon cholesterol efflux (through membrane transporters and proteins) (Fig 9.6) (Chen et al., 2016; Kang et al., 2013; Wu et al., 2014; Yvan-Charvet et al., 2010), free cholesterol is converted to CEs (more hydrophobic form of cholesterol for a more efficient transport (Tosi and Tugnoli, 2005)) by Lecithin: cholesterol acyltransferase (LCAT) that later forms into HDLs (Kuivenhoven et al., 1997). Thereafter, HDLs transport CEs directly to the liver through the scavenger receptor class B type 1 (SR-B1) (Rosenson et al., 2012). 2) CEs are shuttled from HDLs to the LDLs, through CETP, and is delivered to the liver to maintain cholesterol homeostasis (Fig 9.6) (Esau et al., 2016; Tall et al., 2008).

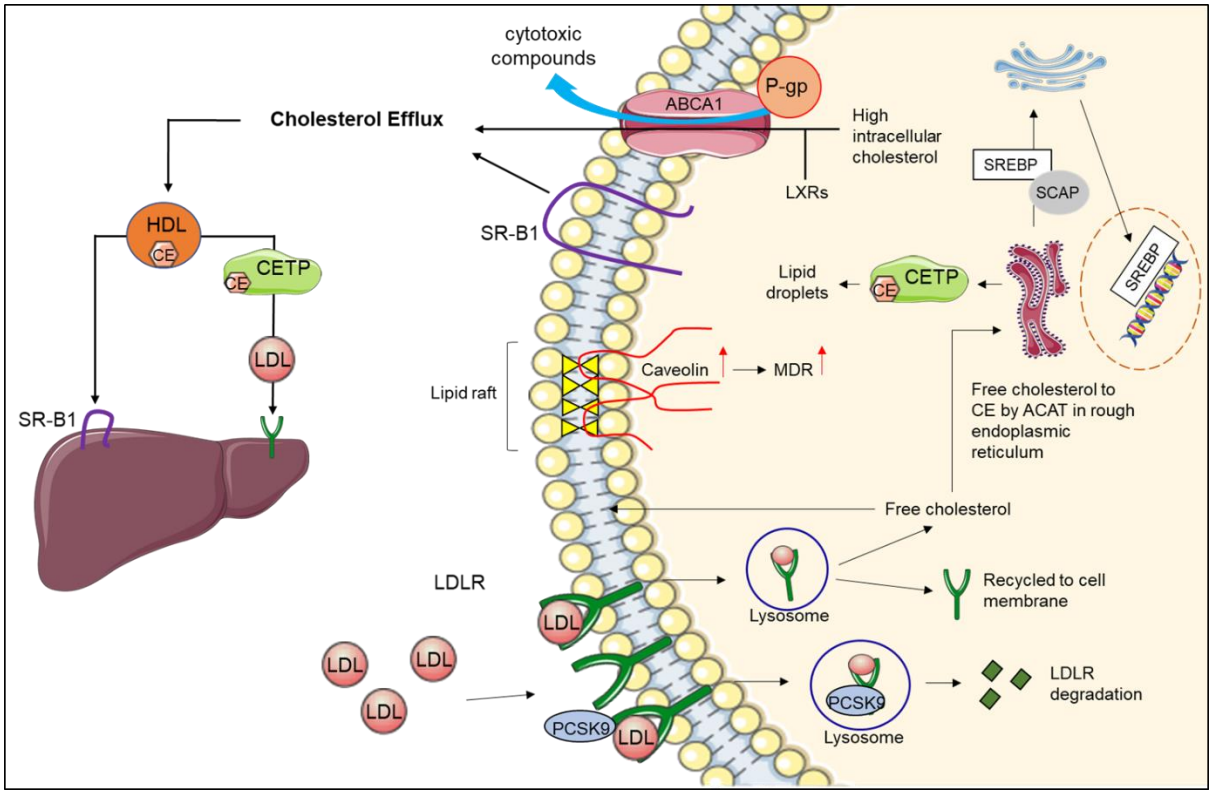

Figure 9.6: Intracellular and extracellular cholesterol homeostasis

[Adopted from Gu et al., 2019]

The above summarises the cholesterol transport system both intracellularly and extracellularly. Cholesterol is transported by LDLs to the cells via LDLR interaction. It is then internalised, and the complex is dissociated in the lysosome into free cholesterol and receptor. In the absence of PCSK9, the LDLRs are recycled to the membrane, however in the presence of PCSK9 it signals LDLR degradation. The free cholesterol is then incorporated into the cell membrane for cell stability and shape, or it is converted to CEs in the rough endoplasmic reticulum by ACAT. CEs are then transported to the storage droplets mediated by CETP. Furthermore, the level of intracellular CEs determines the activity of SREBP. In a low CE environment, SREBP is activated in the golgi body by SREBP cleavage-activating protein (SCAP) and signals cholesterol synthesis. In contrast, SREBP activity is inhibited in a high intracellular CE environment. High intracellular CE environment triggers the activation of membrane cholesterol transporters and proteins ABCA1 and SR-B1 that lead to cholesterol efflux (Gu et al., 2019).

9.9 Cholesterol and Cancer Drug Resistance

As mentioned previously, cholesterol is an important molecule for various purposes and we propose that the increase in cholesterol may be related to drug resistance in cells, especially in cancer cells as these cells are rich in cholesterol. One key protein that maintains intracellular cholesterol level is ABCA1. A high cholesterol content within cells triggers the transport of free cholesterol out of the cells through the interactions with apolipoprotein A-1 (ApoA-1) and liver X receptors (LXRs) (Fig 9.6) (Schroepfer Jr, 2000; Wang et al., 2001; Zhao and Dahlman-Wright, 2010). However, a mutation in these genes result in the accumulation of excess cholesterol within the cell thereby disrupting normal cell immune response (Yvan-Charvet et al., 2010). Similarly, cholesterol and foreign compounds, such as drugs and cytotoxic compounds are transported out of the cell via the P-gp (part of the ATP-binding cassette sub-family B 1 (ABCB1)) resulting in extracellular drug efflux (Fig 9.6) (Mizutani et al., 2008). Consequently, the export of the drugs and cytotoxic compounds reduces intracellular toxicity and as a result cancer cells becomes resistant (Chen et al., 2016; Mizutani et al., 2008; Wu et al., 2014; Yvan-Charvet et al., 2010). Therefore, an elevated expression level of P-gp induces MDR in cancer cells (Chen et al., 2016; Mizutani et al., 2008; Wu et al., 2014; Yvan-Charvet et al., 2010). Cancer drug resistance is also contributed by increased concentration of lipid rafts in cell membranes. Caveolin-1 is a 21-24 kDa integral membrane protein that is involved in the caveolae formation (specialized lipid rafts that are rich in signalling molecules, receptors, effector proteins and transducers) of most mammalian cells (Hoque et al., 2008; Wang et al., 2014). Caveolin-1 has been linked with various membrane transport functions including transcytosis, endocytosis and most importantly cholesterol homeostasis (Frank et al., 2001). Caveolin-1 protein has high-affinity for cholesterol and may transport cholesterol to the plasma membrane through various mechanisms (Fig 9.6) (Arakawa et al., 2000; Frank et al., 2006; Smart et al., 1999). Furthermore, up-regulation of the caveolin-1 protein has also been observed to be involved in the MDR phenomenon (Lavie and Liscovitch, 2000); as increased caveolae would strengthen cell membranes due to an increase in lipid rafts as well as various receptors and signalling molecules for cell proliferation, and cell survival (Hoque et al., 2008). Therefore, targeting cholesterol to reduce drug resistance and increase growth inhibition of cancer cells could possibly be a good anti-cancer therapeutic strategy.

9.10 Targeting Cholesterol for Cancer Treatment

Since cholesterol is found to be abundant in cancer cells, it was predicted that the removal of the excess cholesterol in the plasma membrane, may reduce tumour growth. Therefore, statins (have been the popular choice, readily available on the market (Alla et al., 2013)), a drug in reducing the risk of various cholesterol-related disease development such as cardiovascular diseases, atherosclerosis and Alzheimer's disease (Haag et al., 2009; Rosenson, 2004; Taylor et al., 2011). Moreover, statins have also been found to have anti-cancer properties (Hoque et al., 2008). The mechanism of statins involves the inhibition of HMG-CoA reductase in the mevalonate pathway during the synthesis of cholesterol (Stancu and Sima, 2001). Despite the significant effects of statins a number of side effects (ranging from mild to severe), including impaired cognitive functions and muscle toxicity, have been reported and thus resulted in the controversies surrounding statins (FDA, 2018; Ramsunder, 2015; Sinzinger et al., 2002; Strom et al., 2015).

An alternative strategy that has become increasingly researched, as opposed to blocking the synthesis of cholesterol, is the depletion of excess cholesterol using cholesterol-depleting agents (Esau et al., 2016). Cyclodextrins have been commonly studied as a drug delivery molecule due to their hydrophobic interior that allows the encapsulation of insoluble drugs to increase the solubility in aqueous solutions (Gould and Scott, 2005). The fact that lipids are insoluble in aqueous solutions, allows the cyclodextrins to extract lipid molecules thus enhancing the solubility of lipids to be removed from cells (Zidovetzki and Levitan, 2007). One drug that has been commonly investigated is methyl-β-cyclodextrin (MβCD), however it was found that MβCD is also able to remove cholesterol in the plasma membrane, in non-cancerous cells, involved in cell stability (Mahammad and Parmryd, 2015). Thereby, this non-specific cholesterol depletion ultimately induces cell death to non-cancerous as well as cancerous cells. A closely related cyclodextrin that has been proven to be a better alternative cholesterol depleter than MβCD is the 2-hydroxypropyl-β-cyclodextrin (HPCD). It has been proven to be toxicologically benign up to 10 000 mg/kg in various animal models including; mice, rats, monkeys and dogs (Gould and Scott, 2005). Similarly, in humans, several clinical studies have been performed and patients who have received daily oral doses of up to 16 g of HPCD for two weeks showed no sign of toxicity or side effects (Gould and Scott, 2005). Pharmaceutically, HPCD has been approved to be used to treat Niemann-Pick Type C disease (lysosomal lipid storage disorder) (Yokoo et al., 2015). However, its role in cancer has not yet been well defined. This, therefore, warrants the improvement of currently used drugs or

molecules that will specifically target cells that are high in cholesterol to treat BC. Alternatively, genes involved in cholesterol signalling pathway that can be modified to decrease drug resistance or to increase efficacy of currently available drugs can be targeted. One such gene is the gene that encodes *CETP*.

9.11 CETP

A newly emerged player that could possibly be used as a drug-resistance marker in BC is CETP. The human *CETP* gene, encodes a 74 kDa CETP protein, containing approximately 476 amino acids (Morton and Izem, 2014; Takahashi et al., 1993). *CETP* is found on chromosome 16q13 with a total of 17 exons (NCBI, 2018). As aforementioned, CETP maintains cholesterol homeostasis both intracellularly (transport cholesterol to storage droplets (Fig 9.6) and extracellularly (net transfer of CEs from HDLs to LDLs) (Agerholm-Larsen et al., 2000; Esau et al., 2016; Lagrost, 1994; Tall et al., 2008). Moreover, *CETP*-deficient cells have been found to have lower levels of cholesterol, which could possibly be due to the accumulation of CEs within the endoplasmic reticulum. This accumulation could possibly signal for the down-regulation of proteins involved in cholesterol synthesis and possibly increase or upregulate proteins involved in the cholesterol clearance pathways (Esau et al., 2016; Lagrost, 1994). Additionally, the lack of CETP has shown to increase HDL levels and thus promoting direct removal of plasma cholesterol (Clark et al., 2004; de Grooth et al., 2004; Esau et al., 2016; Lagrost, 1994). This concept of inhibiting *CETP* has been investigated as a possible therapeutic strategy in treating atherosclerosis, cardiovascular disease and possibly Alzheimer's disease (Bisgaier and Newton, 2001; de Grooth et al., 2004; Masson, 2009; Shinkai, 2012). Therefore, the most well-known or studied CETP inhibitor is Torcetrapib. Torcetrapib was initially claimed as a potential drug to treat atherosclerosis and lipid-related diseases by inhibiting CETP and increasing HDL levels (Bots et al., 2007; Clark et al., 2004). Despite the increase in HDL levels, the negative effects of Torcetrapib have been shockingly concerning, these included: increased blood pressure, increased cardiovascular events and no significant decrease in coronary atherosclerosis risks (Barter et al., 2007; Bots et al., 2007; Forrest et al., 2008; Nissen et al., 2007). Due to the toxicity and off-target effects of Torcetrapib and other CETP inhibitors, further research was terminated. This off-target effect of CETP inhibitors could possibly be due to the various, naturally occurring, single nucleotide polymorphisms and alternative splicing that exist in the *CETP* gene (Izem et al., 2020; Suhy et al., 2014). Various CETP variants have also been found to affect the proper functions of CETP thus affecting RCT

process and HDL levels, therefore treatment outcomes may vary between patients (Izem et al., 2020; Suhy et al., 2014). In addition, different CETP variants have been found to be involved in different disease progression, including: age-related macular degeneration, metabolic syndrome and atherogenic dyslipidemia (Lee et al., 2018; Liutkeviciene et al., 2020; Millwood et al., 2018; Prasad et al., 2019). While other polymorphisms (more specifically the rs5882 and rs708272) have been observed to lower the risk of optic neuritis and pituitary adenoma development (Gedvilaite et al., 2019; Sidaraite et al., 2020). Interestingly, it was found that rs5883 highly contributes to the deletion of exon 9 of *CETP* mRNA, creating an exon-9 deleted isoform of CETP (Suhy et al., 2014). This exon-9 deleted isoform of the full length CETP is poorly found in circulation as opposed to the full length CETP isoform (Izem et al., 2020). Furthermore, the exon-9 deleted CETP isoform has been found to reduce the secretion of the full length CETP from the hepatocyte and reduced intracellular levels of the full length CETP isoform (possibly through a decrease in the synthesis of the full length CETP) (Izem et al., 2020). However, this does not affect the storage of triglycerides in maintaining cellular lipid homeostasis. In addition, it was also found the exon-9 deleted isoform can transfer lipids between organelles but not between lipoproteins like the full length CETP (Izem et al., 2020). The effects of the exon-9 deleted CETP isoform on various disease risk and progression has not been well documented, however it has been associated with increased risk of coronary artery disease (Suhy et al., 2014). Therefore, the different genetic variations of CETP could affect individual patient drug treatment and outcome. Thus, it should be considered when developing a CETP inhibitor as a form of treatment for various cholesterol-related diseases.

An important transcriptional regulator of CETP is the LXR. LXR, as previously mentioned, is involved in activating several genes associated with the RCT process and therefore several studies have used LXR agonists by increasing the expression of LXR in treating cholesterol-related diseases, such as atherosclerosis and possibly cancer (Lakomy et al., 2009; Repa and Mangelsdorf, 2002). However, LXR also promotes the transcription of *CETP* and the increased CETP levels have been found to decrease HDL levels involved in RCT (Clark et al., 2004; de Grooth et al., 2004; Lakomy et al., 2009). The fact that CETP is involved in maintaining cholesterol homeostasis and the inhibition of CETP or *CETP*-deficient cells result in lower levels of intracellular cholesterol levels, it was hypothesized that CETP could be used as a target to lower cholesterol levels as a form of anticancer therapy. However, this relationship of CETP in the context of cancer has never been investigated.

9.12 Preliminary Studies on CETP

Preliminary results from Prof. Kaur's previous work showed that downregulation of *CETP* mRNA expression and the use of cholesterol depleting agents (Acetyl Plumbagin (AP), MβCD) resulted in the inhibition of growth and induced increased cancer cell death through mitochondrial-mediated apoptosis. Plumbagin (5-hydroxy- 2-methyl-1, 4-naphthaquinone) (PL) is a molecule that has anticancer properties and is plant-derived (Sagar et al., 2014). In several studies, PL has been found to induce apoptosis by a number of pathways. These include; signalling the production and release of ROS and nuclear factor kappa-light-chain-enhancer of activated B cells (NF-κB), thereby inhibiting the activation of cyclin D to induce apoptosis (Sagar et al., 2014; Sandur et al., 2006; Srinivas et al., 2004; Wang et al., 2008). Due to the high toxicity of this molecule, various derivatives of PL were developed, one being AP (Sagar et al., 2014; Sakao et al., 2009). In my previous preliminary results, I was able to confirm Prof. Kaur's results, where knocking down *CETP* increased TAM's efficacy in both ER+ and ER- BC cells, by increasing cell growth inhibition and apoptosis (Fig 9.7, 9.8). In addition, knocking down *CETP* with a combination treatment of TAM and the cholesterol depletor; AP, increased growth inhibition and cell death by 10-20% compared to single treatments, even at low concentrations (5 µM) (Fig 9.9). Hence, using the preliminary results, we hypothesized that *CETP* mRNA expression can possibly be used as a therapeutic marker, more specifically as a drug-resistance marker for monitoring and modifying the chemotherapeutic effects of drugs such as: TAM. Therefore, this hypothesis formed the bulk of my Master's study and we demonstrated that CETP is possibly involved in drug resistance in BC and *CETP* knock-down showed an enhanced drug efficacy in ER+ BC cells.

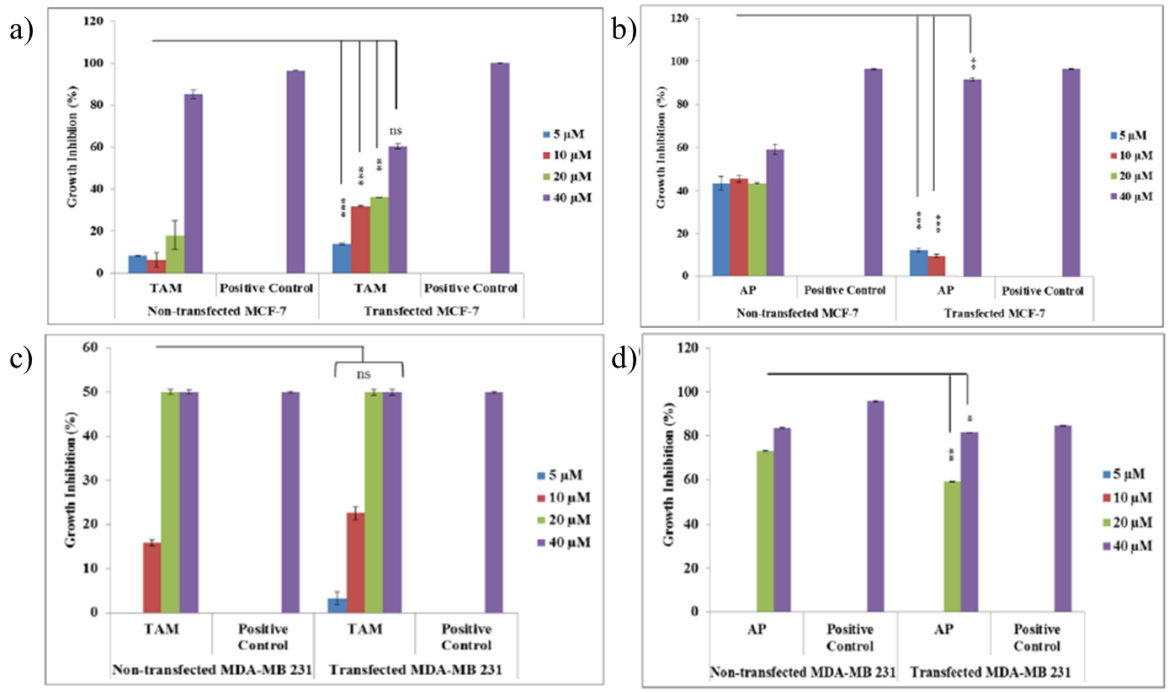

Figure 9.7: Growth inhibition increased in MCF-7 and MDA-MB 231 cells before and after CETP knock-down

*Growth inhibition was measured using the MTT assay and it was observed that growth inhibition was increased in both cell lines post CETP knock-down, with TAM treatment (a and c). However, this was not affected when treated with AP (b and d). Data represents mean ± standard deviation S.D. of raw data (n=3), where *p ≤ 0.05, **p ≤ 0.01 and ***p ≤ 0.001 significant difference to untreated control (ns being non-significant change), calculated using student's t-test.*

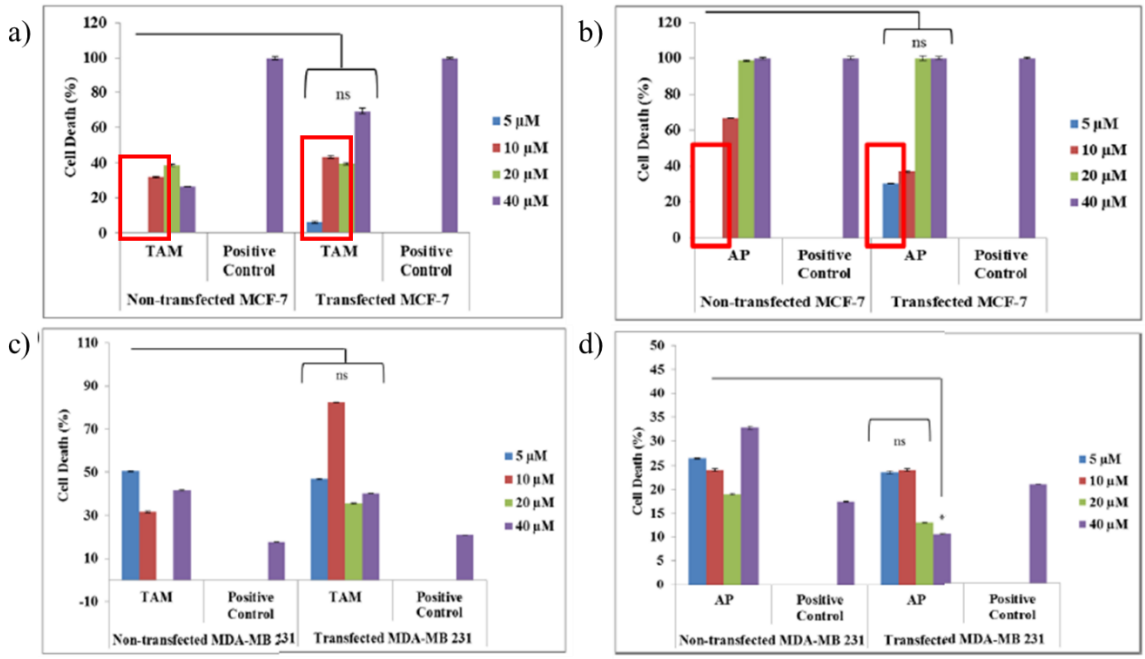

Figure 9.8: Apoptosis increased in MCF-7 and MDA-MB 231 cells before and after CETP knock-down

*CETP knock-down resulted in an increased cell death when treated with TAM and AP in MCF-7 cells (a and b). However, in MDA-MB 231 cells, knocking down CETP only increased TAM's efficacy at 10 and 20 µM (c) and it did not increase AP's efficacy (d). Data represents mean ± standard deviation S.D. of raw data (n=3), where *p ≤ 0.05, **p ≤ 0.01 and ***p ≤ 0.001 significant difference to untreated control (ns being non-significant change), calculated using student's t-test.*

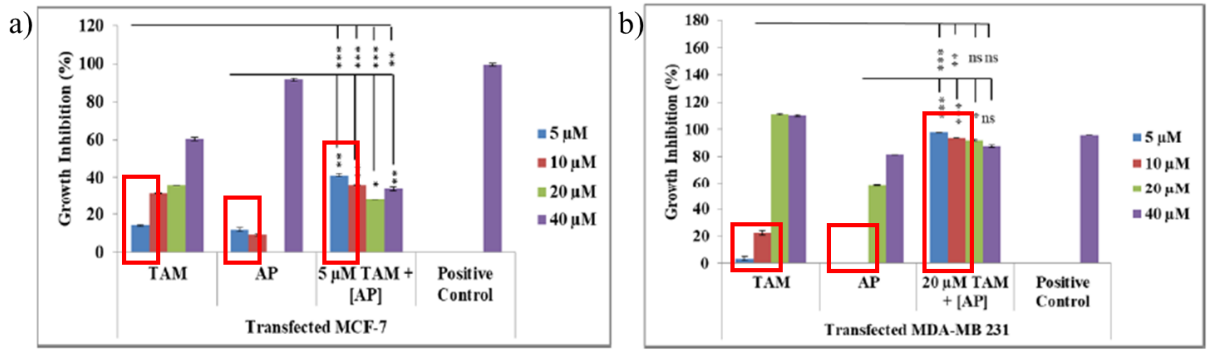

Figure 9.9: Growth inhibition increased in transfected BC cells treated with a combination treatment of TAM and AP

CETP knock-down with a combination treatment of TAM and AP resulted in a further enhancement of cell growth inhibition in both cell lines, even at lower concentrations of 5 and

*10 µM (a and b). Data represents mean ± standard deviation S.D. of raw data (n=3), where *p ≤ 0.05, **p ≤ 0.01 and ***p ≤ 0.001 significant difference to untreated control (*ns *being non-significant change), calculated using student's t-test.*

Therefore, knocking-down *CETP* could be a powerful therapeutic strategy, however the molecular mechanisms underlying CETP's involvement in cancer are unknown. Therefore, this brings us to the aims and objectives of this study.

10. Aims and Objectives

10.1 Aim:

- To elucidate the molecular mechanisms underlying CETP's involvement in cancer.
- To observe the effects of *CETP* knock-down on tumour growth in a mice xenograft study

10.2 Objectives:

- *CETP* knockdown on BC cells in both MCF-7 and MDA-MB 231 cells will be performed to measure the changes in cholesterol content (CE, lipid rafts and free cholesterol) pre and post CETP knockdown
- Identify target genes involved in lipoprotein signalling, and cancer drug resistance that may be affected by *CETP* knockdown using RT-qPCR arrays
- To compare tumour growth between CETP knocked down MDA-MB 231 cells vs non-transfected MDA-MB 231 cells in a mice xenograft study.

10.3 Workflow

The plan of work for this study is summarised in the flowchart below (Fig 10.1). Two cancer cell lines were used in this study: ER+ Michigan Cancer Foundation-7 (MCF-7) and TNBC M.D. Anderson metastatic breast 231 (MDA-MB 231) BC cells. The study was composed of two sections: *in vitro* and *in vivo* part. For the *in vitro* part of the study, the cells were subjected to 72 hrs transfection (*CETP* knock-down) and this was confirmed using RT-qPCR, western blotting and immunofluorescent staining. Cell viability assays: cell counting and MTT assays, as well as apoptosis assays (APO%) were performed on the transfected and non-transfected cells treated with single TAM or AP treatments (5 and 10 µM) and combination of TAM and AP treatment (5 or 10 µM TAM with 5 or 10 µM AP). To confirm whether *CETP* knock-down affected cholesterol levels; cholesterol assay, BODIPY, lipid raft staining and Filipin staining were performed to quantify cholesterol levels pre and post *CETP* knock-down. Thereafter, MOMP assay was performed to see the effects of treatment on the intrinsic apoptotic pathway. Reverse transcription – quantitative polymerase chain reaction (RT-qPCR) arrays were performed to identify gene expression profile changes post *CETP* knock-down in the

lipoprotein signalling and cholesterol metabolism pathways, as well as BC resistance pathways. Kaplan-Meier survival plots were generated to compare mortality in cancer patients with high *CETP* expression compared to patients expressing lower levels of *CETP*. Thereafter, a mice xenograft study was performed to compare tumour growth rate between the non-transfected and CETP knocked down cells (Fig 10.1).

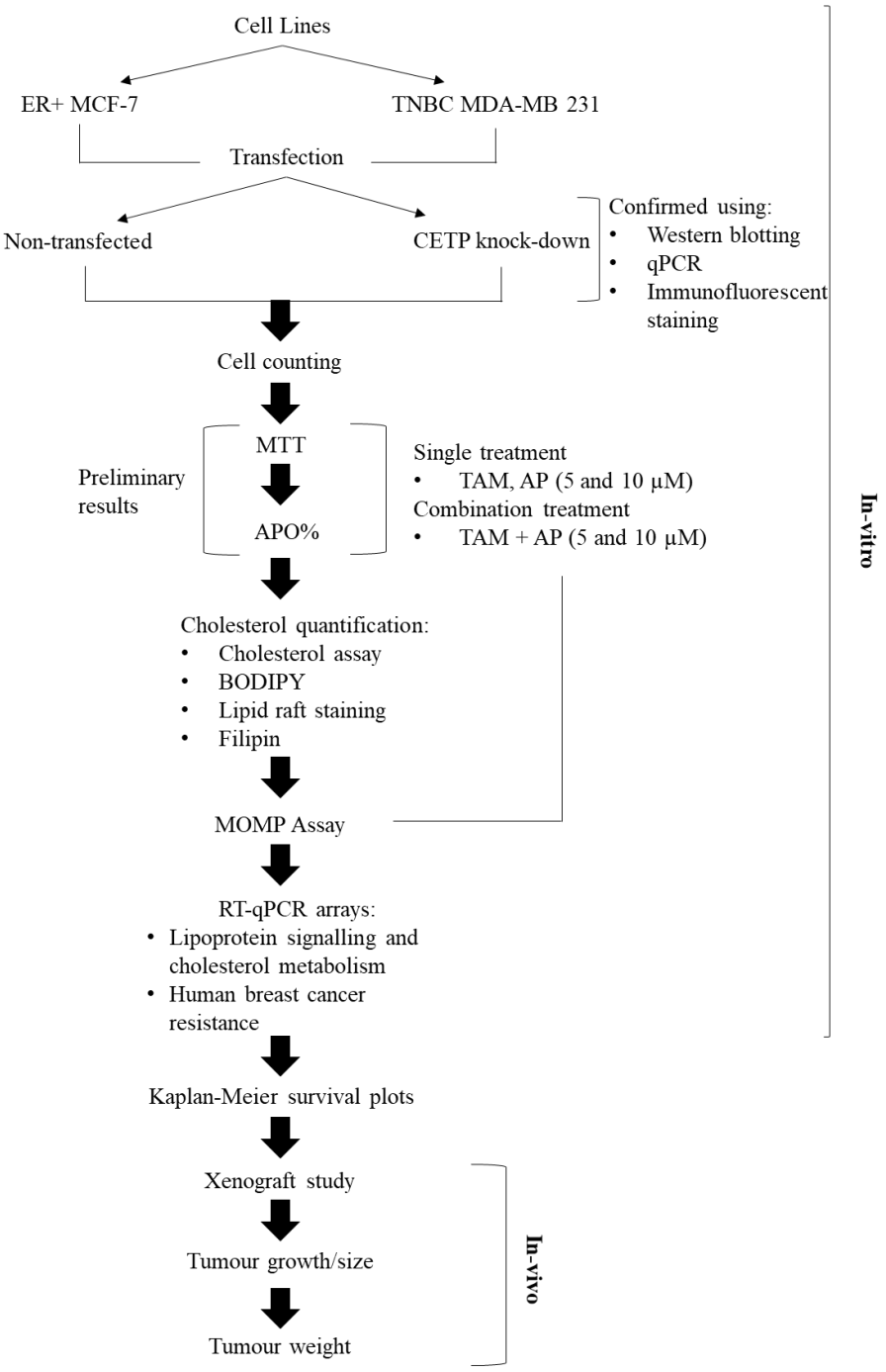

Figure 10.1: Flow diagram of work plan

11. Methods and Material

MCF-7 (The European Collection of Authenticated Cell Cultures (ECACC), UK) and MDA-MB 231 (American Type Culture Collection (ATCC), USA) BC cells were used in this project. Human embryonic kidney 293 cells (HEK293) (ATCC, USA) were also used as a non-cancerous cell line (Supplementary Fig 17.1). All experimental procedures were performed at least three times for reproducibility. The drugs or compounds that were used in this study included TAM (Sigma Aldrich, UK) and AP (synthesised from PL by the School of Chemistry, University of the Witwatersrand), with PL and MβCD (Sigma Aldrich, UK) as positive controls.

11.1 Cell Culture

MCF-7 cells were cultured in Dulbecco's Modified Eagle's Medium (DMEM) (GiBCo, Life Technologies, UK) supplemented with 10% foetal bovine serum (FBS) (Celtic Molecular Diagnostic, SA; Biowest, UK) and 1% penicillin streptomycin (PS) (GiBCo, Life Technologies, UK). MDA-MB 231 cells were cultured in 3:1 DMEM and HAMS F12 (Celtic Molecular Diagnostic, SA; Biowest, UK) also supplemented with 10% FBS and 1% PS. The cells were incubated at 37 ℃ with 5% carbon dioxide (CO_2) to mimic *in vivo* conditions.

Table 11.1: Cell lines used in the study

	MCF-7	**MDA-MB 231**	**HEK293**
Full name	Michigan Cancer Foundation-7 BC cells	M.D. Anderson metastatic breast-231 cancer cells	Human embryonic kidney 293 cells
Receptors	ER+, PR+, HER2-	ER-, PR-, HER2-	Undetectable levels of ER, PR, HER2
Morphology/Type	Epithelial	Epithelial	Epithelial
Disease	Adenocarcinoma, breast mammary gland	Adenocarcinoma, breast mammary gland	Immortalised cell line, non-malignant

Growth mode	Adherent	Adherent	Adherent
Media	DMEM, 10% FBS, 1% PS	3:1 DMEM: HAMS F12, 10% FBS, 1% PS	DMEM, 10% FBS, 1% PS

11.2 Cell Counting

The Neubauer haemocytometer was used for cell counting to accurately seed equal number of cells in each well. A haemocytometer is a cell counting chamber that uses a set of grids with known dimensions to predict the total number of cells in the cell culture flasks. Cell culture media was first removed and 2 ml of 1 × trypsin/Ethylenediaminetetraacetic acid (EDTA) (Celtic Molecular Diagnostic, SA; Biowest, UK) was added to the flasks containing the cells. Trypsin/EDTA is a proteolytic enzyme that disrupts the cell-to-cell and cell-to-substrate adhesion in the absence of calcium and magnesium (Rick, 1974). The cells were then incubated at 37 ℃ with 5% CO_2 for 5 minutes (min) for the activation of trypsin/EDTA to allow detachment of cells. Once the cells were detached, 2 ml of media was added to deactivate the activity of trypsin/EDTA. Subsequently, 100 µl of cells were added to 100 µl of 0.4% trypan blue (Sigma Aldrich, UK) and mixed thoroughly. Trypan blue is a commonly used stain that is excluded by live cells with intact cell membrane and staining the dead cells. Thereafter, 10 µl of the mixture was loaded onto the haemocytometer and cells were counted under an inverted microscope (Nikon Instruments, Tokyo, japan). Cells (live and dead) were counted in the four quadrants of 16 squares (including cells on the lines indicated in red) of the Neubauer grid (A, B, C and D in fig 1).

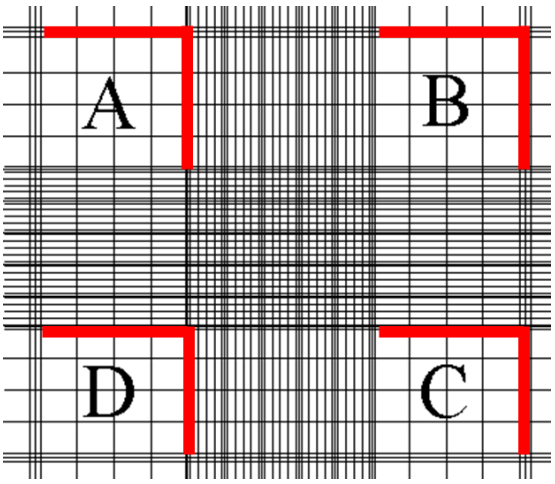

Figure 11.1: Haemocytometer; cell counting chamber

The cells in quadrants A-D are counted, including cells that lie on the two sides of the large squares (highlighted in red) to avoid counting the cells twice.

Equation 11.1: Cell Viability and cell density calculations

$$\% \text{ Cell viability} = \frac{\text{Number of dead cells (unstained)}}{\text{Total cells counted (dead and live)}} \times 100$$

Cells were seeded as follows (96-well plate):

(a) Total volume of media required = 45 µl × total number of wells

(b) Total number of cells required = 5 000 cells/well × total number of wells

(c) Volume of cells required from flask = $\frac{\text{Total volume in flask (µl)} \times \text{total number of cells required}}{\text{Total number of cells counted in flask}}$

Media to be added to the cells (µl) = Total volume required (a) − volume of cells required from flask (c)

45 µl was then pipetted into each well with approximately 5 000 cells/well

Cellular viability was calculated, and cell viability of 95% or above was considered for further experiments and seeded at a desirable density for specific experiments.

11.3 Transient transfection (*CETP* knock-down for 72 hours (hrs))

Transient transfection is the process of manipulating the expression of a particular gene by introducing foreign nucleic acids (DNA, RNA, small interfering RNA (siRNA)) into eukaryotic cells for a short period of time. The siRNAs are approximately 20 – 25 base pairs that is involved in RNA interference (RNAi), more specifically reducing the expression of target genes (Reynolds et al., 2004). The siRNA binds to argonaut that guides the RNA-induced silencing complex (RISC) to the target sequence (Fig 11.2). The RISC complexes, then, induce gene silencing through various processes such as; alternative splicing, transcriptional and translational silencing, thereby repressing target gene expression (Pratt and MacRae, 2009).

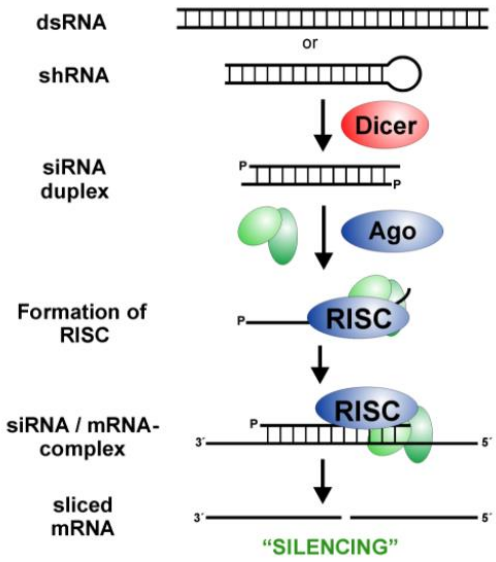

Figure 11.2: Mode of action of siRNAs

(Image adopted from: http://mcmanuslab.ucsf.edu/node/268)

CETP knock-down was performed using the Silencer® Select Pre-designed *CETP* siRNA (Ambion®, Life Technologies, USA) together with a lipid-mediated delivery system; DharmaFECT™ transfection reagent (Dharmacon™, GE Healthcare, UK; Inqaba Biotec™). Cells were seeded into a 6 well-plate at a density of 50 000 cells/well (MCF-7) and 100 000 cells/well (MDA-MB 231, due to slower doubling time) and incubated at 37 °C with 5% CO_2 for 24 hrs to allow attachment. Cells were then transfected as shown below.

Table 11.2: Volumes if siRNA and transfection reagent for a final siRNA concentration of 25 nM

			Tube 1: siRNA/ siRNA negative control (µl/well)		Tube 2: DharmaFECT™ reagent (µl/well)		
Cell type	Cell density	Complete medium	Volume of 5 µM siRNA (µl)	Serum-free medium (µl)	Volume of DharmaFECT™ reagent (µl)	Serum-free medium (µl)	Total volume/well (µl)
MCF-7	5×10^4	1600	10	190	1	199	2000
MDA-MB 231	1×10^5	1600	10	190	2	198	2000

Tubes 1 and 2 were made up according to the table above and the contents were incubated at room temperature for 5 min. Subsequently, tube 2 containing the DharmaFECT™ reagent, was added into tube 1, containing the siRNAs (final volume: 400 µl). The siRNA and DharmaFECT™ reagent-mix was incubated at room temperature for another 20 min. This is to allow the transfection reagent to encapsulate the siRNA for easy delivery into the cell's nucleus. This was then added to the cells (final volume of 2 000 µl/well) and incubated at 37 ℃ with 5% CO_2 for 72 hrs prior to downstream applications. western blotting, reverse transcription - quantitative polymerase chain reaction (RT-qPCR) and immunofluorescent staining were used to confirm *CETP* knock-down.

11.4 Reverse transcription - quantitative polymerase chain reaction (RT-qPCR)

RT-qPCR was used to confirm successful *CETP* mRNA knock-down. RT-qPCR is a rapid and sensitive technique to determine or quantify nucleic acid copies of a gene in biological samples.

11.4.1 RNA Extraction

RNA was extracted from transfected, non-transfected and siRNA negative control samples from both cell lines using the Direct-zol™ RNA MiniPrep kit (Zymo Research, Inqaba biotec™, SA). Firstly, 300 µl TRIzol® reagent (Ambion®, Life Technologies, USA) was added to the cell pellet (10^6 cells) and mixed thoroughly for 5 min at room temperature. Trizol is a commonly used chemical reagent that breaks cell membranes for the isolation or extraction of RNA, DNA and proteins (Simms et al., 1993; Simões et al., 2013). Equal amount of 99.9% room temperature ethanol was added to the samples to precipitate nucleic acids. Thereafter, the samples were transferred to the Zymo-Spin™ IIC Column in a collection tube and centrifuged at 16 000 × g for 30 seconds (s); subsequent centrifugation steps also followed these parameters unless specified otherwise. The flow-through was discarded and the columns were washed with 400 µl RNA wash buffer. DNase solution (5 µl DNase I with 75 µl DNA digestion buffer) was added to the columns and incubated at room temperature for 15 min to prevent any DNA contamination. The samples were then washed with 400 µl of Direct-zol™ RNA PreWash and flow-through was discarded. An additional wash of 2 min with 700 µl of RNA wash buffer, followed by the elution of RNA in 50 µl of DNase/RNase-free water. RNA was stored at 80 ℃ until needed. RNA was quantified using the NanoDrop™ One/One^C Microvolume UV-Vis spectrophotometer (Thermo Fisher Scientific, USA) and RNA samples with 260/280 ratios between 1.9-2 were considered for further applications. RNA integrity was tested on a 1% agarose gel and images were captured with the ChemiDoc XRS+ system (Bio-Rad, USA).

11.4.2 cDNA synthesis

The RevertAid First Strand cDNA synthesis kit (Thermo Fisher Scientific, USA) was used to convert extracted RNA to cDNA. The following reagents were added to the reaction:

Table 11.3: Reagents used in cDNA synthesis for a 20 µl reaction

Reagent	Volume (µl)
Template RNA	2 µg (volume dependent on RNA concentration)
Oligo $(dT)_{18}$ primer	1
Nuclease-free water	Up to 12
Total volume	12
Master Mix	
5× reaction buffer	4
RiboLock RNase inhibitor	1
10 mM dNTP mix	2
RevertAid M-MuLV RT (200U/µl)	1
Final volume	20

The samples were mixed gently and centrifuged briefly prior to a 1 hr incubation at 42 ℃ in the MultiGene PCR machine (Labnet International, UK). The reaction was then terminated at 70 ℃ for 5 min and stored at -20 ℃ until required.

11.4.3 *CETP* mRNA expression through RT-qPCR

The SensiFAST™ SYBR® No-ROX kit was used to determine *CETP* mRNA expression in the transfected, non-transfected and the control samples in both cell lines. SYBR green is a fluorescent cyanine dye that intercalates double-stranded DNA during the annealing and extension step. SYBR green fluorescent signal increases as DNA is amplified at each cycle and is measured in Ct (cycle threshold) values (initial detectable signal of SYBR green). Therefore,

SYBR green fluorescent signal is directly proportional to the amount of template of target mRNA in the reaction. For the study, a half reaction (10 µl) was used as final volume and the components are as follows:

Table 11.4: qPCR reagent composition

Reagent	Volume (µl)	Final Concentration
2× SensiFAST™ SYBR® No-ROX mix	5	1×
10 µM Forward primer	0.4	400 nM
10 µM Reverse primer	0.4	400 nM
cDNA template	2	-
Distilled water (dH_2O)	2.2	-
Final volume	10	-

The primer sequences of *GAPDH* and *CETP* were obtained from previously published study by Ding et al., (2015) (Table 11.5), and synthesised by Integrated DNA Technologies (IDT – Illinois, USA).

Table 11.5: Primer sequences for GAPDH and CETP gene

Gene	Sequence (5'-3')	GC content (%)	Reference
CETP (forward)	GAGTCCCATCACAAGGGTCA	55	(Ding et al., 2015)
CETP (reverse)	GGAAGACTCGCTCAGAGAACC	57.1	
GAPDH (forward)	CGTGTCGGTTGTGGATCTGA	55	
GAPDH (reverse)	TGACGAAGTGGTCGTTGAGG	55	

Subsequently, a 3-step cycling parameter (Table 11.6) was set on the CFX96 Touch™ Real-Time PCR Detection System (BioRad, SA). White, opaque 8-well PCR strips (BIOPlastics,

Netherlands; Celtic Diagnostics, SA) were used. *CETP* mRNA expression was normalised against *GAPDH* and change in *CETP* expression between transfected and non-transfected samples were calculated using the $2^{-\Delta\Delta Ct}$ method (Livak and Schmittgen, 2001). The $2^{-\Delta\Delta Ct}$ method is a well-known formula used to calculate the relative fold change of the expression of a particular gene. It uses the Ct value from the qPCR data, which explained previously is the cycle number where the fluorescence of the sample was first detected. The Δ symbol is the difference between two values (treated and untreated samples, as well as the difference between gene of interest and reference gene). Therefore, it normalises the expression of the gene of interest to the reference gene, that is not affected by the treatment, and compares the expression fold change of the treated sample relative to the expression of the untreated sample (Livak and Schmittgen, 2001).

Table 11.6: 3-step cycling parameter

Cycles	Temperature (°C)	Time	Step
1	95	2 min	Polymerase activation
40	95	5 s	Denaturation
	57.1	10 s	Annealing
	72	15 s	Extension

11.5 Western Blotting

Western blotting was used to confirm CETP protein expression in transfected, non-transfected and control cells in both cell lines. Cells were seeded for transfection, as described previously, for 72 h. Thereafter, cells (at least 10^6 cells) were harvested and pelleted at 4 000 × g for 5 min. The supernatant was removed and 1 × Ripa lysis buffer (Table 7) was added (100 µl/10^6 cells) to disrupt cell membrane, exposing internal proteins and components of the cells. Subsequently, protein concentrations were determined using a bicinchoninic acid (BCA) assay.

Table 11.7: Ripa lysis buffer constitution

	Components/ 100 ml
1 × Ripa lysis buffer	• 300 mM sodium chloride (NaCl) = 0.876g) • 1% Triton-X-100 = 1 ml • 1% Deoxycholate = 1 g • 0.1% sodium dodecyl sulphate (SDS) = 1 ml of 10% SDS • 50 mM Tris = 1.21 g • 10 mM EDTA = 1 ml (all reagents were from Sigma Aldrich, UK)

11.5.1 Protein Quantification: BCA assay

Protein quantification was performed to ensure equal loading of samples during SDS-polyacrylamide gel electrophoresis (SDS-PAGE). BCA assay is a protein quantification technique based on the reduction of copper sulphate (Cu^{2+}) to Cu^{+} (in the presence of protein), which interacts with BCA resulting in the development of purple colour that is measured spectrophotometrically (Smith et al., 1985; Walker, 2009). Test samples with unknown protein concentrations were compared to a known protein standard (example shown below in fig 3). A bovine serum albumin (BSA) (Amresco; Inqaba Biotec™, SA) standard curve was generated using the following BSA concentrations (constituted in 1 × Ripa lysis buffer); 1 mg/ml, 0.8 ml/ml, 0.6 mg/ml, 0.4 mg/ml, 0.2 mg/ml and 0 mg/ml as blank. Subsequently, 25 µl of each concentration was loaded, in triplicates, in a 96-well plate. Test samples of unknown protein concentrations are diluted 5 × (5 µl sample lysate with 20 µl 1 × Ripa lysis buffer) in each well, loaded in triplicates. Thereafter, 200 µl of BCA reagent mix (196 µl of BCA (Sigma Aldrich, UK) and 4 µl of Cu^{2+} (Sigma Aldrich, UK)) was added into each well and the plate was incubated at 37 ℃ with 5% CO_2 for 30 min. The colour intensity of each sample, in the 96-well plate, was measured at 562 nm using the Multiskan GO Microplate reader (SkanIt™ software) (Thermo Fisher Scientific, USA). The total protein concentration of each lysate was calculated in Microsoft Office Excel©.

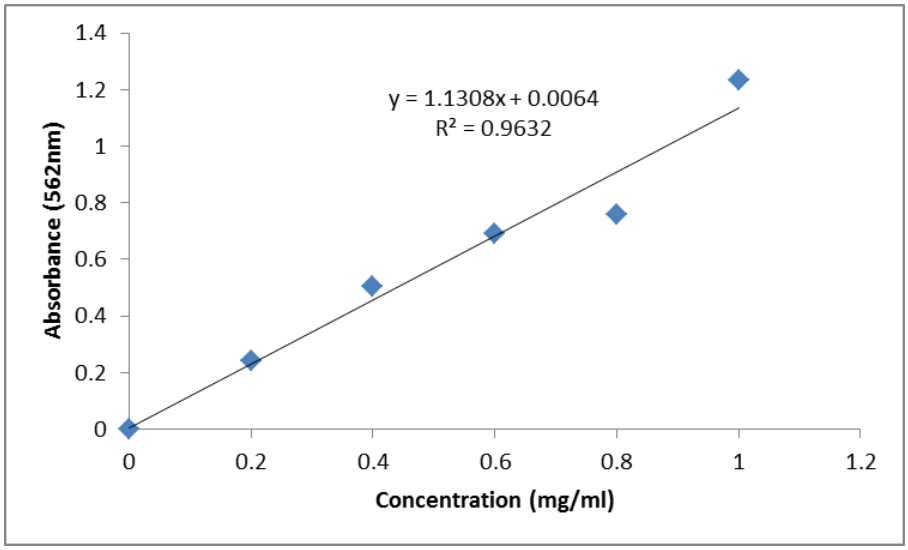

Figure 11.3: BSA protein standard curve

Equation 11.2: Protein quantification formula

Average of samples – average of blanks = (a)
Substituted y-value with (a) in the y = mx + c formula above in BSA protein standard
∴Protein concentration of lysates = calculated x-value × 5 (dilution factor)

The concentrations of protein lysates were calculated using the above formula. Protein lysates were diluted to the same concentration across the samples with 2 × Laemmli buffer (Sigma Aldrich, UK). Once normalised, samples were loaded with equal volume into a 10% SDS-PAGE gel (Table 8 and 9) and electrophoresed at 120 V for 1 hr. Proteins were then transferred onto a 0.22 µM polyvinylidene difluoride (PVDF) membrane (activated/hydrated by methanol) using the Trans-Blot® Turbo™ transfer system (Bio-Rad, USA) for 30 min. PVDF membranes have high binding affinities for proteins through hydrophobic interactions and has high retention of absorbed proteins. Thereafter, the membrane (containing the proteins) was blocked with 3% BSA solution for 1 hr, at room temperature, to prevent antibody from binding directly to the membrane and minimising background noise. Subsequently, the desired primary antibody (anti-CETP or anti-β-tubulin (as the loading control); Sigma Aldrich, UK) (Table 11.10) was added to the blocking solution (1:2 000 dilution) and incubated, in the dark, at 4 °C overnight on a shaker. Unbound primary antibodies were then washed off with 1 × phosphate buffered saline (PBS) for 5 min, which was repeated five times. This was followed by the addition of specific secondary antibodies (anti-mouse or anti-rabbit, dependent on the host of the primary antibody) (Table 11.10) and incubated for 1 hr on a shaker, at room temperature in

the dark. Again, unbound secondary antibodies were washed off with five 5 min 1 × PBS washes. The membrane was then exposed to the Clarity™ western Enhanced Chemiluminescence (ECL) substrate (horseradish peroxidase (HRP) conjugated substrate – 1 ml of reagent A and 1 ml of reagent B) for 5 min in the dark. Protein bands were visualised using the ChemiDoc XRS+ system (Bio-Rad, USA) and densitometry was performed using the Image Lab™ 4.0 Software (Bio-Rad, USA).

Table 11.8: SDS-PAGE gel (10%, 1 mm) components per gel

	Resolving Gel	Stacking Gel
Resolving gel buffer	3 ml	-
Stacking gel buffer	-	750 µl
30% Bis-acrylamide (Sigma Aldrich, UK)	3 ml	500 µl
dH_2O	3 ml	1.75 ml
10% Ammonium persulphate (APS) (Sigma Aldrich, UK)	200 µl	30 µl
Tetramethylethylenediamine (TEMED) (Sigma Aldrich, UK)	20 µl	3 µl

Table 11.9: Buffer components

	Components
1 × Resolving gel buffer	• 36.2 g Tris • 0.8 g SDS • Dissolved in 150 ml dH_2O • pH to 8.9 • Made up to 200 ml with dH_2O
1 × Stacking gel buffer	• 5.9 g Tris

	• 0.4 g SDS • Dissolved in 70 ml dH_2O • pH to 6.8 • Made up to 100 ml with dH_2O
30% Bis-acrylamide (Sigma Aldrich, UK)	• 30 g Acrylamide • 0.8 g Bisacrylamide • 0.1 g SDS • Made up to 100 ml dH_2O
10% APS (Sigma Aldrich, UK)	• 100 mg APS in 1 ml dH_2O

11.6 Immunofluorescent staining

CETP protein knock-down was also confirmed using immunofluorescent staining. Cells were seeded at a density of 20 000 cells/well in a 6-well plate in 2 ml of media and incubated at 37 °C and 5% CO_2 for 24 h. Cells were treated with Torcetrapib (25 µM final concentration; Sigma Aldrich, UK) for 24 hrs at 37 °C, was used as a positive control. Torcetrapib is an inhibitor of CETP and has been highly studied in reducing intracellular cholesterol levels, however, due to the cytotoxicity it did not pass clinical trials (Pearson, 2006). The media was then discarded, followed by three 1 × PBS washes (three washes were performed between each step) prior to cell fixation with 4% formalin (Sigma Aldrich, UK) at room temperature for 10 min. Briefly, the fixation step preserves cellular structures and composition by forming stable, covalent crosslinking between molecules (Thavarajah et al., 2012). Following this, cell membranes were permeabilised with 0.1 Triton™ X-100 (Sigma Aldrich, UK) for 20 min at room temperature. Thereafter, 0.05% BSA (Amresco; Inqaba Biotec™, SA) was added to the cells for 20 min to prevent non-specific binding of CETP antibodies. Anti-CETP primary antibody (Sigma Aldrich, UK) (Table 11.10) was added to the cells (1:1000 dilution) and incubated at 4 °C overnight. Subsequently, secondary antibody-Texas red (Thermo Fisher Scientific, USA) (Table 11.10) was added (1:1 000 dilution) and incubated in the dark for 1 hr at 4 °C. Cells' nuclei were stained using 0.001 mg/ml DAPI (Sigma Aldrich, UK) for 5 min at room temperature. Any unbound antibodies and dye were washed off with three 1 × PBS washes and immunofluorescence was visualised using the FLoid™ cell imaging system (Thermo Fisher Scientific, USA). The fluorescent intensity was measured using ImageJ1 software (Schneider et al., 2012).

Table 11.10: Primary and secondary antibodies used in western blotting and immunofluorescent staining

Primary Antibody	Size (kDa)	Vendor
β-tubulin	50	Sigma-Aldrich
CETP	77	Sigma-Aldrich
SREBP-1 (Supplementary Fig 17.2)	65	Novus Biological
LDLR (Supplementary Fig 17.2)	160	Novus Biological
ER (Supplementary Fig 17.2)	66	Sigma-Aldrich
Secondary Antibody		**Vendor**
Goat Anti-mouse IgG (H+L) – HRP conjugate		Sigma-Aldrich
Goat Anti-rabbit IgG (H+L) – HRP conjugate		Sigma-Aldrich
Goat Anti-rabbit IgG (H+L) Cross-absorbed secondary antibody, Texas red		Thermo Fisher Scientific, USA

11.7 Growth Inhibition Assay

The effects of *CETP* knock-down on growth inhibition was measured through cell counting (as described earlier), where total cell numbers were calculated pre and post transfection in each sample. In addition, an MTT (3-(4,5-dimethylthiazol- 2-yl)-2,5-diphenyl tetrazolium bromide) (Sigma Aldrich, UK) assay was performed to measure the effects of TAM and AP (at varying concentrations; 5 µM, 10 µM, 20 µM and 40 µM), after 24 hrs, on cellular growth pre and post *CETP* knock-down. Furthermore, this was also performed in samples with combination treatments (TAM with varying AP concentrations, 24 hrs) pre and post *CETP* knock-down. This method was used during preliminary results.

Equation 11.3: Cell viability and growth inhibition calculations for MTT assay

Average of absorbance values of test samples − Average of absorbance values of blanks = (a)

% Cell viability = [(a) of test samples ÷ (a) of untreated samples] × 100

% Growth inhibition = 100 − % cell viability

MTT assay is a colorimetric assay that measures the reduction of MTT/tetrazolium salt by metabolically active cells and results in the formation of formazan crystals. Briefly, the mitochondria of viable cells reduces the MTT through the succinate dehydrogenase enzyme, and converts the yellow salts to a blue/purple coloured formazan crystals, which can be dissolved in an organic solvent (Supino, 1995). Cells were seeded into a 96-well plate at a density of 5 000 cells/well and incubated at 37 °C and 5% CO_2 overnight. Cells were then treated with TAM, AP or combination of TAM and AP, at the desired concentrations, in triplicates for 24 hrs at 37 °C and 5% CO_2. MTT (5mg/ml in PBS (Sigma Aldrich, UK)) was added for 3 hrs and the formazan crystals were subsequently dissolved in solubilising solution (10% SDS (Sigma Aldrich, UK) with 10 mM hydrochloric acid (HCl)) for at least 16 hrs. The optical density (OD) was subsequently measured at 570 nm using the Multiskan GO Microplate Reader (Thermo Fisher Scientific, USA; SkanIt™ software) and the percentage of cell growth inhibition was calculated in Microsoft Office Excel©.

11.8 Apoptosis Assay

11.8.1 APOPercentage (APO%) Assay

APOPercentage (APO%) assay was performed using the APO% assay kit (Biocolor, UK) to observe apoptosis post drug treatment (same treatments as in MTT assay). This method was used for preliminary results. APO% assay detects the early stages of apoptosis in adherent cells. The APO% dye is bound to the phosphatidyl ethanolamine that is on the outer leaflet of the cell membrane. Cells that are undergoing apoptosis activates the scramblase enzyme that inhibit flippase activity (flippases maintains membrane structure in normal cells) and thus membrane flip occurs (Biocolor, UK) (Fig 11.4). This membrane flip, therefore, results in the uptake of the APO% dye as phosphatidyl ethanolamine is transferred to the inner leaflet of the membrane, exposing the phosphotidylserine to the extracellular matrix (Biocolor, UK).

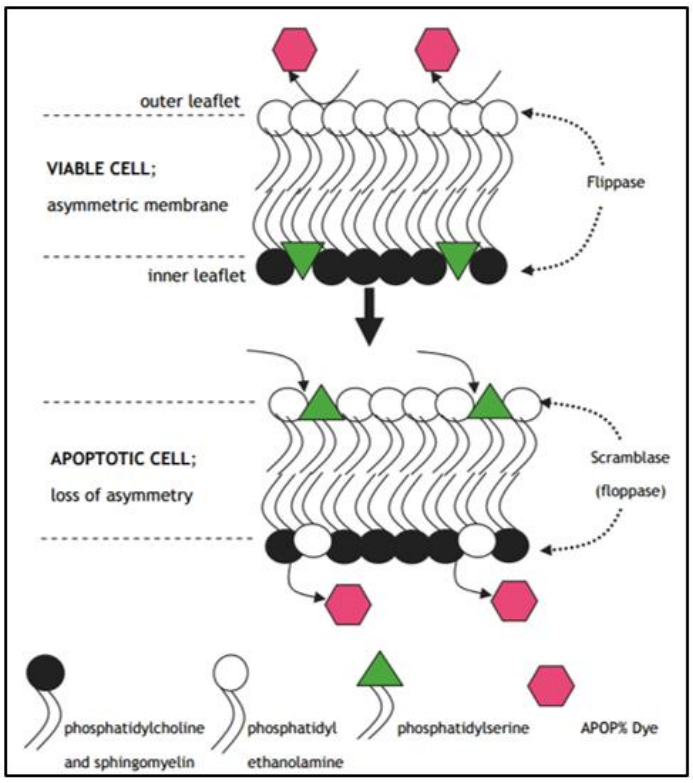

Figure 11.4: Mechanism of action of APO% assay

(Image adopted from: www.biocolor.co.uk)

Cells were seeded at a density of 10 000 cells/well in a 96-well plate and incubated at 37 °C and 5% CO_2 overnight to allow cell adherence. Followed by a 2 hrs drug/ compound treatment at 37 °C. As mentioned earlier, this assay detects the beginning stages of apoptosis therefore, longer treatments may lead to the detachment or disintegration of cells and thus risk of being washed off resulting in inaccurate readings. Thereafter, media was removed from all wells and 65 µl of dye solution (0.5 µl of APO% dye with 64.5 µl 1 × PBS) was added into each well and incubated at 37 °C for 30 min. Subsequently, the wells were washed gently with 100 µl of 1 × PBS. The cells were then submerged in 100 µl of 1 × PBS to prevent dehydration of the cells. The colour intensity was measured at 550 nm using the Multiskan GO Microplate Reader (Thermo Fisher Scientific, USA; SkanIt™ software) and percentage cell death was calculated in Microsoft Office Excel© (formula shown below).

Equation 11.4: Cell death for the APOP% assay

Average of absorbance values of test samples − Average of absorbance values of blanks = (a)

% Cell death = [(a) of treated samples − (a) of untreated samples] ÷ (a) of untreated samples × 100

11.8.2 MOMP assay

MOMP is an additional assay that measures apoptosis, more specifically intrinsic apoptosis. Cells were seeded at a density of 7 500 cells/well into a 96-well plate and incubated at 37 °C and 5% CO_2 overnight. The cells were then treated with the drug/compound, at the desired concentrations, for 24 hrs at 37 °C. Subsequently, 12 µl of 15 mM EDTA was added into each well and incubated at 37 °C for 40 min to detach the adherent cells (Kaur and Esau, 2015). Thereafter, 15 µl of 2 mM cyanine dye; JC-1 (5,5′,6,6′-tetrachloro-1,1′,3,3′-tetraethylbenzimidazolylcarbocyanine iodide) (Sigma Aldrich, UK) was added to the cells for 1 hr at 37 °C in the dark. JC-1 mainly forms aggregates (red) in the mitochondria and less as a monomer (green) in the cytosol of non-apoptotic cells (Reers et al., 1995). In contrast, in apoptotic cells, membrane potential is low and thereby JC-1 only exists as a monomer in the cytosol (Reers et al., 1995). Each well (containing the cells and JC-1) was transferred to a sterile Eppendorf tube and placed on ice, to halt JC-1 activity, until analysis. Fluorescence of JC-1 was detected with the Accuri C6 flow cytometer.

11.9 Cholesterol quantification

11.9.1 Cholesterol assay

Cholesterol assay was performed to determine the effects of drug treatments pre and post *CETP* knock-down on intracellular lipid levels. Briefly this method involves the hydrolysis of CEs by cholesterol esterase, which forms cholesterol. Cholesterol is then oxidised by cholesterol oxidase that results in two products: 1) cholest-4-ene-3-one and 2) hydrogen peroxide (H_2O_2). H_2O_2 is detected with a highly specific colorimetric probe (amplex red – synthesized by the Department of Chemistry, University of the Witwatersrand), The HRP catalyses the reaction between H_2O_2 and amplex red that binds in a 1:1 ratio. This reaction results in the development of a pink colour, which is read at 570 nm (Fig 11.5) (Sigma Aldrich, UK).

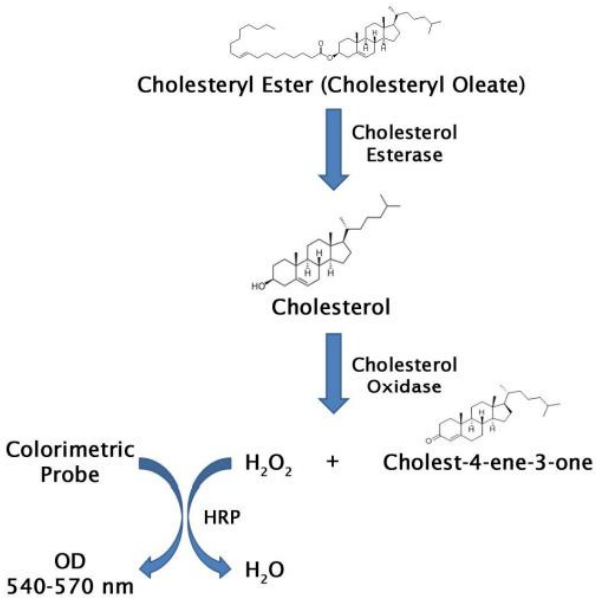

Figure 11.5: Principle of cholesterol assay

(Image Adopted from: https://www.bioscience.co.uk/userfiles/pdf/STA-384-total-cholesterol-colorimetric-assay-kit.pdf)

Cells were seeded into a 96-well plate at a density of 5 000 cells/well, in duplicates in two sets; one set tests for total cholesterol and the other set tests for free cholesterol. The cells were incubated at 37 °C and 5% CO_2 overnight prior to drug treatments for 24 h. Thereafter, the media was removed and discarded from each well and cells were washed, gently, with 50 µl of 1 × PBS. Followed by the addition of 10 µl of 100 U/ml catalase (Sigma Aldrich, UK) into each well and incubated at 37 °C for 15 min. Catalase is an enzyme that degrades excess H_2O_2 into water and thus protects the cells from ROS. In addition, it also prevents background noise. Reagent A was then prepared with the components, in the order, listed below (Table 11.11).

Table 11.11: Components of reagent A in cholesterol assay

Reagent	Set 1: Total cholesterol (with esterase) (µl/well)	Set 2: Free cholesterol (without esterase) (µl/well)
1 M Potassium phosphate buffer (KPO_4) (Sigma Aldrich, UK)	2.5	2.5
1 M NaCl (Sigma Aldrich, UK)	6.25	6.25

100 mM Cholic acid (Sigma Aldrich, UK)	1.25	1.25
100% Triton X-100 (Sigma Aldrich, UK)	0.25	0.25
20 U/ml Cholesterol oxidase (Sigma Aldrich, UK)	2.5	2.5
150 U/ml HRP (Sigma Aldrich, UK)	1.44	1.44
25 U/ml Cholesterol esterase (Inqaba Biotec™, SA)	3.33	-
Isopropanol: NP-40 (9:1) (Merck, SA)	6.48	9.81
10 mM Amplex red (School of Chemistry, University of the Witwatersrand)	1	1

Subsequently, 25 µl of reagent A (with esterase and without esterase respectively) was added to the respective wells and incubated, in the dark, for 30 min at 37 °C. The absorbance was then measured using the Multiskan GO Microplate Reader (Thermo Fisher Scientific, USA; SkanIt™ software) and CE levels were calculated against a cholesterol standard curve (5, 10, 15, 20 and 0 µg/ml as blank) in Microsoft Office Excel© (formula shown below).

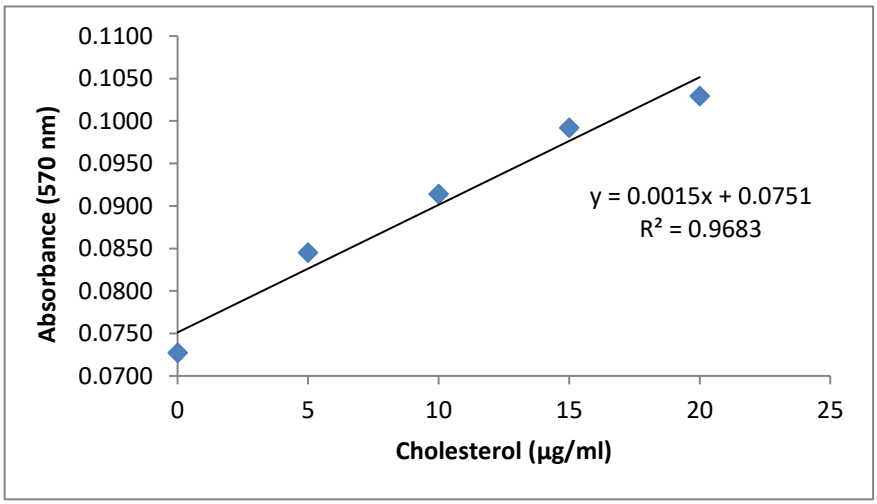

Figure 11.6: Cholesterol standard curve

Equation 11.5: Cholesterol ester quantification

Average of samples – average of blanks = (a)

Substituted y-value with (a) in the y = mx + c formula above in the cholesterol standard curve

∴ Calculated x-value for total cholesterol and free cholesterol

x-value = total/free cholesterol concentration (µg/ml)

µg/ml converted to µg/µl → x-value ÷ 1000 × total volume in well = total/free cholesterol concentration (µg/µl)

Total cholesterol – free cholesterol = CE

11.9.2 Immunofluorescent lipid staining

Several lipid staining methods were used to quantify cholesterol levels in transfected cells relative to non-transfected cells. The following steps were followed through for all staining procedures. Transfected and non-transfected cells were seeded into a 6-well plate at a density of 50 000 cells/well and incubated at 37 °C and 5% CO_2 overnight. A concentration of 1 mM MβCD (24 hrs at 37 °C) was used as the positive control. Cells were then fixed with 4% formalin as described earlier. Cell were washed with 1 × PBS three times in between each step unless stated otherwise.

Filipin staining

Filipin is a naturally fluorescent antifungal antibiotic that was first identified or isolated from *Streptomyces Filipinesis* (Whitfield et al., 1955). In addition, it has been found that filipin has high affinity to sterols and membrane cholesterol (Le Lay et al., 2006; Norman et al., 1972). Due to this interaction, filipin has been used as a cytochemical probe in numerous sterol-related studies (Sohn et al., 2018; Wilhelm et al., 2019). In this study, filipin was used to determine cholesterol levels pre and post *CETP* knock-down. Once cells were fixed, it was incubated with 1 ml of filipin (0.05 mg/ml in PBS) (Sigma Aldrich, UK), in the dark at room temperature, for 2 hrs (Esau et al., 2016). Cells were then washed with 1 × PBS and the nuclei were stained using the NucRed™ Dead 647 (Thermo Fischer Scientific). Fluorescent intensity was measured under the FLoid™ cell imaging system (Thermo Fisher Scientific, USA).

Boron-dipyrromethene (BODIPY) staining

BODIPY is a fluorophore that can be structurally modified to form conjugations with proteins, hormones, DNA and lipids for fluorescence labelling (Li et al., 2006b; Osati et al., 2016). In this study, BODIPY was used to fluorescently label CEs pre and post *CETP* knock-down. Once the cells were fixed with 4% formalin (Sigma Aldrich, UK) and washed with 1 × PBS, cell membranes were permeabilised using 0.1% triton X-100 (Sigma Aldrich, UK) at room temperature for 20 min. Thereafter, 1 µl of 1 mg/ml BODIPY was added and incubated at 37 °C for 15 min in the dark. The nucleus was then stained with 0.001 mg/ml DAPI (Sigma Aldrich, UK) for 3 min and fluorescence was measured using the FLoid™ cell imaging system (Thermo Fisher Scientific, USA).

Lipid raft staining

Lipid rafts are areas in the cell membrane that are highly concentrated in cholesterol and sphingolipids (Blank et al., 2007). Lipid rafts were stained using the Vybrant™ Alexa Fluor™ 594 Lipid Raft Labelling kit (Thermo Fisher Scientific, USA). This kit is composed of cholera toxin subunit B (CT-B) labelled with Alexa Fluor 594 dye (component A) and an anti-CT-B antibody (component B). CT-B binds to the glucosphingolipid ganglioside (GM1) in the plasma membrane (concentrated in the lipid rafts) therefore, making it possible to fluorescently tag CT-B to study the lipid rafts (Blank et al., 2007). Once cells were fixed, the cell membranes were permeabilised with 0.1% triton X-100 (Sigma Aldrich, UK) at room temperature for 20 min. Thereafter, cells were submerged with component A (2 µl in 1 ml PBS) and incubated at 37 °C, in the dark, for 30 min. The cells were then washed with 1 × PBS and component B (10 µl in 1 ml PBS) (anti-CT-B antibody that binds to component A and forms crosslinks in the plasma membrane) was added to the cells and incubated at 37 °C, in the dark for another 30 min. The nucleus was stained using 0.001 mg/ml DAPI (Sigma Aldrich, UK) for 3 min. at room temperature and fluorescence was measured using the FLoid™ cell imaging system (Thermo Fisher Scientific, USA).

11.10 RT² Profiler™ PCR arrays

RT² Profiler™ PCR arrays (Qiagen, Germany; Whitehead Scientific, SA) were used to identify the expression levels of a total of 168 genes (involved in human cancer drug resistance

pathway, as well as human lipoprotein signalling and cholesterol metabolism pathways; 84 genes in each pathway) pre and post *CETP* knock-down. These array panels are based on the same principle as the conventional RT-qPCR, where it involves the amplification of target gene sequence and the detection of copy numbers of the target gene with SYBR® green. Each panel (96-well plates, white) comes as ready-prepared plates with different primer pairs in each well (84 wells for 84 different genes) (Qiagen, Germany; Whitehead Scientific, SA). The remaining 12 well includes five housekeeping genes (β-actin, β-2-microglobulin, glyceraldehyde-3-phosphate dehydrogenase, hypoxanthine phosphoribosyltransferase 1 and ribosomal protein large P0), control to monitor genomic DNA contamination, three reverse transcription controls and three positive PCR controls (Qiagen, Germany; Whitehead Scientific, SA). RNA was extracted using the Direct-zol™ RNA MiniPrep kit (Zymo Research, Inqaba Biotec™, SA) as described previously. Extracted RNA was quantified using the NanoDrop™ One/One^C Microvolume UV-Vis spectrophotometer (ThermoFisher Scientific, USA). Thereafter, 500 ng of RNA sample was used for cDNA synthesis using the RT^2 First Strand Kit (Qiagen, Germany). This kit consists of two steps: genomic DNA elimination step and the reverse transcription step.

Table 11.12: Genomic DNA elimination mix

Component	Volume/concentration
RNA samples	500 ng
Buffer GE	2 µl
RNA-free water	Made up to 10 µl
Total volume	10 µl

The reaction was then incubated at 42 °C for 5 min and placed on ice for 1 min to stop the reaction. Thereafter, the reverse transcription mix was added to the reaction (Table 11.13) and incubated for another 15 min at 42 °C. The reaction was then halted by a 5 min incubation at 95 °C. Subsequently, 91 µl nuclease-free water was added to the reactions and mixed with 1 350 µl of 2 × RT^2 SYBR green mastermix. The reaction mix was then made up to a total

volume of 2 700 µl with nuclease-free water. 25 µl of the reaction mix was loaded into each well of the RT² Profiler™ PCR array plate.

Table 11.13: Reverse transcription mix

Component	Volume (µl)
5 × buffer BC3	4
Control P2	1
RE3 reverse transcriptase mix	2
RNase-free water	3
Total volume	10

The CFX96 Touch™ Real-Time PCR Detection System (BioRad, SA) was used to measure the gene expressions in transfected and non-transfected cells (parameters listed in table 11.14).

Table 11.14: CFX96 Touch™ Real-Time PCR parameters

Cycles	Temperature (°C)	Duration
1	95	10 min
40	95	15 s
	60	1 min

Gene expression changes in transfected and non-transfected samples were analysed using the RT² Profiler™ PCR array template (lipoprotein signalling array code: PAHS-080ZA, BC resistance array code: PAHS-004Z) (https://www.qiagen.com/de/resources/resourcedetail?id=b3396407-ecb5-4656-ac5d-5ea7b83a397e&lang=en) (Qiagen, Germany) on Microsoft Office Excel©. The gene expressions from these arrays were also compared to the data obtained from Gene Expression

Profiling Interactive analysis (GEPIA) using multiple gene analysis tool (http://gepia.cancer-pku.cn/).

11.11 Heatmap and gene network map

Omicsnet (https://www.omicsnet.ca/) (Zhou and Xia, 2018) was used to predict interaction networks between the selected genes obtained from the RT² Profiler™ PCR array. Cystoscape (Shannon et al., 2003) was then used to create the gene network map including the expression profiles obtained from RT² Profiler™ PCR array. Briefly, the gene names and expression data (log2 fold change) were analysed by these software programs to generate a network map, where lines represent the interaction between the genes and nodes representing the expression of the genes post *CETP* knock-down.

11.12 Kaplan-Meier survival plots

Kaplan-Meier survival plots were generated using the online KM plotter software (https://kmplot.com/analysis/index.php?p=service&cancer=breast) on 05-12-2021 (Győrffy, 2021). The software has built-in patient data for various gene expression profiles. *CETP* (gene ID: 206210_s_at) was selected as the gene of interest and Kaplan-Meier plots were generated in accordance with the absence or presence of the ER, PR and HER2 surface receptors.

11.13 Mice Xenograft study

This *in vivo* study was approved by the Wits Animal Ethics Screening Committee (AESC number: 2016/09/41/D). MDA-MB 231 cells were used for this xenograft study as tumours were formed more easily as opposed to MCF-7 cells in a previous xenograft study performed by a colleague. Unfortunately, due to various reasons, stable transfection was not successful. Therefore, for the mice study, transient transfection was performed. In the study, 8 mice were used (4 transfected and 4 non-transfected, however one mouse from each group had to be euthanised due to unforeseen complications) to compare tumour growth rate. Mice were acclimatised for a week before injection of BC cells and weights of each mice were recorded thrice a week. Transfected and non-transfected MDA-MB 231 cells (±5 million cells per mice) were pelleted at 1400 rpm for 8 min. in a 1.5 ml Eppendorf tube. The media was removed, and the cells were resuspended in 55 µl of PBS and 55 µl of complete media. The cells were then kept in a 37 ℃ heating block until injection into the mice. The cells were injected

subcutaneously in the left flank of each mouse. The mice were euthanised after 18 days from the time the tumour was detected. This was due to the fact that the tumour from the first mice grew very aggressively and it was starting to hamper the animal's well-being. Therefore, to keep parameters the same, all other tumours (untreated) were extracted after 18 days. The mice were euthanised using 0.2 µl of Eutha-naze (Bayer, Germany) with a 23 Gauge needle. Blood was extracted and thereafter, saline solution was used for perfusion before the organs were harvested. Organs included: heart, lungs, kidneys, liver, colon, stomach, brain, pancreas and spleen, which were snap frozen in liquid nitrogen or dry ice and stored in -80 ℃. The tumours' volumes were measured (length, width and depth) thrice a week and post extraction using a digital calliper. The weight of the tumours was also measured post tumour extraction. The tumours were cut into 3 equal parts to be stored in different medium for different downstream experiments; 1) RNA*later*™ (RNA stabilisation solution; ThermoFisher Scientific, USA), 2) 4% formaldehyde and 3) snap frozen in liquid nitrogen or dry ice.

11.14 Statistical analysis

The statistical analyses were performed using Microsoft Office Excel©. The experimental procedures were performed in triplicates and repeated at least 3 times for reproducibility. Furthermore, the statistical significance was calculated using student's t-test. A p-value of less than 0.05 was used to estimate the significance of the observations. A Z-factor (Zhang et al., 1999) was calculated for each 96-well plate and assays having Z-factor above > 0.5 were included in the statistical analysis as it is the acceptable range in which the technicality of the experiments was trustworthy.

12. Results

Cancer and cancer therapies have been extensively studied worldwide, despite this the heterogeneity of tumours, as well as resistance towards treatments, serve as the main reason for complications in treating cancer. Research on the link between cholesterol and cancer are slowly emerging, where cholesterol has been implicated in several processes in carcinogenesis (Cruz et al., 2013). However, targeting cholesterol as a form of anti-cancer therapy remains controversial. There are currently two approaches targeting cholesterol as a possible therapeutic strategy. The first being the use of cholesterol synthesis inhibitors, such as statins, to block the mevalonate pathway and in turn reducing the levels of cholesterol (Chae et al., 2015). The second approach looks at the cholesterol depleting agents, such as cyclodextrins (e.g. MβCD), plumbagin and its derivative, AP, in reducing excess cholesterol as opposed to blocking the synthesis. For this study, we focused more on the second approach of depleting excess cholesterol as a possible alternative anticancer therapy. In our preliminary data, we showed that cholesterol contributes to cancer survival and drug resistance, where the particular gene/protein: *CETP* has been proven to be a cell survival gene and can possibly be used as a drug resistance marker for BC (Esau et al., 2016). However, the molecular mechanisms underlying *CETP's* involvement in cancer are unknown. Therefore, we knocked down *CETP* in two BC cell lines; ER+ (MCF-7) and ER- (MDA-MB 231) prior to all downstream experiments.

12.1 CETP Knockdown

The successful knock-down of *CETP* was confirmed using three different techniques; western blotting, immunofluorescent staining, as well as qPCR to determine *CETP* mRNA expression pre and post *CETP* knock-down. All three methods showed successful decrease in *CETP* protein and mRNA expression in both MCF-7 and MDA-MB 231 cells (Fig 12.1 and 12.2). Densitometry from western blotting showed 51% and 35.4% decrease in CETP protein levels in MCF-7 and MDA-MB 231 cells respectively (Fig 12.2a and 12.2b). This was also confirmed in immunofluorescent staining showing 68.4% and 46.2% decrease in CETP protein expression in MCF-7 and MDA-MB 231 cells respectively post *CETP* knock-down (Fig 12.2e and 12.2f). CETP mRNA expression was also confirmed to be knocked down showing a significant 72.8% and 60.7% decrease in CETP levels in MCF-7 and MDA-MB 231 cells respectively (Fig 12.2e

and 12.2d). Once *CETP* knock-down was confirmed, we performed a cell count to compare cellular growth and proliferation before and after knock-down.

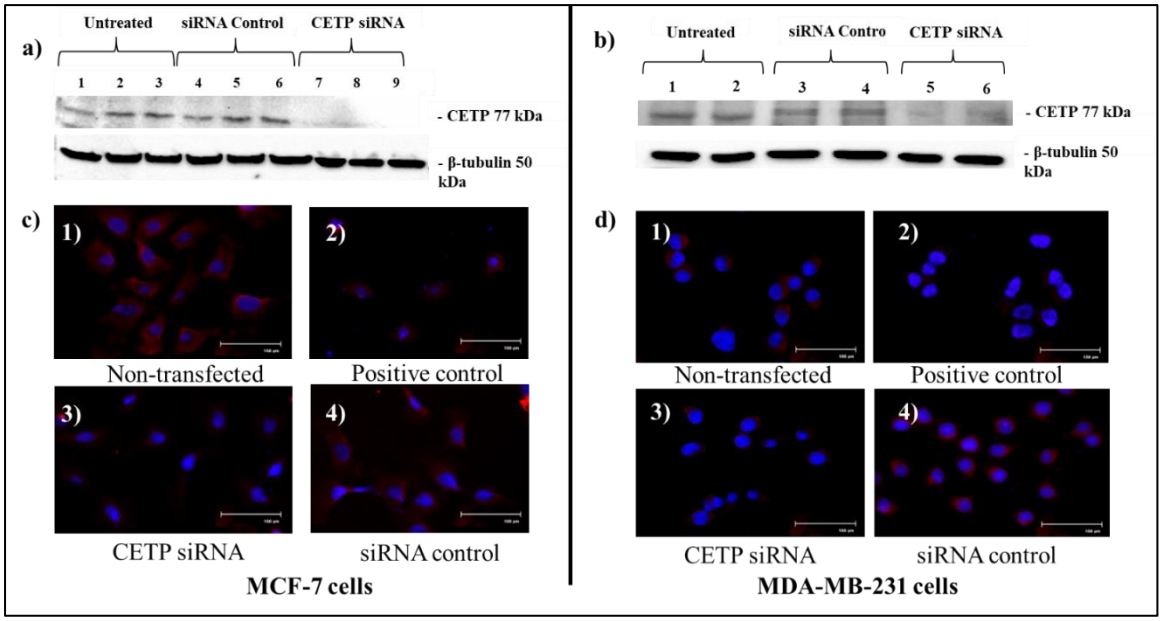

Figure 12.1: CETP knock-down was confirmed in both MCF-7 and MDA-MB 231 cells

CETP *knock-down was confirmed in both MCF-7 and MDA-MB 231 cells using western blotting and immunofluorescent staining. B-tubulin was used as the loading control and the blots showed equal bands indicating equal loading. The extent of knock-down was calculated using densitometry and ImageJ tools (calculations shown in next figure). Scale bar: 1 cm is 100 µm.*

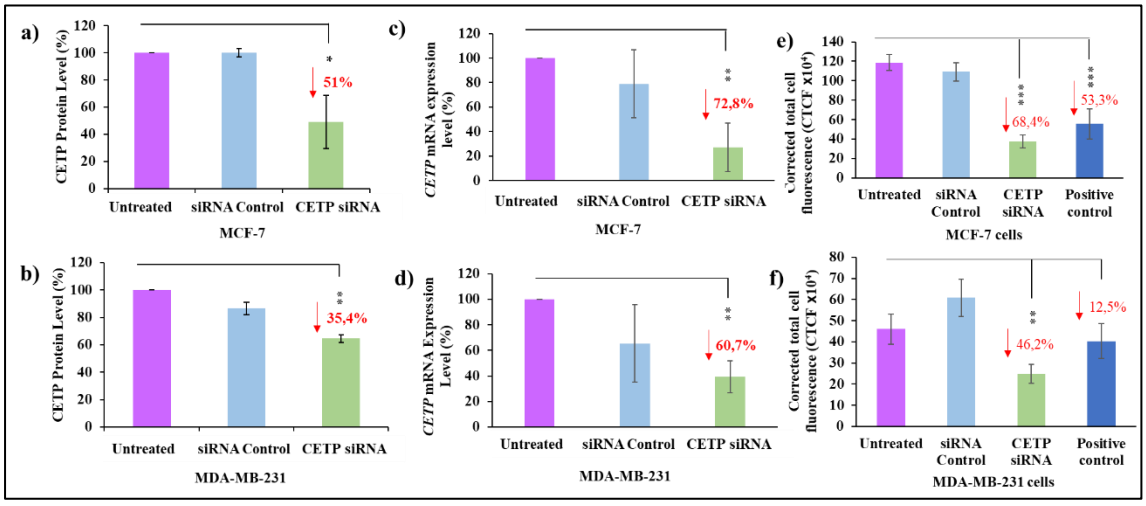

Figure 12.2: Confirmation of CETP protein and mRNA knock-down in MCF-7 and MDA-MB 231 BC cells

Knock-down of CETP *protein was confirmed using western blotting in both MCF-7 and MDA-MB 231 cells.* CETP *protein level was normalised against β-tubulin (loading control) and it was quantitively calculated relative to the untreated cells using densitometry analysis. There*

was a 51% CETP *protein knock-down in MCF-7 cells (a) and 35,4%* CETP *protein knock-down in MDA-MB 231 cells (b). CETP mRNA expression was also measured using RT-qPCR and upon CETP knock-down there was, on average, 72,8% reduction in CETP mRNA expression in MCF-7 cells (c) and 60,7% reduction in CETP mRNA expression levels in MDA-MB 231 cells (d). Relative CETP protein levels were detected with anti-*CETP *primary antibody and anti-rabbit, Texas red secondary antibodies. Upon CETP transfection (knock-down) there was a decrease in fluorescence intensity in both cell lines when CETP was knocked down compared to non-transfected cells. Analyses showed that there was an overall of 68.4% decrease and 46.2% decreased in* CETP *protein levels in MCF-7 and MDA-MB 231 cells respectively (e and f). Data represents mean ± standard deviation S.D. of raw data (n=3), where *p ≤ 0.05, **p ≤ 0.01 and ***p ≤ 0.001 significant difference to untreated control (ns being non-significant change), calculated using student's t-test.*

12.2 Cell growth post CETP knock-down

CETP's role in cardiovascular disease and atherosclerosis has been well explored however, the link between CETP and cancer is limited. Prof. Kaur's previous published work, in addition to the preliminary data gathered in my MSc degree has shown that *CETP* is implicated as a cell survival gene, where knocking down *CETP* resulted in an increase in cell death in MCF-7 cells when treated with an anticancer drug, TAM, even at lower concentrations. To confirm this, and to test the effect in MDA-MB 231 cells, a cell count was performed after 72 hours of transfection and from these results, it can be seen that proliferation was greatly reduced in both MCF-7 and MDA-MB 231 cells (68.2% and 51.3% respectively) (Fig 12.3). This could explain the reduced resistance in the absence of *CETP* and thus the increased cell death that was observed when cells were treated with TAM.

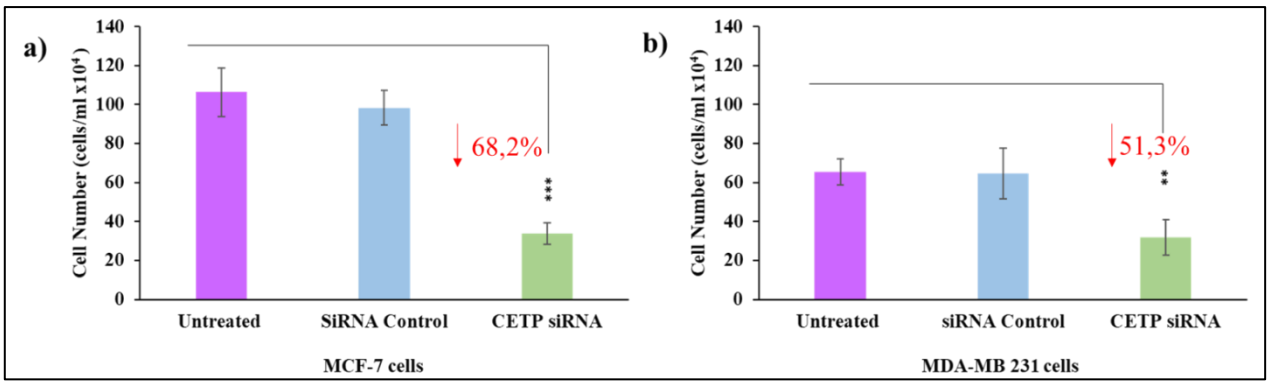

Figure 12.3: CETP knock-down reduced cell growth in MCF-7 and MDA-MD-231 cells using haemocytometer cell counting method

*CETP knock-down decreased cell proliferation by 68,2% in MCF-7 cells and 51,3% in MDA-MB 231 cells. Thereby confirming previous results, where CETP was identified as a cell survival gene. Data represents mean ± standard deviation S.D. of raw data (n=3), where *p ≤ 0.05, **p ≤ 0.01 and ***p ≤ 0.001 significant difference to untreated control (ns being non-significant change), calculated using student's t-test.*

It is known that CETP is involved in the shuttling of CEs and therefore, knocking down *CETP*, we would expect a decrease in cholesterol levels within the cells. Therefore, several cholesterol assays and staining assays were performed to confirm this (Fig 12.4 – 12.7).

12.3 Cholesterol levels post *CETP* knock-down

Several different cholesterol quantification assays were performed to confirm the effects of *CETP* knock-down on CE levels, lipid rafts and free cholesterol.

12.3.1 Cholesterol assay analysis

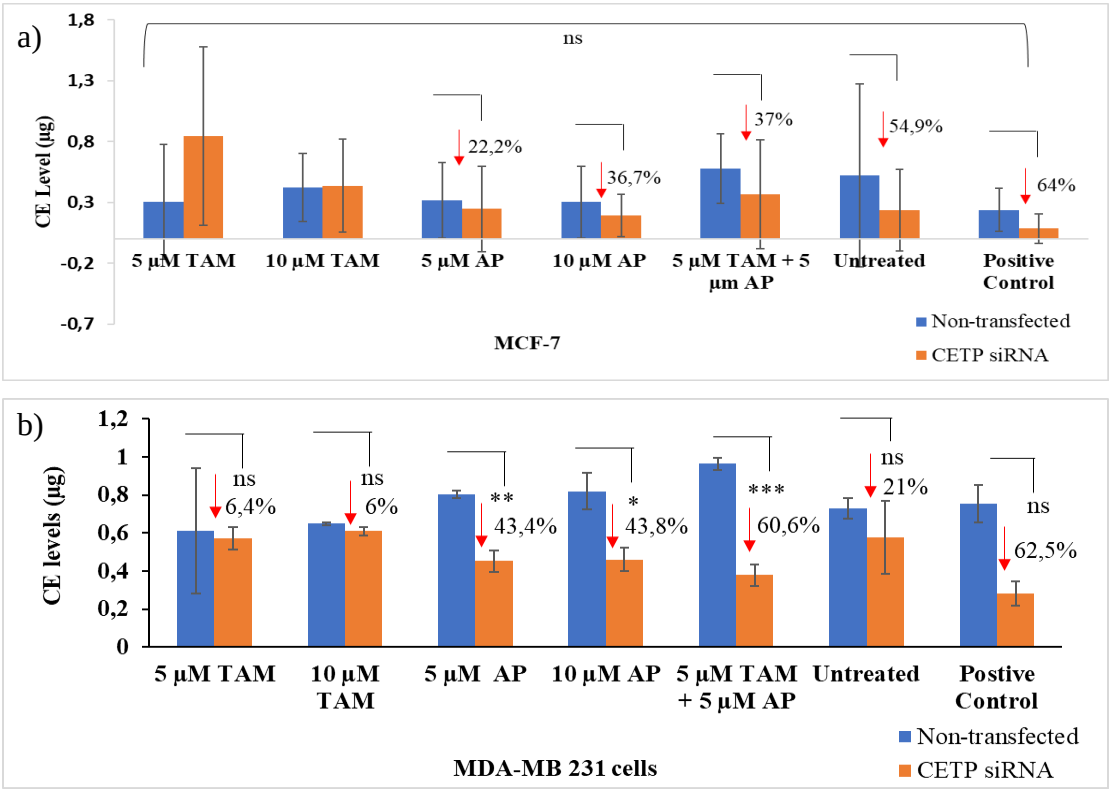

Figure 12.4: *CETP* knock-down results in a decrease in CE levels in MCF-7 and MDA-MB 231 cells

Overall, CETP knock-down resulted in a decrease in CE levels in both MCF-7 (except at 5 µM and 10 µM of TAM, which has not been found to have any cholesterol depleting properties) (a)

*and MDA-231 (b) cell lines. CETP knock-down alone, with no additional drug treatments, resulted in a 54.9% and 21% reduction in CE levels in MCF-7 and MDA-MB 231 cells respectively. CETP knock-down with 5 and 10 µM TAM treatment did not decrease CE levels but rather increased CE levels in MCF-7 cells (a) and non-significantly increased in MDA-MB 231 cells at both concentrations (6.4% and 6% respectively). Transfected cells treated with a cholesterol depleting agent; AP, caused a greater reduction in CE levels at 5 µM AP (22.2% in MCF-7 cells, 43.4% in MDA-MB 231 cells) and 10 µM AP (36.7% in MCF-7 cells, 43.8% in MDA-MB 231 cells). Transfected cells with the combination treatment of 5 µM TAM and 5 µM AP did not significantly change the reduction in CE levels in MCF-7 cells (37%). However, in MDA-MB 231 cells, knock-down of CETP with the combination treatment significantly reduced CE levels by 60.6%. Data represents mean ± standard deviation S.D. of raw data (n=3), where *p ≤ 0.05, **p ≤ 0.01 and ***p ≤ 0.001 significant difference to untreated control (ns being non-significant change), calculated using student's t-test.*

The cholesterol assay measured the intracellular CE levels in both BC cell lines, and an overall decrease was observed in CE levels within both MCF-7 and MDA-MB 231 cells, treated and untreated with TAM and AP. Specifically, in the untreated transfected cells, there was a 54.9% and 21% decrease in CE in MCF-7 and MDA-MB 231 cells respectively, post *CETP* knock-down (Fig 12.4). Interestingly, in the transfected MDA-MB 231 cells treated with 5 and 10 µM AP (known cholesterol depleter), there was a further 43.4% and 43.8% decrease in CE levels post CETP knock-down (Fig 12.4b). This was also observed in the BODIPY fluorescent staining, where transfected cells 56.8% and 76% decrease in CE levels in MCF-7 and MDA-MB 231 cells respectively (Fig 12.5). CE accumulation have been implicated in pancreatic and prostate cancer resistance and aggressiveness (Li et al., 2018; Yue et al., 2014). Therefore, this decrease in CE levels post *CETP* knock-down in both BC cell lines suggest that this is involved in the increased TAM efficacy in our preliminary results (Fig 9.7 - 9.9).

12.3.2 BODIPY staining analysis

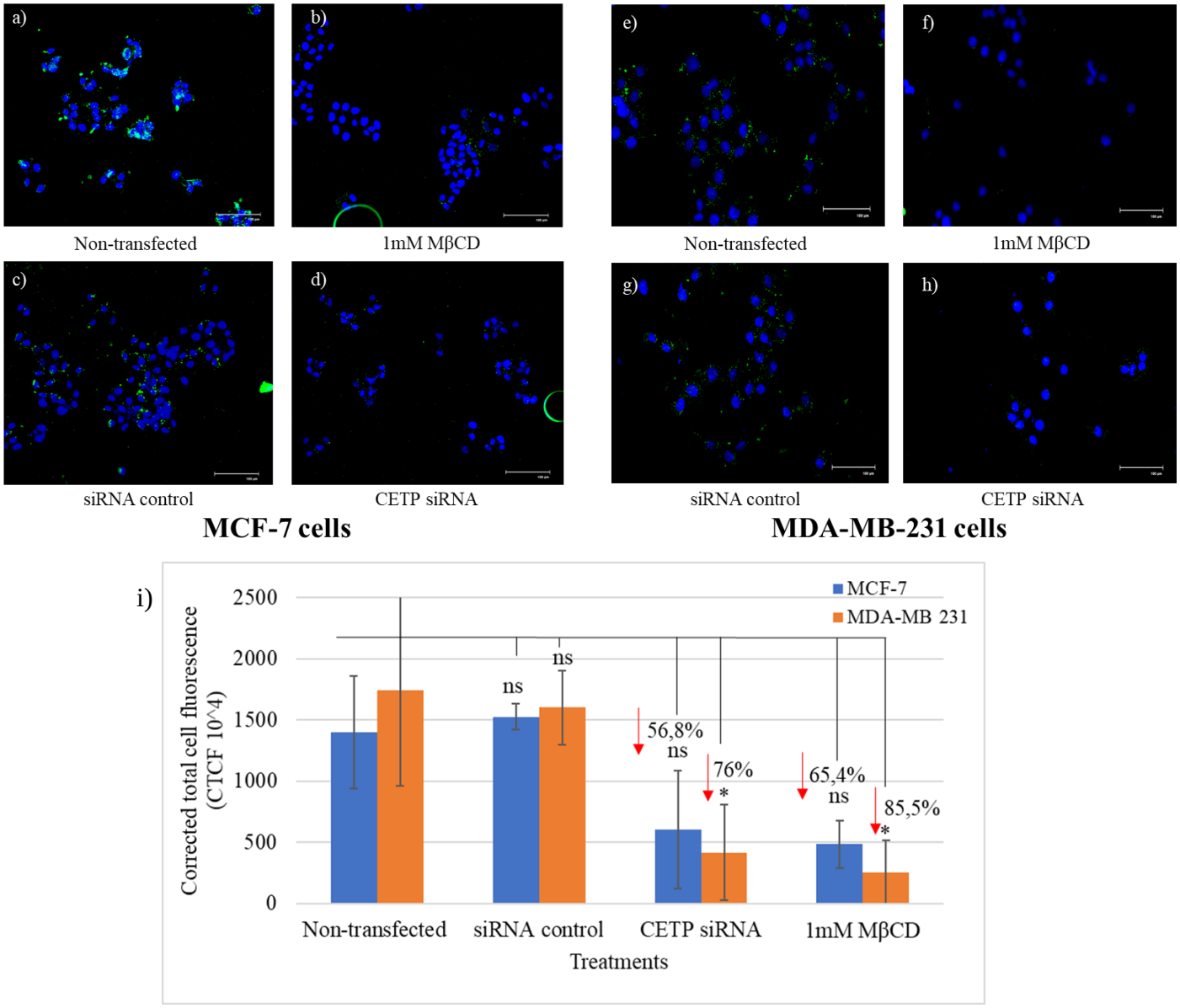

Figure 12.5: CE reduction was also confirmed in both MCF-7 and MDA-MB 231 cells using BODIPY staining

The reduction of CE levels was also confirmed through immunofluorescent staining using BODIPY. The immunofluorescent images (a-h) are representative images to visually observe the reduction in CE levels in both cell lines post CETP knock-down. In both MCF-7 and MDA-MB 231 cells, there was a 56.8% and 76% reduction in CE levels respectively (CEs shown as green fluorescent dots, while the nucleus was stained blue with DAPI). 1 mM MβCD was used as a positive control, which reduced CE levels by 65.4% and 85.5% in MCF-7 and MDA-MB 231 cells respectively (i). This decrease in CE levels was not observed in the siRNA control in both cell lines (i). Relative percentage decrease in fluorescence compared to the non-

transfected cells were analysed using ImageJ1 software. *Data represents mean ± standard deviation S.D. of raw data (n=5), where *p ≤ 0.05, **p ≤ 0.01 and ***p ≤ 0.001 significant difference to the non-transfected sample (ns being non-significant change), calculated using student's t-test. Scale bar: 1 cm is 100 µm.*

12.3.3 Filipin staining analysis

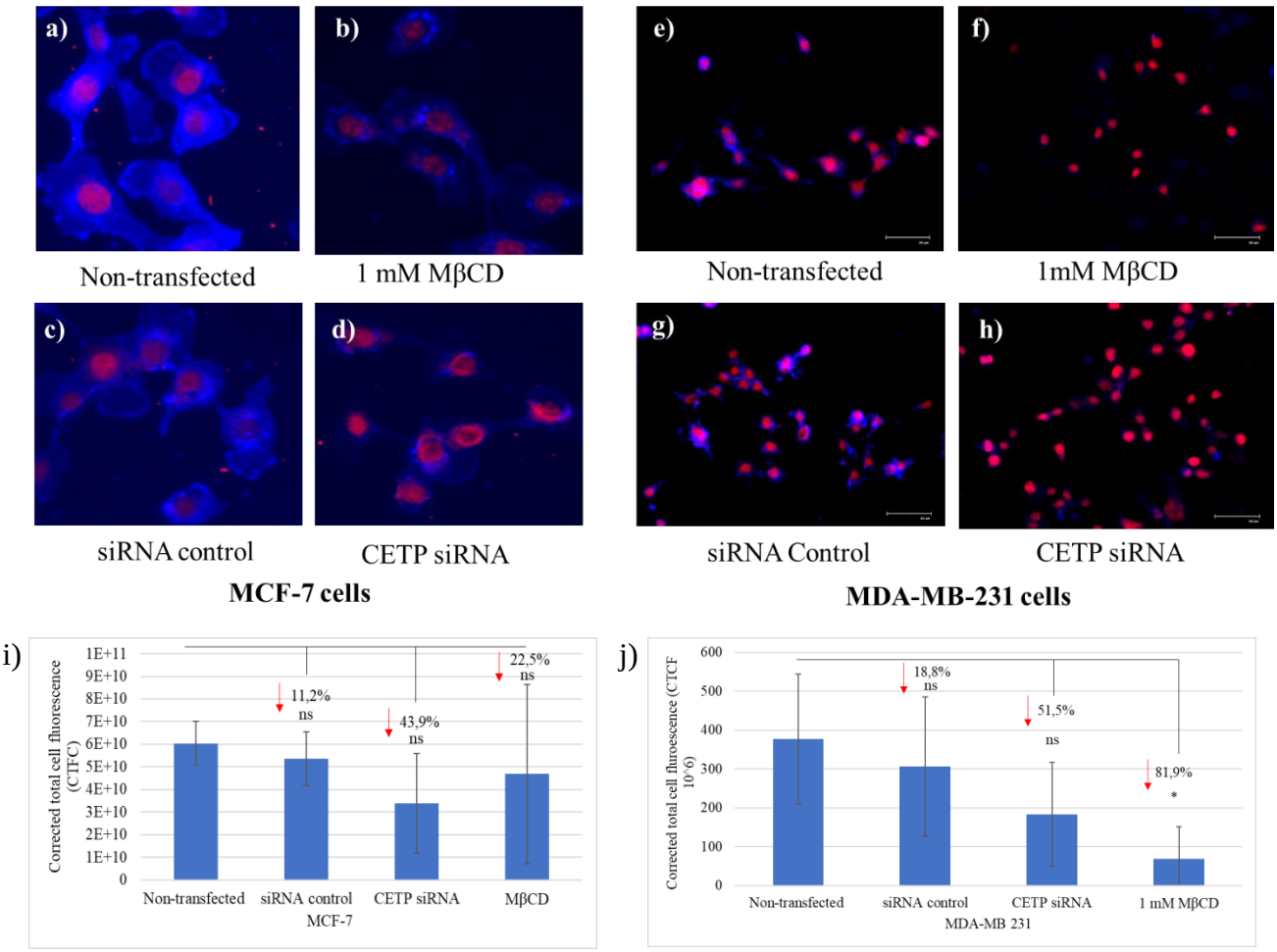

Figure 12.6: CETP knock-down resulted in a reduction in free cholesterol in both MCF-7 and MDA-MB 231 cells

Intracellular cholesterol was stained using Filipin in both cell lines pre and post CETP knock-down. From the figures above, it can be clearly observed that CETP knockdown reduces intracellular cholesterol level in MCF-7 cells (a-d) by 43.9% (i) and MDA-MB 231 cells (e-h) by 51.5% (j) as shown by the reduced blue fluorescent colour (nucleus was stained red with NucRed™ Dead 647). MβCD is a known cholesterol depletor and therefore it was used as the positive control with 22.5% and 81.9% decrease in intracellular cholesterol in MCF-7 and MDA-MB 231 cells respectively (b and f). Relative percentage decrease in fluorescence compared to the non-transfected cells were analysed using ImageJ1 software. *Data represents*

*mean ± standard deviation S.D. of raw data (n=5), where *p ≤ 0.05, **p ≤ 0.01 and ***p ≤ 0.001 significant difference to the non-transfected sample (ns being non-significant change), calculated using student's t-test. Scale bar: 1 cm is 100 µm.*

12.3.4 Lipid raft staining analysis

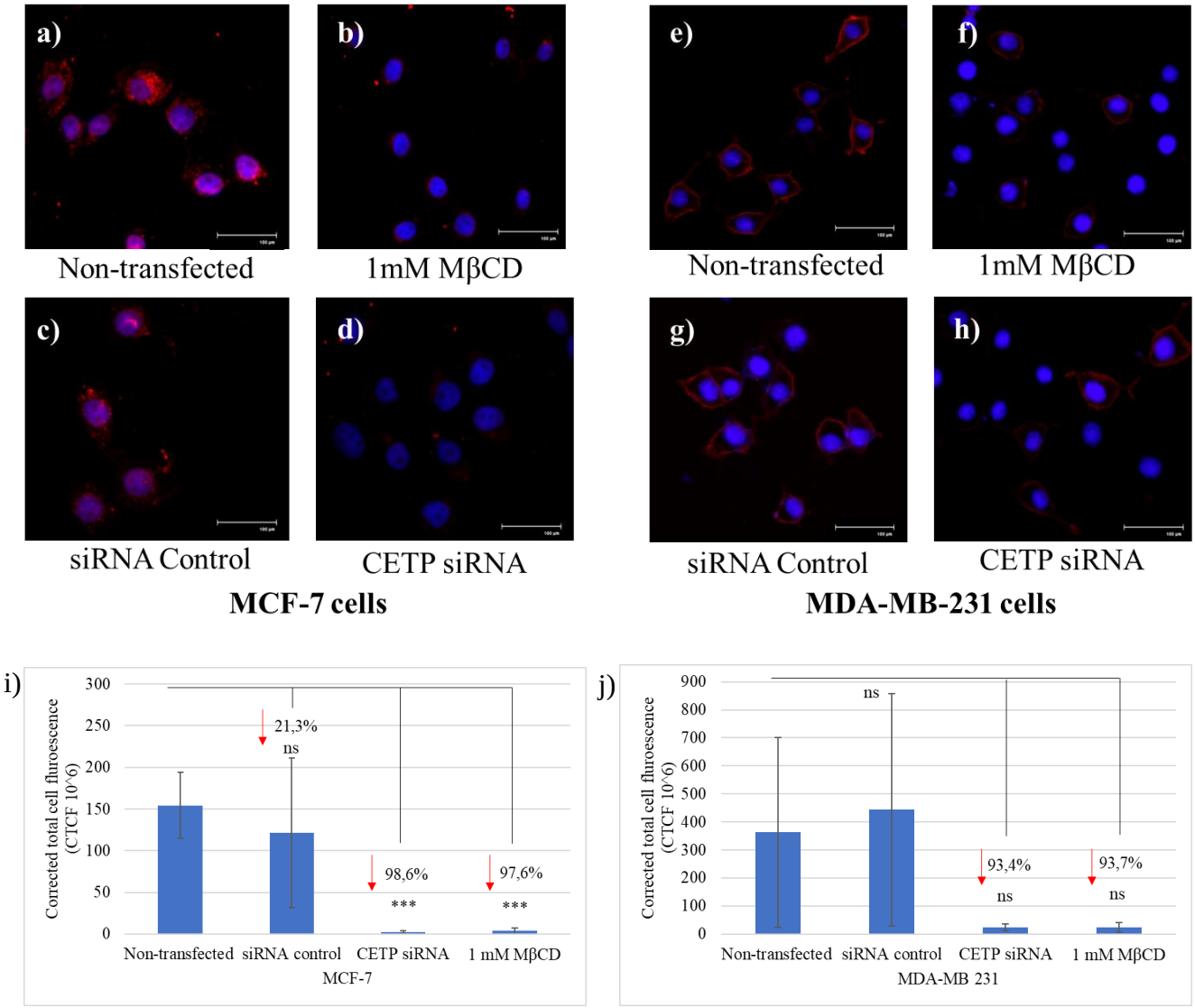

Figure 12.7: CETP knock-down decreases the lipid rafts in both MCF-7 and MDA-MB 231 cells

Lipid rafts were stained using the Vybrant™ Alexa Fluor™ 594 Lipid Raft Labelling kit. Upon staining, it was observed that lipid raft was indeed decreased post CETP knock-down in both cell lines, shown by the reduced red fluorescence (nucleus stained with DAPI) (a-h). In MCF-7 cells, there was a significant 98.6% decrease in lipid raft post CETP knock-down (i). Similar level of decrease in lipid raft was observed in the positive control (1 mM MβCD) in MCF-7 cells, 97.6%. While in the siRNA control, there was a 21.3% decrease in lipid raft levels (i). Similarly, in MDA-MB 231 cells, there was a 93.4% decrease in lipid raft post CETP knock-

down (j). Furthermore, there was a 93.7% decrease in lipid raft in the positive control MβCD, while there was no significant decrease in lipid raft in the siRNA control group (j). Relative percentage decrease in fluorescence compared to the non-transfected cells were analysed using ImageJ1 software. *Data represents mean ± standard deviation S.D. of raw data (n=5), where *p ≤ 0.05, **p ≤ 0.01 and ***p ≤ 0.001 significant difference to the non-transfected sample (ns being non-significant change), calculated using student's t-test. Scale bar: 1 cm is 100 µm.*

In normal cells, cholesterol homeostasis is a highly regulated process through cholesterol efflux via various membrane proteins or transporters (Liscovitch and Lavie, 2000). *CETP* knock-down resulted in a decrease in intracellular free cholesterol (Fig 12.6), as well as lipid rafts (Fig 12.7) in both MCF-7 and MDA-MB 231 cells. This could suggest that there was an increase in cholesterol efflux or a decrease or halting of the cholesterol synthesis process. This decrease in cholesterol level is an additional confirmation that cholesterol is attributed to drug resistance, as we've seen previously that post *CETP* knock-down, there was a reduction in cellular growth and proliferation, as well as an increased drug efficacy.

12.4 MOMP post *CETP* knock-down

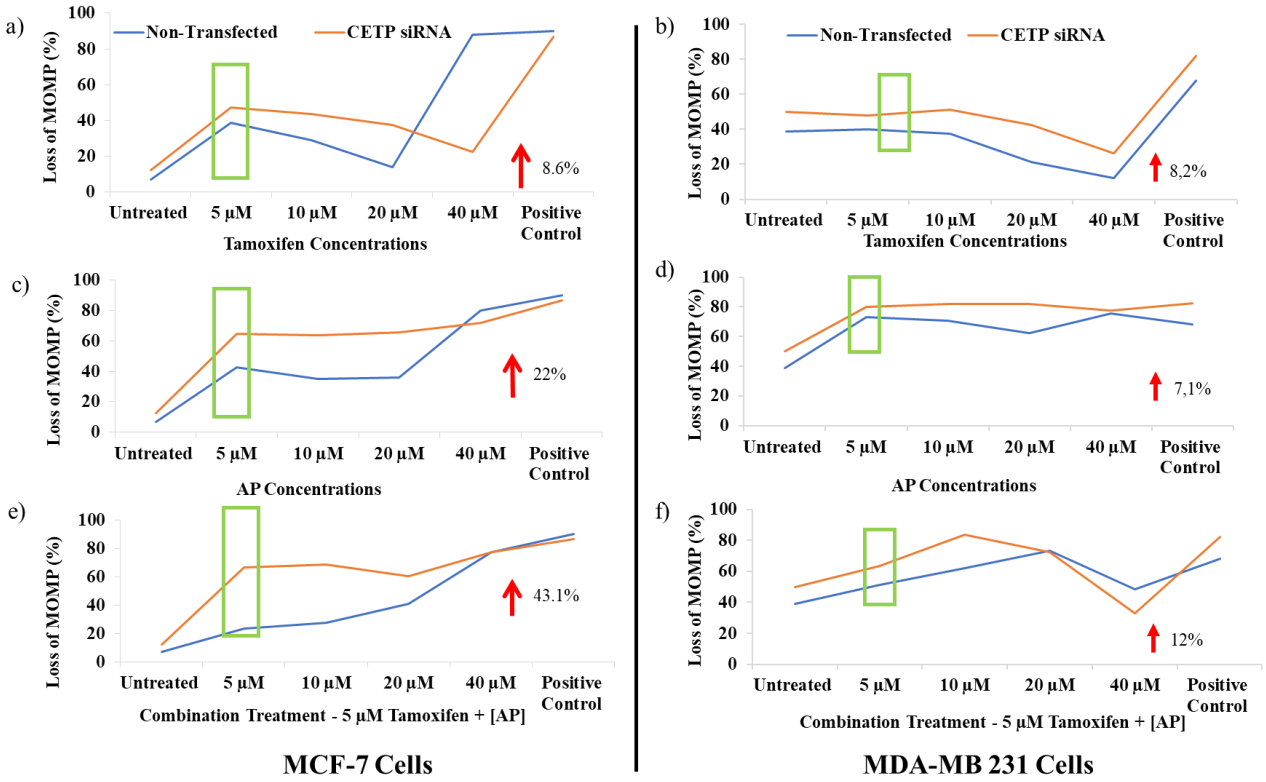

Figure 12.8: CETP knock-down with the combination treatment of TAM and AP increases intrinsic apoptosis in MCF-7 cells

CETP knock-down increased the loss of membrane potential in MCF-7 and MDA-MB 231 cells treated with various concentrations of TAM, AP and combination treatment of TAM and AP (a-f). However, this membrane loss was greater in MCF-7 cells; 8.6%, 22% and 43.1% at 5 µM TAM, 5 µM AP and combination of 5 µM TAM and 5 µM AP respectively (a,c and e). In MDA-MB 231 once cells, CETP knock-down increased the loss of membrane potential by 8.2%, 7.1% and 12% at 5 µM TAM, 5 µM AP and combination of 5 µM TAM and 5 µM AP respectively (b, d and f). 40 µM PL was used as positive control. [(Gu et al., 2019)]

We further looked at the effects of *CETP* knock-down on the mitochondrial outer membrane potential in both MCF-7 and MDA-MB 231 cells. Interestingly, in both cell lines there was an increase in loss of mitochondrial membrane potential post *CETP* knock-down at 5 µM TAM and AP treatment (Fig 12.8). Although, this was a minor increase when the drugs were used apart, when we combined the treatment of TAM and AP, the effect almost doubled in both cell lines. This is indicative that at least 43.1% and 12% of apoptosis (in MCF-7 and MDA-MB 231 cells respectively) was through the intrinsic pathway when treated with the combination treatment of TAM and AP post *CETP* knock-down. This, however, does not elucidate the

mechanism of CETP's role in BC resistance and therefore the lipoprotein signalling and cholesterol metabolism array, as well as the BC resistance array was performed in both cell lines post *CETP* knock-down.

12.5 Molecular mechanisms of CETP in the involvement of BC resistance

The strong link between *CETP* and cancer resistance therefore led us to measure the expression levels of several genes that are involved in the human BC resistance and lipoprotein signalling pathways post *CETP* knock-down to deduce the molecular basis of involvement of *CETP* in BC (Fig 12.9). Overall, there was a demarcated decrease in expression of majority of genes involved in the lipoprotein and cholesterol signalling pathways post *CETP* knock-down in MCF-7 cells, however little to no change was observed in transfected MDA-MB 231 cells (Fig 12.9). Furthermore, we observed a decrease in expression of several genes involved in BC drug resistance of which also included; proliferative transcription factors, growth factor receptors, hormone receptors, genes involved in drug metabolism, cell cycle and DNA damage and repair genes in transfected MCF-7 cells (Fig 12.9 and 12.10). However, the effects of *CETP* knock-down on expression of these genes were not as significant in MDA-MB 231 cells as compared to MCF-7 cells. These results could therefore share insight into some possible explanations to the involvement of CETP in cellular survival.

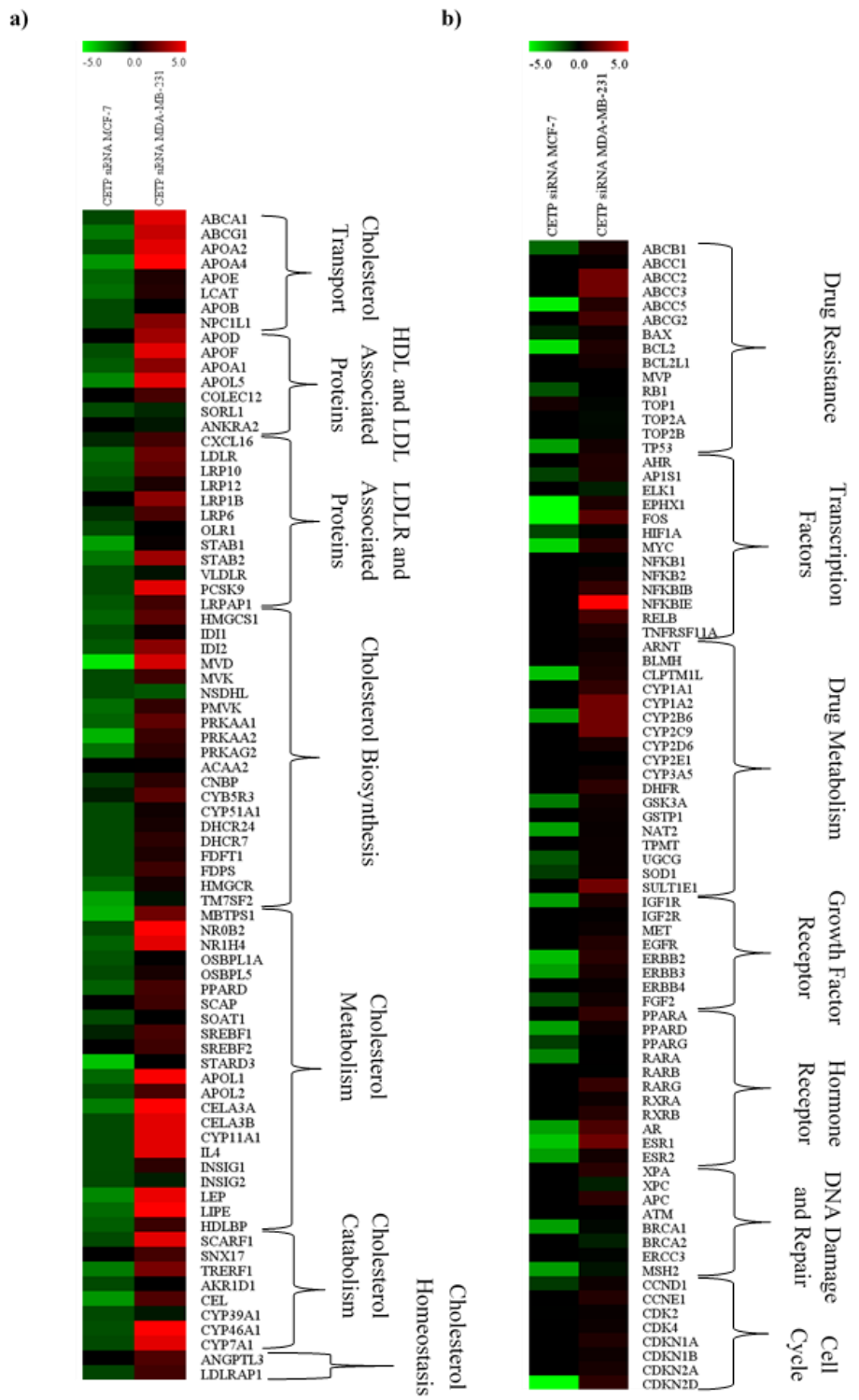

Figure 12.9: Heatmap representing the gene expression profiles in the lipoprotein signalling and cholesterol metabolism pathways and human BC resistance pathways in both cell lines post CETP knock-down

The above figure represents the expression of the 84 genes involved in a) the lipoprotein signalling and cholesterol metabolism pathways and b) human BC resistance pathways post CETP knock-down in MCF-7 and MDA-MB 231 cells. These genes were categorised according

to their functions. The various shades of green represent the level of decreased expression of a gene, where the brighter the colour, the more reduced the expression of a gene is relative to the non-transfected cells. In contrast, the red represents the increased level of gene expression compared to the non-transfected cells, where the brighter the red, the higher the level of increased expression. This is also shown on the gradient bar above the heat maps, where the colour spectrum is from -5 to 5 (negative values representing a decreased gene expression, while the positive represents an increased gene expression in log2 values and 0 representing no change post CETP knock-down). Log2 was used to normalise the data against 1 for easier interpretation. In general, CETP knock-down in MCF-7 cells decreased various genes involved in cholesterol metabolism, synthesis transport, as well as genes in drug resistance. While in MDA-MB 231 cells, opposite effects were observed or minimal change in gene profiles.

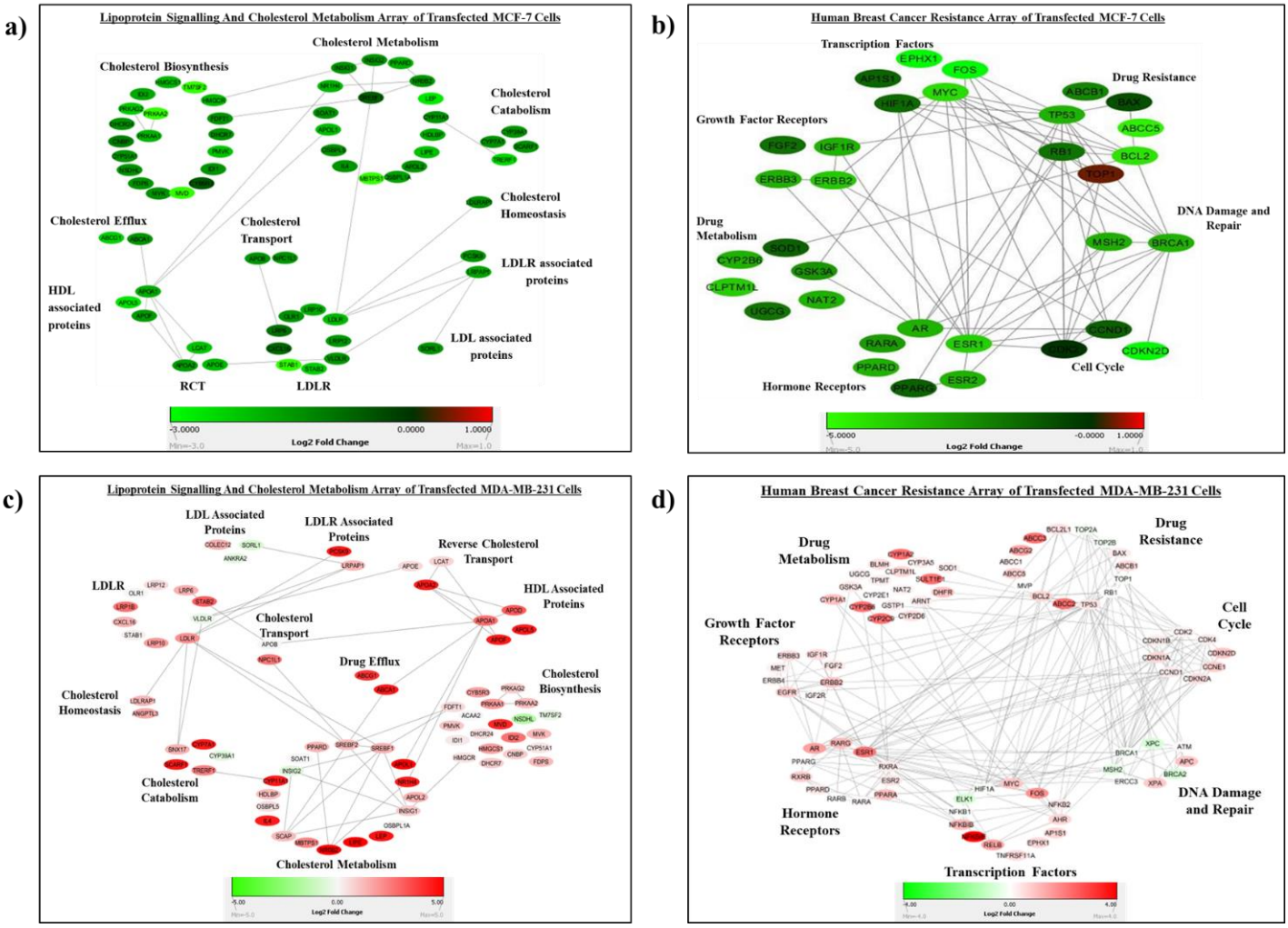

Figure 12.10: The effects of CETP knock-down on differentially expressed genes involved in lipoprotein signalling and cholesterol metabolism pathways and human BC resistance pathways in MCF-7 and MDA-MB 231 cells represented as a gene network map

CETP knock-down resulted in a decrease in several genes involved in the lipoprotein signalling and cholesterol metabolism pathway as well as human BC resistance pathways in MCF-7 cells (a and b respectively). Conversely, CETP knock-down increases or had a very low effect on genes involved in the two pathways in MDA-MB 231 cells (c and d). Gene networks were obtained from Omicsnet (https://www.omicsnet.ca/) and Cytoscape software was used to create the gene network map. Gene expression values were obtained from the RT² Profiler™ PCR array.

Table 12.1: Gene expression shifts (log2 fold changes) using RT² Profiler™ PCR arrays of human BC resistance and lipoprotein signalling and cholesterol metabolism between MCF-7 cells, MDA-MB 231 cells and GEPIA data (http://gepia.cancer-pku.cn/)

Lipoprotein Signalling and Cholesterol Metabolism (Log2 fold change)					Breast Cancer Resistance (Log2 fold change)				
Gene	MCF-7	MDA-MB-231	GEPIA	Pathway	Gene	MCF-7	MDA-MB-231	GEPIA	Pathway
ABCA1	-1,433175292	4,451629182	-0,544320516	Cholesterol Efflux	ABCB1	-2,052916876	0,545184666	-1,14684139	Drug resistance
ABCG1	-2,347081832	3,904178513	0,243925583		ABCC1	0	0,168876893	0,118644496	
APOA2	-1,570979948	4,451629182	0	Reverse Cholesterol Transport	ABCC2	0	2,220556113	-1	
APOA4	-2,936442229	6,058794534	0		ABCC3	0	2,220556113	-0,22948185	
APOE	-1,987562499	0,606822978	0,113956189		ABCC5	-4,707604281	0,711802677	0,256339753	
LCAT	-2,166116658	0,707982032	-0,540568381		ABCG2	0	1,334285098	-1,20163386	
APOB	-1,433175292	0	0	Cholesterol Transport	BAX	-0,70577198	0,272743973	0,215012891	
NPC1L1	-1,433175292	2,590734591	-0,584962501		BCL2	-4,370753019	0,61131729	-0,1740294	
APOD	0	3,150926604	-0,536753408	HDL Associated Proteins	BCL2L1	0	0,455472326	0,119298928	
APOF	-1,546947401	4,451629182	0		MVP	0	-0,002006724	0,164386818	
APOA1	-1,787973155	2,711555717	1		RB1	-1,589194844	-0,005460578	-0,06413034	
APOL5	-2,635066869	4,451629182	0		TOP1	0,427233144	-0,115426421	0,132450296	
COLEC12	0	1,405681813	-0,427421224	LDL Associated Proteins	TOP2A	0	-0,189005411	1,64385619	
SORL1	-1,433175292	-0,793428046	-0,187627003		TOP2B	0	-0,148164746	0,04580369	
ANKRA2	0	-0,44074345	-0,072149786		TP53	-3,126527399	0,407083776	0	
CXCL16	-0,780053842	1,304024978	-0,074000581	LDL Receptors	AHR	0	0,62938942	-0,32862275	Transcription Factors
LDLR	-1,986850288	2,070674715	-0,067114196		AP1S1	-1,267670258	0,625512399	0,234465254	
LRP10	-1,762856169	1,793822566	-0,04508789		ELK1	0	-0,608278168	0,134301092	
LRP12	-1,483365827	0,558517201	-0,263034406		EPHX1	-6,02848664	0,58301867	-0,06054154	
LRP1B	0	2,726091068	-2,807354922		FOS	-7,244380615	1,701340695	-0,5849625	
LRP6	-0,918385311	1,435730063	-0,30256277		HIF1A	-1,367087277	-0,093382052	0	
OLR1	-1,433175292	0	1,137503524		MYC	-4,178140336	0,892324949	-0,25457283	
STAB1	-3,129989799	0,182800824	-0,257797757		NFKB1	0	-0,064454055	-0,06140054	
STAB2	-2,296369753	3,080920847	-2,321928095		NFKB2	0	0,32291498	0,131244533	
VLDLR	-1,433175292	-0,335880691	-0,567040593		NFKBIB	0	1,029351161	0,2410081	
PCSK9	-1,433175292	4,451629182	1	LDL Receptors Associated Protein	NFKBIE	0	7,47301256	0,321928095	
LRPAP1	-1,693816567	1,290984027	0,044394119		RELB	0	1,377978312	0,285402219	
HMGCS1	-1,952081014	1,790290141	0,122856748	Cholesterol Biosynthesis	TNFRSF11A	0	0,519595003	-0,6520767	Drug Metabolism
IDI1	-1,433175292	0,280999388	0,085729874		ARNT	0	0,260102389	-0,0931094	
IDI2	-1,737045338	2,702022669	0		BLMH	0	0,486859591	0,097297201	
MVD	-4,516112136	4,165558139	0,144389909		CLPTM1L	-3,789107941	0,602693163	0,086156644	
MVK	-1,433175292	1,224762285	0,118644496		CYP1A1	0	0,977439431	0	
NSDHL	-1,433175292	-1,672121516	0,131244533		CYP1A2	0	2,220556113	0	
PMVK	-2,13731887	0,994716317	0,175849835		CYP2B6	-3,126527399	2,220556113	0	
PRKAA1	-1,947443777	1,871296082	-0,314873337		CYP2C9	0	2,220556113	0	
PRKAA2	-3,534753294	1,131886222	-0,106915204		CYP2D6	0	0,488367018	-0,22239242	
PRKAG2	-2,231818923	0,862372823	-0,140862536		CYP2E1	0	0,030954045	-0,4150375	
ACAA2	0	0,043735844	-0,199308808		CYP3A5	0	0,284883281	-1,13750352	
CNBP	-1,102086327	0,846513889	-0,05246742		DHFR	0	0,900724762	0,034765418	
CYB5R3	-0,565411658	1,703058477	-0,565411658		GSK3A	-2,423096408	0,329047345	0,149377624	
CYP51A1	-1,433175292	0,313845227	0,115477217		GSTP1	0	0,247585245	-0,20249286	
DHCR24	-1,433175292	0,456846941	0,176877762		NAT2	-3,126527399	0,179675446	0,584962501	
DHCR7	-1,433175292	0,876818209	0,236067358		TPMT	0	0,230070069	0,197939378	
FDFT1	-1,433175292	0,593407535	-0,043068722		UGCG	-1,673354337	0,198855895	0,176877762	
FDPS	-1,433175292	1,209653366	0,125530882		SOD1	-1,170619714	0,228415741	0,053111336	
HMGCR	-1,958775779	0,419486347	0,140862536		SULT1E1	0	2,220556113	0	
TM7SF2	-3,178371822	-0,332922061	-0,11783649		IGF1R	-3,126527399	0,519595576	0,065588342	Growth Factor Receptor
MBTPS1	-3,420060643	2,214311248	-0,074000581	Cholesterol Metabolism	IGF2R	0	0,089242793	-0,09114789	
NR0B2	-1,433175292	5,546654652	0		MET	0	0,222449984	-1	
NR1H4	-1,919682722	4,451629182	0		EGFR	0	0,678361199	-1,29278175	
OSBPL1A	-1,639536725	0,071264954	-0,292180751		ERBB2	-3,696091719	0,839802006	0,110182918	
OSBPL5	-1,433175292	0,481137732	0,070389328		ERBB3	-3,126527399	0,488145419	0,225881407	
PPARD	-1,881312773	1,343852563	0,072149786		ERBB4	0	0,163039567	-0,06413034	
SCAP	0	1,229987471	-0,028569152		FGF2	-1,543116572	0,337760919	-2,03952836	
SOAT1	-1,433175292	0,0030608	0,084888898		PPARA	0	0,965044533	-0,71989208	Hormone Receptor
SREBF1	-0,652631062	1,388511984	0,172467196		PPARD	-3,126527399	0,292156272	0,072149786	
SREBF2	0	1,225671131	0,027480736		PPARG	-1,209592302	0,021584208	-1,13750352	
STARD3	-3,833441385	0	0,055495113		RARA	-2,604103219	0,045874055	0,230297619	
APOL1	-2,025695671	4,928593529	0,087462841		RARB	0	-0,031185941	-0,78427131	
APOL2	-1,433175292	1,401073285	0,095157233		RARG	0	1,052914049	0	
CELA3A	-2,454647457	7,13444512	0		RXRA	0	0,291634312	-0,05889369	
CELA3B	-1,433175292	4,451629182	0		RXRB	0	0,743831125	-0,03037365	
CYP11A1	-1,433175292	4,451629182	-1,415037499		AR	-3,126527399	1,481209745	0,101879614	
IL4	-1,433175292	4,451629182	0		ESR1	-3,858369426	2,168329468	0,339486466	
INSIG1	-1,433175292	0,883717014	-0,030373649		ESR2	-3,126527399	0,381707989	-1,80735492	
INSIG2	-1,41572507	-0,589546348	-0,034765418		XPA	0	0,818805181	-0,14809864	DNA Damage and Repair
LEP	-2,676402212	4,638336686	-4,906890596		XPC	0	-0,618567966	-0,12553088	
LIPE	-2,084423774	5,067333354	-1,234465254		APC	0	0,893844989	-0,28010792	
HDLBP	-1,832498651	1,166283892	0,072149786		ATM	0	0,052003558	-0,23446525	
SCARF1	-1,433175292	4,451629182	-0,485426827	Cholesterol Catabolism	BRCA1	-3,126527399	-0,140556187	0,362570079	
SNX17	0	1,352136282	0,022720077		BRCA2	0	-0,615867524	0,765534746	
TRERF1	-2,417838675	2,388530262	0,452512205		ERCC3	0	-0,084739282	0	
AKR1D1	-1,433175292	0	0		MSH2	-3,093437061	-0,386479537	0,101879614	
CEL	-2,954624579	1,562817676	0,222392421		CCND1	-1,137134733	0,290377282	0,154328146	Cell Cycle
CYP39A1	-1,433175292	-0,451853386	-1,447458977		CCNE1	0	0,705065098	1	
CYP46A1	-1,561611801	5,047103738	-1,137503524		CDK2	-0,020075918	0,181557642	0,120294234	
CYP7A1	-1,433175292	4,451629182	0		CDK4	0	0,262028595	0,065095028	
ANGPTL3	0	1,561954051	0	Cholesterol Homeostasis	CDKN1A	0	0,618703514	-0,07400058	
LDLRAP1	-1,338459391	1,296678405	0,033947332		CDKN1B	0	0,280492416	0,026472211	
					CDKN2A	0	0,463976589	0,777607579	
					CDKN2D	-10,45693395	0,86565669	0,402098444	

The table above represents the log2 fold change of the gene expression profiles post CETP knock-down, as well as patient samples from GEPIA (gene expression profiles were generated from breast cancer patient vs normal patient samples from the The Cancer Genome Atlas

(TCGA) and the Genotype-tissue Expression (GTEx) projects). From the table above, the expression profiles in patient samples did not have a drastic difference in cancer patients as compared to normal patients. While CETP knock down showed a significant shift in gene expression profiles (especially in MCF-7 cells) as compared to the non-transfected cells. Log2 was used to normalise the data against 1 for easier interpretation.

The BC resistance RT² Profiler™ PCR array revealed that upon *CETP* knock-down, there was a reduction in gene expression of *ESR1* (ER) and the lipid signalling RT² Profiler™ PCR array showed a reduced expression of *LDLR* (3.7 and 2 log2 fold decrease respectively) in MCF-7 cells (Fig 12.9 and Table 12.1). ER is a hormone receptor known to initiate growth and cell proliferation when bound with its ligand; estrogen, thus resulting in the rapid proliferation of ER+ BC cells. Although MCF-7 cells are poorly invasive, it is becoming progressively more difficult to treat with the various available endocrine therapies due to drug resistance. Therefore, the decrease in ER and LDLR mRNA expression levels post *CETP* knock-down, in MCF-7 cells, suggests that the decreased proliferation (Fig 12.2a) could be a result of decreased ER. This is possibly due to the fact that extracellular cholesterol and estrogen (which are both involved in cancer proliferation and resistance) uptake are reduced through these receptors, consequently reducing cellular proliferation and in turn drug resistance. LDLR protein levels are tightly regulated by PCSK9. PCSK9, when bound to LDLR, initiates lysosomal degradation of LDLR thus reducing cholesterol uptake (Lagace, 2014). Knock-down of *CETP* in MCF-7 cells resulted in a decrease in *PCSK9* expression by 1.4 log2 folds (Table 12.1). This suggests that PCSK9 activity is possibly activated via surface LDLR and cholesterol levels. Studies have shown that by knocking-down *PCSK9* increases hepatic LDLR for an increased removal of circulating cholesterol to treat cholesterol-associated diseases, such as hypercholesterolemia (Frank-Kamenetsky et al., 2008; Lopez, 2008). Furthermore, it has also been found that *PCSK9* expression is directly proportional to sterol regulatory element binding transcription factor 2 (*SREBF2*) (Schulz et al., 2015) and CETP inhibitors have been found to downregulate *LDLR* and *PCSK9* expression levels through a decreased SREBF2 levels (Dong et al., 2014). Therefore, *CETP* knock-down reduces *PCSK9* expression in addition to a decline in *LDLR* resulted in a decrease in intracellular cholesterol level in MCF-7 cells (Fig 12.9) and could thus be a possible approach in reducing cholesterol levels in treating other cholesterol-related diseases. Perhaps, the decrease in *ER*, *LDLR* and *PCSK9*, in conjunction with several other gene expression fluctuations, may have sensitised ER+ cancer cells to various treatments. Conversely, in MDA-MB 231 cells the opposite was observed, where *CETP* knock-down

caused a surge in *ER*, *LDLR* and *PCSK9* (2, 2 and 4.5 log2 folds increase respectively) (Fig 12.9 and Table 12.1). Although these receptors are commonly known for their involvement in cell growth and proliferation, as well as an increase in intracellular cholesterol levels, an enhanced expression of these receptors in MDA-MB 231 cells is not necessarily ominous. This increase could signify that these previously non-targetable TNBC cells, due to the lack of surface receptors, are now expressing targetable receptors and thus possibly sensitised to various endocrine therapies, such as TAM (Fig 9.7 – 9.9). Although *CETP* knock-down resulted in an increase in LDLR in transfected MDA-MB 231 cells, there was a concurrent surge in *PCSK9*, which presumably is an attempt of cells to regulate intracellular cholesterol levels. However, as mentioned previously, *PCSK9* is regulated by *SREBF2* (Schulz et al., 2015) (which upon *CETP* knock-down showed an increased in expression in MDA-MB 231 cells) (Fig 12.9). This, therefore, is an additional explanation to the increased *PCSK9* and *LDLR* levels in MDA-MB 231 cells.

Apart from the reduced gene expression of some hormone receptors in MCF-7 cells post *CETP* knock-down, there was also a decrease in several growth factor receptor expressions such as; insulin-like growth factor 1 receptors (*IGF1R*), receptor tyrosine-protein kinase erbB (*ERBB2/ ERBB3*) and fibroblast growth factor receptors (FGFR) (Fig 12.9b). It is well known that these growth factor receptors are responsible for cellular proliferation, growth and repair (Babina and Turner, 2017; Stuhlmiller et al., 2015). Furthermore, it has been found that these genes are often upregulated in cancer cells, thus activating cell survival signalling pathways to overcome endocrine therapies (Fedele et al., 2012). Therefore, *CETP* knock-down in MCF-7 cells significantly reduces the expression of *IGF1R, ERBB2/ERBB3* and *FGFR* (by 3.1, 3.7, 3.1 and 1.5 log2 fold respectively) (Table 12.1) and possibly reprogramming cells for normal cellular proliferative rates thus mitigating endocrine resistance. Unfortunately, this was not observed in MDA-MB 231 cells post *CETP* knock-down thus reiterating the resistant nature of TNBC cells.

CETP knock-down revealed an overall decrease in expression levels of genes invovled in cholesterol transport, biosynthesis and metabolism in MCF-7 cells (Fig 12.10a). In contrast, a number of genes in these pathways were upregulated or unchanged upon *CETP* knock-down in MDA-MB 231 cells (Fig 12.10c), suggesting that *CETP* may trigger different pathways depending on intracellular environment. Upon *CETP* knock-down in MCF-7 cells, there was a decrease in expression levels of enzymes that are involved in the cholesterol biosynthesis mevalonate pathway including; mevalonate pyrophosphate decarboxylase (*MVD*), HMG-CoA

reductase (*HMGCR*) and mevalonate kinase (*MVK*) (Fig 12.10a). However in transfected MDA-MB 231 cells, there was a slight increase in expression levels of these genes possibly to conteract the loss of cholesterol levels from *CETP* knock-down. In addition, several other genes are also closely associated with the regulation/ signalling for cholesterol synthesis when cholesterol levels drop within cells. These included; *SREBF1* (that encodes for the protein SREBP), SCAP and insulin induced gene 1 (*INSIG1*). Intracellular cholesterol homeostasis is tightly regulated by the interactions of these proteins with one another. SREBP is located in the endoplasmic reticulum and upon cholesterol depletion, SCAP mediates the translocation of SREBPs from the endoplasmic reticulum to the golgi body, where it is proteolytically cleaved to signal for cholesterol synthesis in the nucleus (Sato, 2010). In a cholesterol-rich environment, the sterols cause SCAP to bind to INSIG thus inhibiting SREBP translocation/ activation thereby impeding the signal for sterol synthesis (Sato, 2010). In cancer, SREBP activity is increased for continuous cancer cell growth and proliferation, therefore an increasing number of studies have used the SCAP/SREBP interaction as a target for anticancer therapy (Cheng et al., 2018; DeBose-Boyd and Ye, 2018). We have found that *CETP* knock-down resulted in a decrease in expression levels of *SREBF1* and I*NSIG1* (by 0.7 and 1.4 log2 fold respectively) (Table 12.1) and no change in SCAP expression in MCF-7 cells (Table 12.1). The decreased *SREBF1* could suggest that SREBP protein translation would be decreased, therefore halting the signals for continuous proliferation. Interestingly, protein Kinase AMP-Activated Catalytic Subunit Alpha 2 (*PRKAA2*), an important enzyme in the adenosine monophosphate-activated protein kinase (AMPK) pathway that protects cells from metabolic stress and stops ATP consuming biosynthetic pathways e.g cholesterol synthesis through inhibition of *SREBF1* transcriptional activity (Khan and Frigo, 2017; Randrianarisoa et al., 2019), was downregulated (by 3.5 log2 fold) in MCF-7 cells post *CETP* knock-down (Fig 12.9a and Table 12.1). This is possibly due to the decrease in *MVD* and *HMGCR* expression thus the cells already have lowered cholesterol synthesis. In addition, this decrease would also result in excess energy depletion, as cells will be unable to restore the loss of ATP, thus sensitising MCF-7 cells to drug treatment. In contrast, *PRKAA2* was increased (by 1.1 log2 fold) in MDA-MB 231 cells upon *CETP* knock-down (Fig 12.10c and Table 12.1). This could be a counter action to inhibit *SREBF1* activity to limit cholesterol synthesis and possibly reducing cancer resistance.

Another important pathway that keeps cholesterol levels balanced is the RCT system. This process comprises of a network of proteins; including HDLs, LDLs, apolipoproteins, ABCA1

transporters, LCAT and CETP, that act together in transporting excess cholesterol from cells to the liver to be excreted (Trajkovska and Topuzovska, 2017). The accumulation of intracellular cholesterol signals for cholesterol efflux through ABCA1 transporter membrane proteins, where ApoA1 initiates cholesterol esterification via LCAT in HDLs to prevent re-entering of the cholesterol into peripheral cells (Cooke et al., 2018; Phillips, 2014). CETP then mediates the transfer of these CEs from HDL to LDLs for excretion by the liver. In cancer cells, these processes are deregulated thus leading to cholesterol dyshomeostasis. *CETP* knock-down in MCF-7 cells resulted in several HDL associated genes, such as *ApoA1* and *LCAT*, as well as ABC transporter genes to be downregulated (by 1.8, 2.2 and 1.4 log2 fold respectively) in response to the lack of cholesterol efflux (Fig 12.10a and Table 12.1). Conversely, in transfected MDA-MB 231 cells, these genes were upregulated (by 2.7, 0.7 and 4.4 log2 folds respectively) (Fig 12.10c and Table 12.1), therefore result in an increase in cholesterol efflux and consequently decrease in resistance. Furthermore, RCT can also be disrupted through the inactivation of CETP through a lipid transfer inhibitor protein known as ApoF (Morton et al., 2019; Shen et al., 2015). ApoF activity is elevated in cancer cells and thereby causing an inefficient excretion of excess cholesterol (Morton et al., 2019; Shen et al., 2015). *CETP* knock-down in MCF-7 cells, resulted in a decrease in ApoF expression (1.5 log2 fold decrease) and therefore cholesterol transport resumes as normal. In MDA-MB 231 cells however, expression level of *ApoF* was increased (4.5 log2 fold increase) (Table 12.1), this could suggest that *CETP* knock-down in MDA-MB 231 cells favours HDL mediated CE removal as opposed to HDL-LDL cholesterol removal (Shen et al., 2015).

In addition to these findings, *CETP* knock-down also resulted in several genes associated with BC drug resistance to be downregulated in MCF-7 cells compared to non-transfected cells (Fig 12.9b). The most pronounced gene expression changes were observed in ATP Binding Cassette Subfamily C Member 5 (*ABCC5*) and *BCl-2* and minor expression changes in ATP-binding cassette subfamily B member 1 (*ABCB1*), *BAX*, and tumour protein 53 (*TP53*) (Fig 12.9b and Table 12.1). These genes, are however, slightly increased in MDA-MB 231 cells after *CETP* knock-down. Resistance, or more specifically MDR, is a key barrier that is preventing the effectiveness and efficiency of chemotherapies. A significant portion of MDR in cancer cells is caused from upregulation of various drug efflux pumps that transport a myriad of chemotherapeutic drugs out of the cell (Bai et al., 2018). ABCC5 and ABCB1 are examples of these drug efflux pumps and utilise ATP to transport substances across the plasma membrane thus mediating MDR (Jansen et al., 2015). *CETP* knock-down drastically decreased the

expression of *ABCC5* (4.7 log2 fold decrease) and to a less extent, *ABCB1* (2 log2 fold decrease), in MCF-7 cells (Table 12.1). This decrease would result in a decline in extracellular transport of drugs and therefore providing a possible explanation to the increased cell death when treated with TAM and AP (Fig 9.8). However, in *CETP* knocked down MDA-MB 231 cells, there was a slight increase in *ABCC5* and *ABCB1*, with *ABCC2* and *ABCC3* having a more prominent increase in expression (2.2 log2 fold increase for both) (Fig 12.10d and Table 12.1). ABCC2 and ABCC3 are more commonly known for the excretion of bilirubin diglucuronides from the liver and gallbladder (van der Schoor et al., 2015). Apart from the glucuronides, ABCC2 and ABCC3 have also been observed to transport various chemotherapeutic molecules out of the cells as a toxic defence mechanism and thus expression levels have been found to be elevated in various tumours (van der Schoor et al., 2015). This rise in expression of these two genes after *CETP* knock-down in MDA-MB 231 cells suggest that TNBC cells have a more active defence mechanism and thus contributing to the resistant nature of these cells, hence TAM and AP treatments were less effective in MDA-MB 231 cells compared to MCF-7 cells (Fig 9.7-9.9).

Drug metabolism or detoxification is another decisive factor for poor clinical outcome that works closely with drug efflux pumps. This means that with the increased drug efflux, there would be a comparable amount of drug elimanation through the liver (Krishna Vadlapatla et al., 2013). While other drug metabolising enzymes (DME) are capable of activating certain drugs for therapeutic effects (Chang, 2012). Cytochrome P450 (CYP) enzymes, for example, are capable of either inactivating drugs or activating pro-drugs and it is involved in the detoxification process (Krishna Vadlapatla et al., 2013; Singh et al., 2011). TAM is a pro-drug metabolised by various CYP enzymes, such as CYP3A5 and CYP2D6, into its active form thus carrying out its functions (Singh et al., 2011). These genes are, however, neither increased nor decreased after *CETP* knock-down in MCF-7 cells, while slightly increased in MDA-MB 231 cells post *CETP* knock-down with various other CYP enzymes (Fig 12.9b and Table 12.1). As mentioned previously TNBC cells lack hormone receptors and thus endocrine therapies are ineffective in causing apoptosis in MDA-MB 231 cells, however, upon *CETP* knock-down we observed an increase in ER in MDA-MB 231 cells. Therefore, in conjunction with this increase with an increase in CYP genes could explain the improvement of TAM efficacy in TNBC cells (Fig 9.7-9.9).

Another crucial factor that devotes to cancer drug resistance is the evasion of apoptosis. Apoptosis is a well-known, and by far the most studied, process that initiates cell death of

damaged cells thus preventing cancer progression. However, cancer cells circumvent apoptosis and acquire uncontrolled proliferation, sustained angiogenesis, metastasis to neighbouring organs (Hanahan and Weinberg, 2000), suppression of pro-apoptotic genes in support of tumorigenesis (Su et al., 2015) and thus resulting in eventual organ failure. Anti-apoptotic and pro-apoptotic genes belonging to the BCl-2 family were affected differently after *CETP* knock-down in both cell lines (Fig 12.9b), these included; *BCl-2* and *BAX* respectively. BCl-2 is associated with the inhibition of apoptosis (anti-apoptosis) and is often upregulated in resistant BC cells, more specifically TNBC cells, to counteract the activities of BAX, which is a promoter of apoptosis in response to cell stress or DNA damage (Pearce et al., 2019). For this reason, several studies have looked at BCl-2 inhibitors or *BAX* overexpression/mimics as a possible therapeutic strategy in treating cancer (Bozgeyik, 2019; Li et al., 2019; Luo et al., 2019). *CETP* knock-down lowered the expression of *BCl-2* (4 log2 fold decrease) and to a lesser extent *BAX* expression levels (0.7 log2 fold decrease) in MCF-7 cells (Table 12.1). This suggests that *CETP* knock-down mitigates MCF-7 resistance by causing a downregulation in *BCl-2*, while *BAX* remains relatively unchanged. In contrast, *BCl-2* and *BAX* were elevated in transfected MDA-MB 231 cells compared to the non-transfected cells (0.61 and 0.27 log2 fold increase) (Fig 12.9b and Table 12.1). This increase in *BCl-2* expression is possibly a compensatory mechanism in response to the increase in *BAX* expression in attempt to evade apoptosis. A closely related gene to *BAX* is *TP53*. *TP53* is a commonly known proto-oncogene that is often mutated in cancer cells as it functions as a tumour suppressor by tightly regulating the cell cycle checkpoint (Humpton and Vousden, 2019). In addition, *TP53* has been found to directly activate the transcription of BAX, under normal conditions to nullify the activities of BCl-2 and thus preventing unrestrained cell proliferation (Hemann and Lowe, 2006). Although *TP53* is downregulated in MCF-7 cells upon *CETP* knock-down (3.1 log2 fold decrease), *BCl-2* is significantly less compared to the non-transfected MCF-7 cells (4.4 log2 fold decrease) (Table 12.1), which could suggest an alternative route in which BCl-2 is being inhibited. On the contrary, no significant change in *TP53* was observed in MDA-MB 231 cells after *CETP* knock-down. In contrast, the extrinsic apoptotic pathway is initiated through a family of death receptors, TNFRs that activate downstream caspases to initiate apoptosis (Green and Kroemer, 1998). However, it has also been found that TNFR is also involved in pro-inflammatory pathway by regulating the activity of NF-κB to suppress apoptosis thereby conferring to drug resistance (Bharti and Aggarwal, 2002; Nair et al., 2014). *CETP* knock-down did not affect the expression of NF-κB in both cell lines, therefore *CETP* knock-down neither increased or decreased drug resistance though NF-κB (Fig 12.9b). Interestingly, there was a drastic increase

in the *nuclear factor of kappa light polypeptide gene enhancer in B-cells inhibitor, epsilon* (*NFKBIE*) in MCF-7 cells post *CETP* knock-down by 7.45 log2 fold (Table 12.1). This indicates that there might have been an increased inhibition of NF-κB protein post *CETP* knock-down in MCF7 cells. This was however, not observed in MDA-MB 231 cells.

Cancer cells are able to reprogramme their metabolic pathways to sustain or promote cell proliferation, growth and survival. The Warburg effect is an example of how cancer cells adapt in hypoxic conditions to maintain proliferation through HIF1α (Bubici and Papa, 2019; Hanahan and Weinberg, 2011). Therefore, *HIF1α* expression would be expected to be elevated in cancer cells. Interestingly, in the RT² Profiler™ PCR array, we observed a reduction in *HIF1α* expression (1.4 log2 fold decrease) in MCF-7 cells after *CETP* knock-down (Fig 12.9b and Table 12.1) and thus halting anaerobic glycolysis thereby inhibiting cancer cell growth. Consequently, this reduced the resistance of the cells towards anaerobic conditions and hence increased cell death in transfected MCF-7 cells compared to non-transfected cells (Fig 9.7 – 9.9). However, no change in *HIF1α* expression was observed in transfected MDA-MB 231 cells compared to the non-transfected cells (Fig 12.9). It is known that *HIF1α* is closely associated with *Myc* in cancer cells. *Myc* is a proto-oncogene/transcription factor that, under normal conditions, maintains normal cellular growth and proliferation (Hydbring and Larsson, 2010). However, Myc has high oncogenic potential and is often dysregulated or overexpressed in cancer cells (Doe et al., 2012; Levens, 2013). Furthermore, this increased *Myc* expression has been found to exaggerate the expression of *HIF1α* and in turn escalates energy production for increased cancer cell proliferation (Doe et al., 2012). Therefore, it is safe to say that *CETP* knock-down in MCF-7 cells decreases the expression of *HIF1α* and further causes an immense drop in *Myc* expression (4.2 log2 fold decrease) (Table 12.1), which would result in a reduction in cancer cell proliferation (Esau et al., 2016). However, again, there was no drastic change in expression levels of these two genes upon *CETP* knock-down in MDA-MB 231 cells (Table 12.1).

Many chemotherapeutic drugs that are developed generally target DNA in causing unrepairable damage or by disrupting the DNA repair mechanisms to induce cancer cell death (Bouwman and Jonkers, 2012). A well known gene that is involved in DNA repair and maintaining genomic integrity by regulating cell cycle checkpoints is the BC type 1/2 susceptibility protein encoded by BRCA1/2 (O'Donovan and Livingston, 2010). However, *BRCA1/2* gene is highly prone to mutations and thus increasing the risk of BC , and other cancers, development in women up to 85% (Konishi et al., 2011). Upon *CETP* knock-down, we observed a 3.1 log2

fold and 0.1 log2 fold decrease in *BRCA1* gene expression in MCF-7 cells and MDA-MB 231 cells respectively, with a further 0.6 log2 fold decrease in *BRCA2* gene in MDA-MB 231 cells (Table12.1). This suggest that *CETP* knock-down possibly reduces DNA repair through a decline in *BRCA1/2* activity in both cell lines and in turn reduces drug resistance.

12.6 Patient survival outcomes based on their *CETP* expression

Kaplan-Meier survival plots were then generated to compare our results to patient survival outcomes depending on their *CETP* expression. Based on the survival plots, high *CETP* expression decreases patient survival outcome in different BC types. In 'luminal A' BC patients (ER+, PR+, HER2-) exhibiting high *CETP* levels, the probability of survival of up to 150 months is dropped to 60% as compared to 70% for patients exhibiting low *CETP* levels. While 'luminal A' patients with low *CETP* expression is anticipated to survive up to 111 months (Fig 12.11a). Interestingly, overexpression of *CETP* in 'luminal B' BC patients' (ER+, PR+, HER2+) showed a better survival outcome (up to 80 months) as compared to patients with low levels of *CETP* (Fig 12.11b). However, probability of survival after 80 months is drastically decreased to approximately 30%, while patients with low levels of *CETP* expression show 60% survival probability of up to 200 months (Fig 12.11b). Similarly, basal-like patients (TNBC) with lower levels of *CETP* expression have a better probability of survival up to 200 months (about 70%) compared to patients with high *CETP* expression (probability of survival up to about 75 months is reduced to roughly 50%) (Fig 12.11c). Additionally, these patients are expected to live up to 11 months longer than patients with higher levels of *CETP* (Fig 12.11c). This is extremely significant as TNBC is, undoubtedly, the most difficult to treat and by reducing *CETP* levels it appears to repress the resistance of TNBC. Consequently, increasing the efficacy of drug treatments, which is what we have observed (Fig 9.7-9.9). Lastly, under-expressed *CETP* is also beneficial to HER2+ BC patients, whereby survival probability is increased by 18 months compared to patients with high *CETP* expression (Fig 12.11d). HER2+ BC patients, expressing lower levels of *CETP*, have a 10% higher survival probability of up to 50 months as compared to HER2+ BC patients expressing higher levels of *CETP* (Fig 12.11d). Evidently, *CETP* plays a crucial role in patient survival outcome and can possibly be used as a BC resistance marker in predicting treatment effectiveness. This confirms our previous results, as well as Prof. Kaur's previously published work, whereby *CETP* knock-down decreased cell proliferation and lowered drug resistance, thereby reiterating that *CETP* is a cell survival gene.

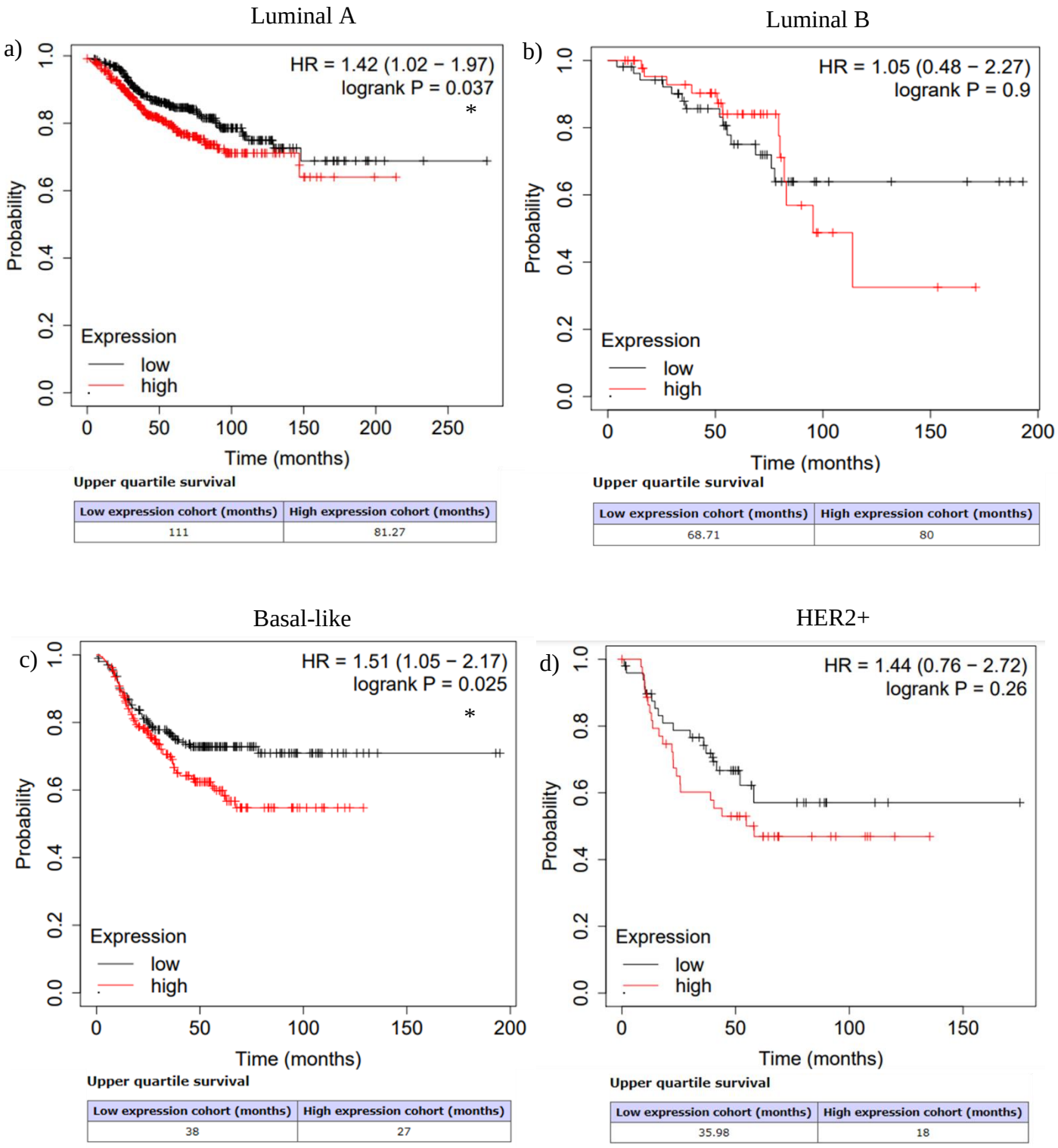

Figure 12.11: The effects of CETP expression profiles on cancer patient survival outcome in different BC types

Survival plots were generated using the online Kaplan-Meier Plotter (Győrffy et al., 2010) (https://kmplot.com/analysis/index.php?p=service&cancer=breast). An overall reduction in

*patient survival was observed, across all types of BC, when CETP is overexpressed (represented as red lines). In ER+ BC subtype 'luminal A', CETP overexpression reduces survival by 29 months (a). In 'luminal B' BC subtype, the probability of a patient with high CETP expression surviving over 100 months is roughly 30%, whereas the probability (y-axis) of a patient with low CETP expression (represented by the black lines) has over 60% chance of surviving up to 200 months (x-axis) (b). In addition, on average, 'luminal B' patients expressing lower levels of CETP survive up to 57.3 months as opposed to 36.99 months for patients expressing higher levels of CETP (d). An overexpression of CETP in TNBC (basal-like) and HER2+ BC subtype reduced survival by 11 and 18 months respectively (c and d). The logrank probability score is used to test whether survival distribution between two groups (that occurred at any given time) are different or significant (while a student's t-test assumes normal distribution of data with same variance) (Bland and Altman, 2004). Similar to the student's t-test, the smaller the p value, the more significant the data is, where *$p \leq 0.05$, **$p \leq 0.01$ and ***$p \leq 0.001$ significant. Although the logrank probability calculates the significance between two groups, it does not consider the odds of patient survivability. The hazard ratio (HR) calculates the relative risk or odds of patients' probability of survival up to a certain time period (Spruance et al., 2004). HR value of one means that there was no difference between the two groups at a specific time point, while a value of above one means that survivability in one group is better than the other (as shown here where patients with low CETP expression had an overall better survival outcome compared to patients expressing high levels of CETP).*

12.7 *In vivo* xenograft study

We additionally looked at the rate of tumour growth pre and post *CETP* knock-down in a mice xenograft study, where 4 mice were injected with non-transfected MDA-MB 231 cells and 4 mice injected with *CETP* knocked down cells (transiently transfected for 72 hrs). MDA-MB 231 cells were used as these cells are TNBC cells. They are highly aggressive and do not require estrogen for growth, whereas MCF-7 cells would require estrogen pellets to support tumour development as nude mice express very low amounts of estrogen. Unfortunately, one mouse from each group (transfected and non-transfected) had to be euthanized due to complications (rectal prolapse and haemorrhagic gastro-entiritis). From the *in vivo* study, we observed an average of 86.45% decrease in tumour growth rate in *CETP* knocked down MDA-MB 231 cells compared to the non-transfected cells (Fig 12.12). Although transient transfection/ knock-down is not typically used in mice xenograft studies, as it does not last long enough in the cells

and tumours usually take about 2 to 3 weeks to develop. However, we were able to observe a clear reduction in tumour growth, especially at week 2 (Fig 12.13). The tumour size grew exponentially from week two in mice that were injected with non-transfected cells, while the tumours in mice injected with the transfected cells had a steady growth for 3 weeks (Fig 12.13). These data correlates to what was previously found where tumours treated with AP for 21 days showed a 35% reduction in *CETP* mRNA level and reduced tumour growth in mice injected with MCF-7 cells (Esau et al., 2016). There were no signs of metastasis observed post-mortem and therefore remained in stage 0, where it was benign but aggressive in growth. There was also a steady increase in mice body weight, even after injecting the mice with the cells and therefore, it did not affect the mice's diet or visible behavioural changes (Fig 12.14). Mouse number 14 did show a decrease in body weight around week 10, however that could be due to human error whilst weighing the mouse (Fig 12.14). This *in vivo* pilot study successfully confirms using MDA-MB 231 cells that *CETP* is a cell survival gene, and its expression levels can be used to determine the level of cancer resistance as well as possible chemotherapeutic outcome.

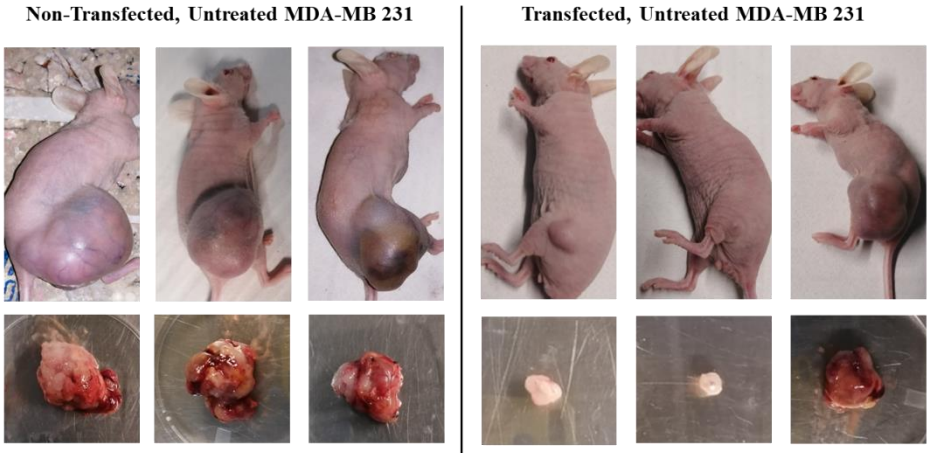

Mice ID	2	3	14	6	15	16
Tumour weight (g)	8,41	7,76	4,41	0,19	0,02	4,00
Tumour size (mm^3)	8532,34	7109,53	3086,70	140	18,73	2378,56
Average tumour size (mm^3)		6242,86			845,76	
% Decrease in tumour size			86,45%			

Figure 12.12: Non-transfected and *CETP* transfected tumours extracted from mice

Transfected and non-transfected MDA-MB 231 cells (±5 million cells) were injected subcutaneously into the left or right flank. The mice were euthanised on day 18 as the first

tumour that developed was very aggressive and was highly impacting the wellness of the animal and therefore to keep the parameters the same as much as possible, all mice (whether transfected or non-transfected) were terminated on day 18. From the images, we can clearly see that on average, tumours grew much slower when CETP expression is low compared to the non-transfected cells; 845.76 mm^3 and 6242.86 mm^3 respectively, which is a significant 86.45% reduction in tumour growth.

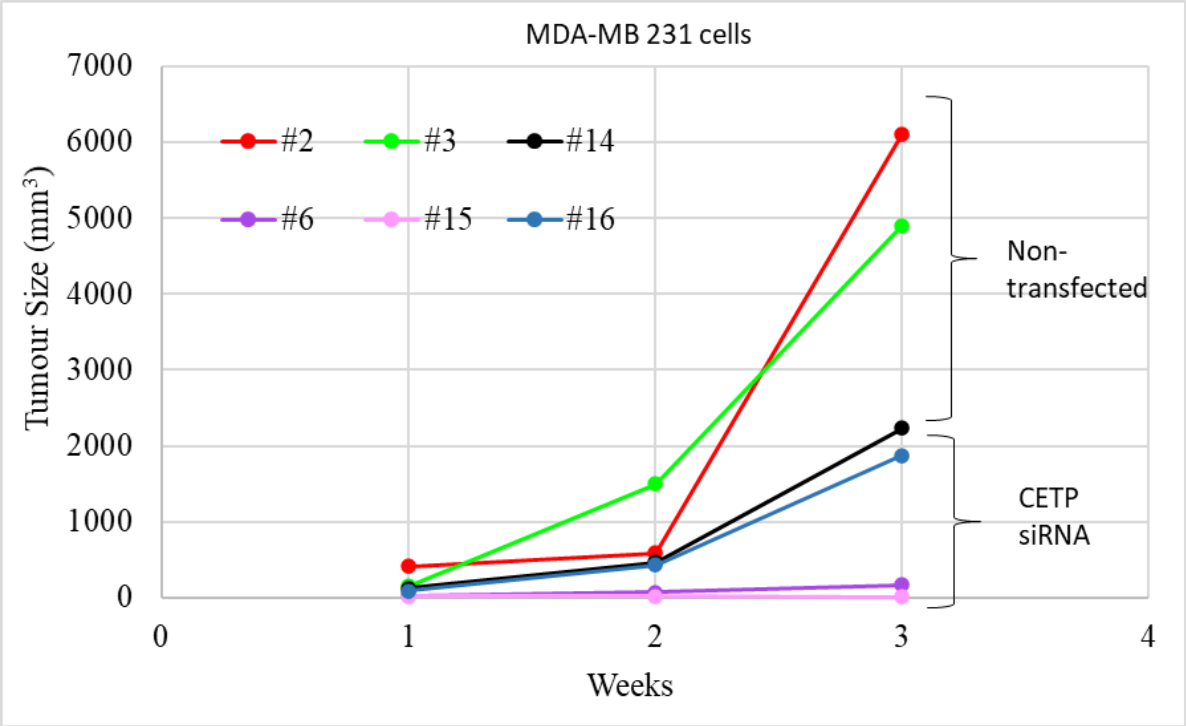

Figure 12.13: Average tumour volume per week

The non-transfected MDA-MB 231 tumours started to grow aggressively at day 14/ week 2 as can be observed in the graph above for mice number 2, 3 and 14. Whereas for the transfected cells, especially for number 6, the tumour growth rate was much slower compared to the non-transfected cells.

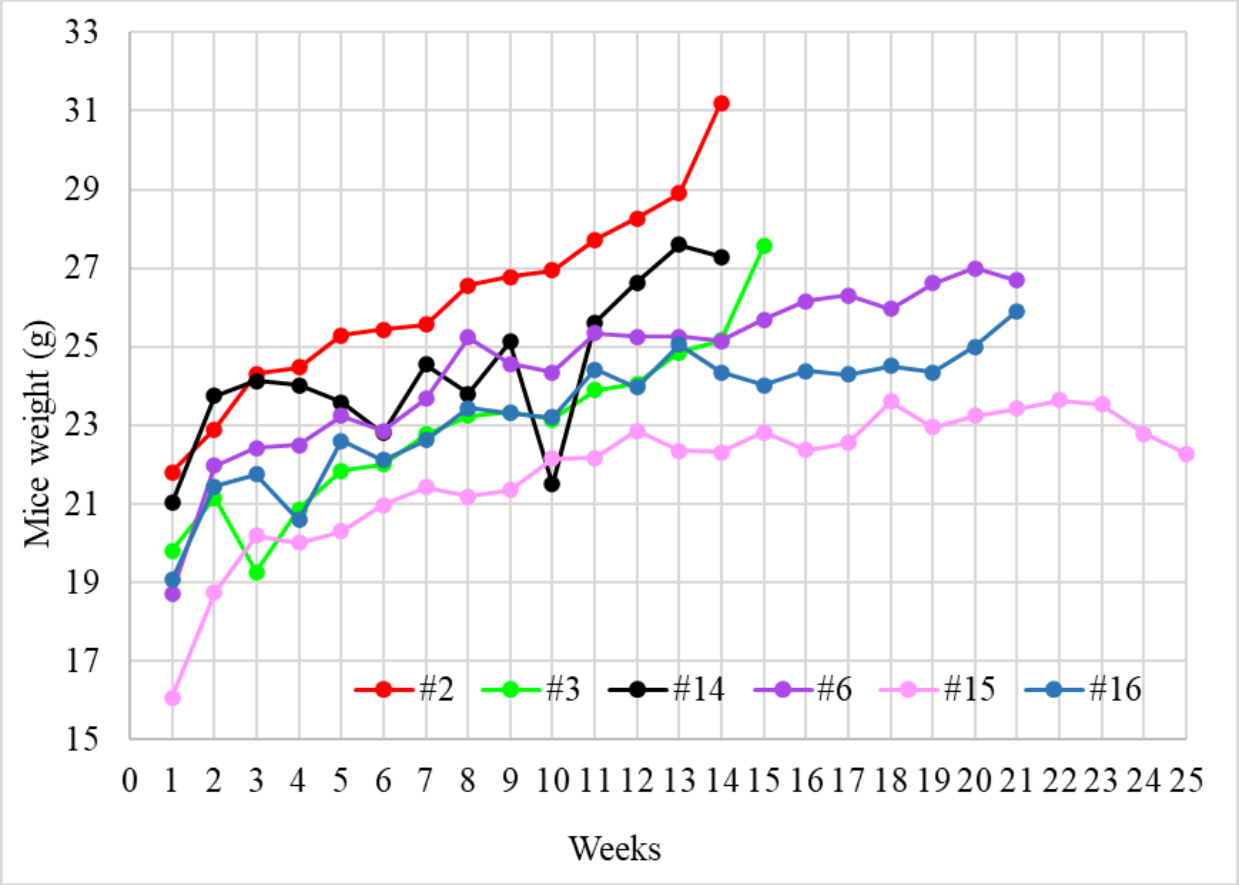

Figure 12.14: Weight changes in mice throughout the study

The figure above represents the weight changes from the time of mice procurement until the mice were euthanised in weeks. There was no abnormal growth of the mice and there was a consistent increase in the weight of the mice. However, mouse number 14 showed a drop in weight on week 10. This could possibly be due to weighing errors, or the mice was slightly dehydrated, however the mouse was healthy, and no unusual activities were observed.

13. Discussion

Cholesterol homeostasis is maintained by several networks or pathways, which is essential in sustaining normal cellular functions (Howe et al., 2016). Since cholesterol is partially soluble in blood, it requires water-soluble molecules for the transport of cholesterol through the circulatory system via lipoproteins (HDLs, LDLs and VLDLs) (Cruz et al., 2013). CETP is an important component of cholesterol transport and has a close working relationship to membrane cholesterol transporters and extracellular lipoproteins for cholesterol efflux and RCT (Ohashi et al., 2005), and thus maintaining homeostasis (Cruz et al., 2013). In addition, intracellular free cholesterol is insoluble and thus toxic within cells (Tabas, 2002). Therefore, free cholesterol is transported to the cell membrane for cell stability and shape or converted to CE through esterification by ACAT (Rogers et al., 2015; Shim et al., 2018). In several cancer studies, it was found that CE accumulation within cells significantly contributes to cancer resistance and aggressiveness (de Gonzalo-Calvo et al., 2015; He et al., 2017; Neuwirt et al., 2020; Simoes et al., 2020). This said, the increased CE accumulation commonly observed in cancer cells has been associated with the upregulation of the PI3K-AKT pathway, involved in cell proliferation, growth and survival (Cruz et al., 2020; Giunchi et al., 2019). Furthermore, lipid droplets (carrying CEs) have been found to be major instigators in prostaglandin E_2 (PGE_2) synthesis in colon cancer cells and it has been associated with tumour cell proliferation (Cruz et al., 2020). In addition, it is also known that cholesterol levels are six to eight times higher in cancerous cells compared to normal cells to compensate for increased energy production for the signalling of cell growth, proliferation and survival (Cruz et al., 2020; Li et al., 2006a).

There are currently two strategies that may target cholesterol as a form of anticancer therapy. The first approach investigates the blocking of the cholesterol synthesis pathway to lower the production of cholesterol and thereby decreases intracellular cholesterol levels. The most widely researched method in blocking the cholesterol synthesis pathway is by using statins. Statins, is by far, the most prescribed drug, currently on the market, to lower cholesterol levels in the prevention of cardiovascular events and atherosclerosis (Rosenson, 2004; Yebyo et al., 2019). Statins inhibits the action of HMG-CoA reductase in the mevalonate pathway, which halts downstream processes in which cholesterol is produced (Sultan et al., 2019). This inhibition of the rate limiting step has been found to elevate hepatic LDLRs involved in RCT, hence cholesterol clearance in circulation and thus reducing LDL levels (Maron et al., 2000). In addition, it has also been found that statins can lower LDL production through the inhibition

of hepatic apolipoprotein B-100 synthesis (Maron et al., 2000). Due to statins' effectiveness in reducing cholesterol levels, numerous studies have emersed on the possibility of statins having anticancer properties (Chae et al., 2015; Dulak and Józkowicz, 2005; G Vallianou et al., 2014). Although this is a novel avenue to explore, there have been several controversial studies on the safety of statin use. Numerous adverse effects of statins have been reported that should not be ignored, including: liver and muscle toxicity, loss of cognitive functions, neuropathy and pancreatic dysfunction (Golomb and Evans, 2008; Longo et al., 2020). In addition, there was a significant increase in mortality of type 2 diabetes mellitus patients on statin treatment and hospitalized for COVID-19 (Cariou et al., 2021). Furthermore, evidence from studies also show that roughly 25% of patients show statin intolerance and therefore do not respond to statins (Snejdrlova et al., 2020; Stroes et al., 2015). Therefore, further clinical trials would have to be conducted for better understanding of statins' effects as an anticancer drug.

In this study, we looked at the second approach in which excess cholesterol is depleted as opposed to blocking the synthesis. Cyclodextrins, more specially β-cyclodextrins, are the most studied cholesterol depleters. Its unique hydrophilic exterior with a hydrophobic cavity allows it to extract hydrophobic molecules, such as cholesterol, and thus allows the molecule that's being encapsulated to be soluble in aqueous solutions (Zidovetzki and Levitan, 2007). Previous studies have shown that MβCD was able to remove 80-90% of membrane cholesterol. Furthermore, it has been shown to induce apoptosis in various cancer cells and thus been suggested as a possible anticancer drug (Onodera et al., 2013; Zidovetzki and Levitan, 2007). However, it was found that MβCD was non-specific and could deplete cholesterol in normal cells, therefore causing cytotoxicity (Ulloth et al., 2007; Zidovetzki and Levitan, 2007). Recently, it was found that another cholesterol depleter, known as AP, was able to deplete excess cholesterol in MCF-7 cancer cells with no known toxicity to normal cells (Esau et al., 2016). AP is derived from plumbagin (known apoptotic inducer) and it was found that AP treated cancer cells reduced *CETP* mRNA expression by 33% and decreased tumour growth in mice (Esau et al., 2016; Sagar et al., 2014). In addition, it was found that *CETP* knock-down resulted in a 20% reduction in cell growth after six days and increased caspase 3/7 activity when treated with TAM (Esau et al., 2016). Therefore, we hypothesized that *CETP* could be used as a drug resistance marker. This was successfully proven as we observed a significant decrease in cell growth and proliferation (without drug treatment) post *CETP* knock-down for 72 hrs in both MCF-7 and MDA-MB 231 cells. In addition, through the cell viability and apoptosis assays, *CETP* knock-down resulted in an increase in TAM's efficacy in both MCF-

7 cells and MDA-MB 231 cells. Moreover, *CETP* knock-down in combination with AP further increased TAM's efficacy and thus highly supports the roles of *CETP* as a cell survival gene, as well as in cancer resistance. Further analysis confirmed that this increased efficacy was due to a decrease in CE levels, lipid rafts as well as free cholesterol.

CETP is an important protein in maintaining cholesterol homeostasis, however increased levels of CETP have been associated with increased risk of coronary heart disease and atherosclerosis (Boekholdt et al., 2004; de Vries-van der Weij et al., 2009). This is due to the fact that CETP is involved in the RCT process and thereby increased CETP levels result in a decrease in circulating HDLs, which increase adverse coronary events (Barter, 2000). Therefore, inhibiting *CETP* was suggested as a possible therapeutic strategy. Torcetrapib is a widely studied *CETP* inhibitor, however upon further clinical trials, it showed severe toxicity and increased risk of death and cardiac events (Barter et al., 2007). In addition, the use of *CETP* inhibitors have been associated with an increased risk of BC (Nowak and Ärnlöv, 2018). Recently, it was published that the failures of using CETP inhibitor to treat cardiovascular disease is the heterogeneity between the different CETP inhibitor compounds (Schmidt et al., 2021). Therefore, although targeting *CETP* may be a promising field of research as a therapeutic strategy, the non-specificity or the insufficient target inhibition of these CETP inhibitors need to be eradicated. However, *CETP* as a drug resistance marker to predict the outcome of therapeutic strategies, especially anticancer therapies, could be useful in clinical practices.

The molecular pathways were then elucidated to explain the decreased resistance post *CETP* knock-down. The qPCR arrays displayed very different results between ER+ MCF-7 and TNBC MDA-MB 231 cells when *CETP* was knocked down. It was noted that post *CETP* knock-down in MCF-7 cells, there was a decrease in expression profiles of several genes involved in the lipoprotein signalling and cholesterol metabolism pathway, as well as genes implicated in the BC resistance pathways. Most noticeably, the cholesterol synthesis, transport, efflux, HDL and LDL related pathways were all significantly downregulated, therefore coinciding with our cholesterol staining results which showed decreased intracellular cholesterol levels upon *CETP* knock-down in MCF-7 cells (Fig 13.1). In addition, cholesterol intake was possibly reduced through a decrease in LDLR as we observed a reduced *LDLR* gene expression. This would result in a reduced intracellular free cholesterol levels, therefore cell stability may be hampered thus reducing resistance. Cholesterol efflux pump, ABCA1 was decreased as a possible response to a reduced intracellular cholesterol levels as a combating mechanism. In MDA-MB 231 cells, however, the genes in the same pathways were increased,

therefore displaying the resistant nature of MDA-MB 231 cells. Although cholesterol synthesis was elevated, there was a concomitant increase in the degradation of LDLR through PCSK9 and upregulation of the cholesterol efflux pump, ABCA1. This is significant as it would result in a surge in cholesterol efflux and simultaneously, a decrease in cholesterol intake as cell surface LDLR would be degraded rather than redistributed to the surface for continuous cholesterol intake.

Lipid metabolism plays a pivotal role in cancer development and progression as it is involved in providing energy for the increased proliferation, membrane synthesis and metastatic potential of cancer cells (Liu et al., 2017). Cancer cells are able to reprogramme their lipid metabolism to adapt and maintain their aggressive proliferative rate (Liu et al., 2017). A study showed that BCR-Abl-transformed precursor B cells (BCR-Abl: chimeric oncogene between the Abelson (Abl) tyrosine kinase gene and break point cluster gene (BCR)) incubated in lipid-deficient media resulted in growth inhibition as well as cell death (Huang et al., 2016). However, cell proliferation was restored when lipids were supplemented back into the growth medium and thus highly supports the role of cholesterol's involvement in cancer proliferation (Huang et al., 2016). In addition, as aforementioned, CE levels are significantly increased in cancer cells stored as lipid droplets and is associated with cancer resistance (Cotte et al., 2018; Englinger et al., 2020; Hultsch et al., 2018; Tirinato et al., 2020). This increased lipid droplet accumulation within cancer cells is a result of either *de novo* fatty acid synthesis pathway or the increased exogenous cholesterol uptake (Cruz et al., 2020; Liu et al., 2017). The signalling for fatty acid synthesis is highly regulated by SREBP (which also regulates cholesterol synthesis) and the upregulation of SREBP is associated with increased lipid droplets and cholesterol accumulation and tumour growth (Ye and DeBose-Boyd, 2011). *CETP* knock-down resulted in a decrease in *SREBF1* gene, in MCF-7 cells thereby lowering intracellular cholesterol accumulation resulting in a decreased drug resistance. This was not observed in MDA-MB 231 cells, however there was an increase in *PRKAA2* expression post *CETP* knock-down, which is involved in the inhibition of *SREBF1*, with a simultaneous increase in cholesterol efflux pumps' expression. This, therefore, shows that *CETP* knock-down affects different pathways in which intracellular lipid accumulation is decreased, thereby decreasing drug resistance. This is in line with several studies where it was found that an increased expression of SREBP had a protective effect against cytotoxic agents, while the inhibition or knock-down of SREBP increased sensitivity of these cells to chemotherapeutic drugs and increased apoptosis in different cancer types (Gao et al., 2019; Xu et al., 2021; Yin et al., 2019;

Zhang et al., 2019). In addition to lipid trafficking through lipid droplets and its involvement in cancer development, it has also been implicated in inflammation (Cruz et al., 2020). It is well-known that inflammation and cancer progression are closely related, whereby inflammation accounts for approximately 25% of cancer-causing factors (Murata, 2018). This is accounted by the increased production in cytokines and ROS by inflammatory cells, such as leukocytes, at the site of damage in response to stress and signals for enhanced cell proliferation, thereby increasing the risk of cancer development (Coussens and Werb, 2002; Murata, 2018). In addition, eicosanoid synthesis (pro-inflammatory active lipid compounds such as PGE_2) through lipid droplets is highly elevated in cancer cells to enhance cell proliferation during tumorigenesis (Cruz et al., 2020; Howe, 2007). Furthermore, it has been found that PGE_2 is involved in the evasion of immune responses during tumorigenesis by inhibiting macrophages, T cells and natural killer cell activation, while inducing myeloid-derived suppressor cells (Greene et al., 2011). Moreover, lipid droplets have been found to be a central organelle in which a plethora of signalling-associated proteins localise, including PI3K, ERK1/2 and p38, which are involved in the MAPK signalling pathway associated with cell growth, proliferation and survival (Bozza and Viola, 2010; Cruz et al., 2020). As we observed, *CETP* knock-down reduced intracellular lipid droplets/ CE levels in both MCF-7 and MDA-MB 231 cells and therefore possibly reduced lipid-droplet-mediated resistance and proliferation.

a) Effects of *CETP* knock-down on lipoprotein signalling and cholesterol metabolism in MCF-7 cells

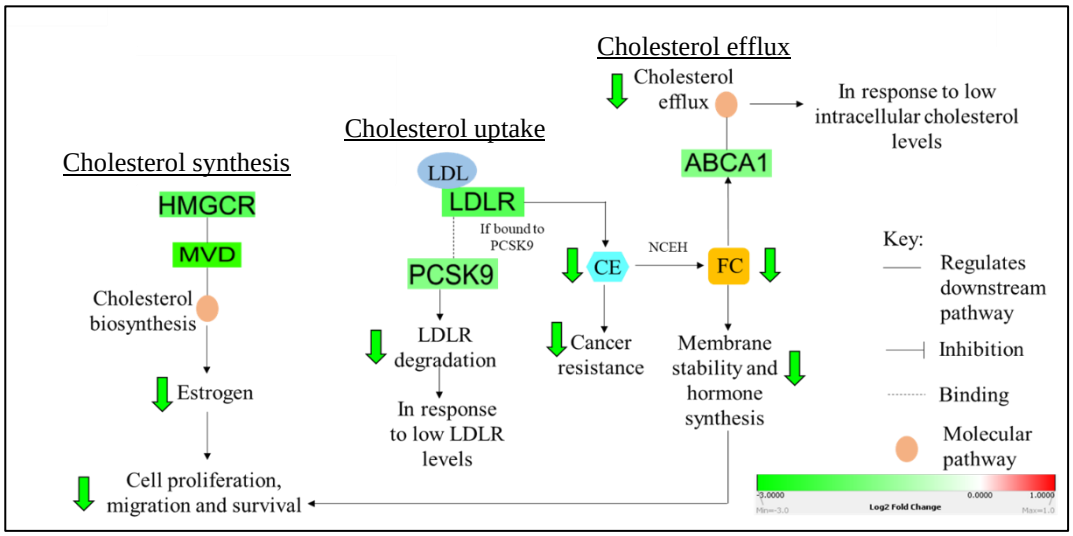

b) Effects of *CETP* knock-down on lipoprotein signalling and cholesterol metabolism in MDA-MB 231 cells

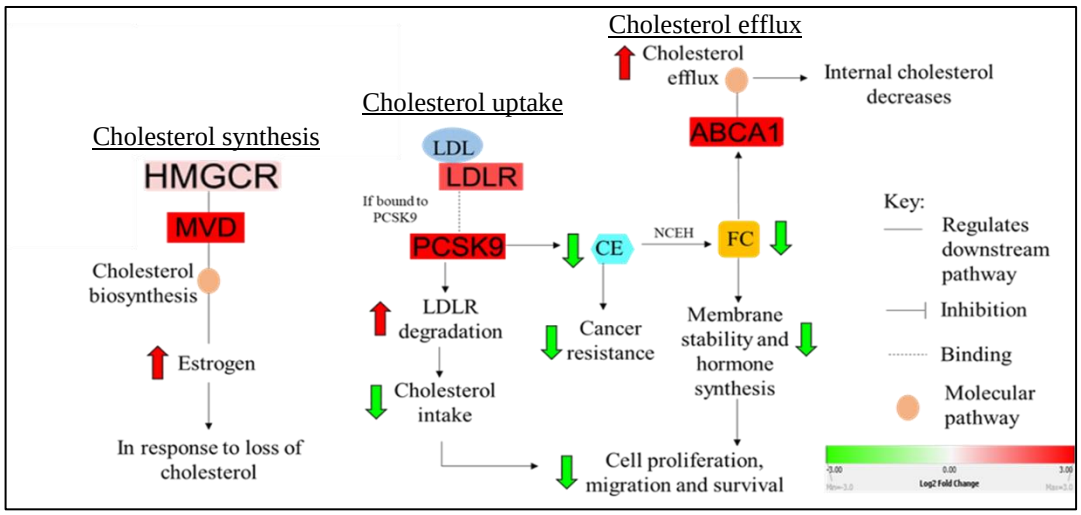

c) Effects of *CETP* knock-down on BC resistance in MCF-7 cells

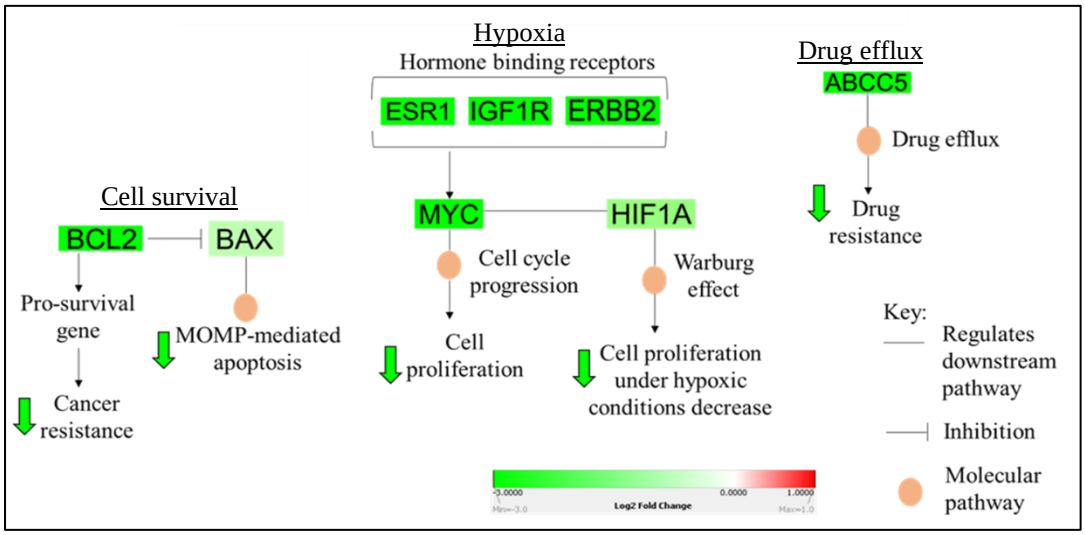

d) Effects of *CETP* knock-down on BC resistance in MDA-MB 231 cells

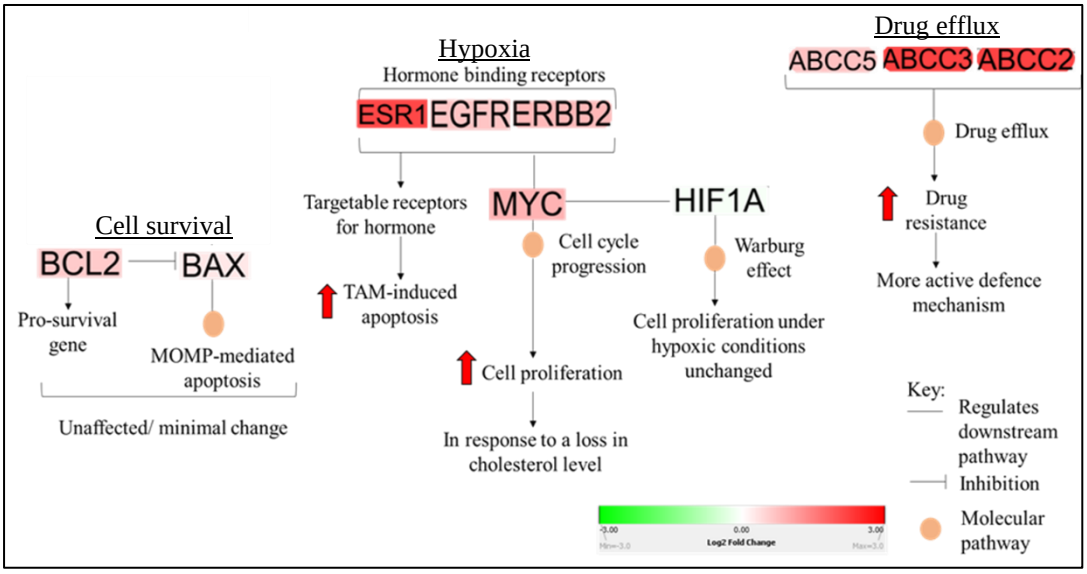

Figure 13.1: Diagram illustrating several genes and pathways affected post CETP knock-down

Cholesterol biosynthesis, maintained through HMGCR and MVD, are both downregulated in MCF-7 cells post CETP knock-down, thus decreasing estrogen synthesis, thereby decreasing cellular proliferation (a). These genes are, however upregulated in MDA-MB 231 cells (b). In addition, ESR1 is downregulated in MCF-7 cells upon CETP knock-down thus leading to a decrease in estrogen uptake and cell proliferation (c). ESR1 in MDA-MB 231 cells were upregulated d). LDLR and PCSK9 expression levels are decreased in MCF-7 cells leading to a decreased cholesterol uptake. In contrast, these genes were upregulated in MDA-MB 231 cells (in response to increased SREBF2), which increases cholesterol uptake however it is limited by PCSK9-LDLR lysosomal degradation. Cholesterol efflux pump (which removes

excess CE by converting it to free cholesterol, (FC) through neutral cholesteryl ester hydrolase (NCEH)) was also downregulated upon CETP knock-down in MCF-7, while increased in MDA-MB 231 cells. TP53, BCl-2 and BAX expression were reduced upon CETP knock-down in MCF-7 cells (c), however there was no significant change in the expression of these genes in MDA-MB 231 cells (d). Furthermore, hormone binding receptors gene expressions; ESR1, IGF1R and ERBB2 were all decreased in MCF-7 cells upon CETP knock-down (c) leading to decreased cell proliferation. MYC is also down regulated in MCF-7 cells thus preventing cell cycle progression (c). While these genes were slightly elevated in MDA-MB 231 cells post CETP knock-down (d). HIF1α expression was also reduced in MCF-7 cells (c) thus sensitising MCF-7 to hypoxic conditions. CETP knock-down did not affect HIF1α expression in MDA-MB 231 cells. Lastly, drug efflux pump; ABCC5 was reduced in MCF-7 cells (c) thus reducing drug resistance. On the contrary, drug efflux pumps; ABCC2, ABCC3 and ABCC5, were all increased in MDA-MB 231 cells showing that TNBC cells have a more active defence mechanism. The colours of the genes in each block represents the log2 fold change expression (same as the heat map). Green represents a downregulation of the gene and red represents the upregulation of the gene. The darker the colour is, the more downregulated or upregulated the gene is. The scale bar shows from -3 to 3 fold change expression.

Similarly, in the BC resistance array, most pathways were downregulated in ER+ BC cells post *CETP* knock-down, while in TNBC cells, there were little to no change (Fig 13.1). These genes: *HIF1α, Myc, TP53, BCl-2* and *BAX* are all targeted genes in the BC signalling pathways; PI3K-AKT and MAPK pathways (Fig 13.2). These pathways are often altered in cancer patients as they are involved in cell growth, differentiation, and survival (Mor and Philips, 2006; Porta et al., 2014; Rawlings et al., 2004).

One of the most well studied hallmarks of cancer is the evasion of apoptosis pathway. Apoptosis can be initiated through the intrinsic or the extrinsic pathway (Azimian et al., 2018). Extrinsic pathway involves the activation of downstream signalling through death receptors that activates various caspases, which cleaves ICAD to initiate DNA fragmentation (Green and Kroemer, 1998). Apart from the pro-apoptotic involvement of TNFRs, it has been found to be involved in the pro-inflammatory pathway through the signalling or activation of NF-κB (Nair et al., 2014). NF-κB is a transcription factor and the activation of NF-κB dimerizes with various members of the Rel family, such as p65, that allows the translocation of NF-κB from the cell cytosol to the nucleus (Bharti and Aggarwal, 2002). This activation of NF-κB lead to the pro-inflammatory signalling or activation of downstream transcription of proliferative genes, ROS

(as explained previously is prone to cause cancer progression) and tumour suppressor protein, p53 (Tilborghs et al., 2017). Several studies showed that cancer cells have highly elevated levels of NF-κB, which is associated with cancer aggression and could thus be a promising target in treating cancer (Ding et al., 2020; Tilborghs et al., 2017; Wu et al., 2018). Some studies that have shown that the inhibition of NF-κB suppressed ROS productions and favours anti-inflammatory pathway in reducing proliferation (Ghasemi et al., 2019; Kim et al., 2019; Nguyen et al., 2019). Interestingly, post *CETP* knock-down resulted an increase in *NFKBIE,* which is a gene involved in the inhibition of NF-κB protein and thereby possibly reducing NF-κB-mediated resistance in MCF-7 cells. As briefly mentioned earlier, that nuclear translocation of NF-κB through p65 is involved in p53 accumulation and thereby signalling for various cell proliferative pathways and pro-inflammatory pathways (Becatti et al., 2010). In contrast, the inhibitory subunit of NF-κB (IκBα) inhibits the activity of the p53 by forming p53-IκBα complex, thus preventing p53-mediated apoptosis (Zhou et al., 2003). In our study, we did not observe any difference in NF-κB expression pre and post *CETP* knock-down in both cell lines, which was an indication that *CETP* knock-down did not affect NF-κB-mediated resistance. However, we did observe a decrease in *TP53* expression post *CETP* knock-down in MCF-7 cells but not in MDA-MB 231 cells. This could indicate that *CETP* knock-down possibly decreased drug resistance through a decrease in p53-mediated DNA repair response/apoptosis in ER+ BC cells. Apoptosis mediated by p53 is initiated through a series of phosphorylation that signals for the downstream activation of pro-apoptotic genes, one of which includes *BAX* (Yogosawa and Yoshida, 2018). BAX is involved in the intrinsic apoptotic pathway, where the activation of BAX leads to the release of cytochrome c from the mitochondria and interacts with Apaf-1, thereby inducing caspase-mediated apoptosis (Azimian et al., 2018). The intrinsic pathway is also tightly regulated by *BCL-2*, anti-apoptotic gene, which maintains mitochondrial membrane potential and thus preventing the release of cytochrome c (Azimian et al., 2018). An overexpression of *BCl-2* increases the inhibition of apoptosis and therefore it is often upregulated in cancer cells (Azimian et al., 2018). This apoptotic resistance was also observed in BC patients receiving chemoradiotherapy (Azimian et al., 2018). *CETP* knock-down was observed to downregulate both *BCl-2* and *BAX* genes in MCF-7 cells, while it remained relatively unchanged in MDA-MB 231 cells. The downregulation of *BAX* in MCF-7 cells post *CETP* knock-down is possibly correlated to the decrease in *TP53* expression, while the decrease in *BCL-2* gene expression, post CETP knock-down, could indicate a reduced resistance through a decrease in apoptotic evasion. This was also supported by the increased

loss of MOMP that we observed post *CETP* knock-down in both cell lines, in both treated (single and combination treatment) and untreated cells.

In ER+ BC cells, steroid hormones are especially vital in maintaining the rapid cellular proliferation through the MAPK and PI3K-AKT pathways and have been found to inhibit apoptosis by enhancing the expression of the *BCL-2* gene, thereby conferring to drug resistance (Liang and Shang, 2013). In addition, it was found that in BC cells, estrogen rapidly enhances the transcription of Myc through the interaction between ER and activator protein 1 (Liang and Shang, 2013). Myc is an important oncogene involved in the signalling of cell cycle progression and proliferation and it has been found to be overexpressed in 20-30% of BCs (Wang et al., 2011). One of the main functions of Myc is the regulation of glycolysis and its contribution to the Warburg effect, where cancer cells are able to generate energy under both aerobic and anaerobic conditions for the enhanced cell proliferation (Akram, 2013; Miller et al., 2012). Similarly, the HIF1α transcription factor is involved in the activation of downstream genes that may be involved in angiogenesis, cell proliferation and survival under hypoxic conditions (Podar and Anderson, 2010). Therefore, it is not a surprise that an increase in Myc and HIF1α is associated with enhanced cancer cell proliferation, poor prognosis and chemoresistance (Cruzeiro et al., 2018; Hong et al., 2020; Hu et al., 2019; Pan et al., 2019). While the inhibition of Myc and HIF1α has shown to decrease cell proliferation and suppressed tumour growth (Cruzeiro et al., 2018; Hong et al., 2020; Hu et al., 2019; Pan et al., 2019). Our results showed that upon *CETP* knock-down in MCF-7 cells, there was a decreased expression of hormone receptors and a corresponding decreased *Myc* expression (Fig 13.1). In addition, the expression of *HIF1α* was also reduced. This is indicative that *CETP* knock-down reduces cell proliferation and cancer resistance via the repression of hypoxia-related genes in ER+ BC cells, as energy production through the glycolysis pathway would be limited. Interestingly, the hormone binding receptors increased slightly in MDA-MB 231 cells (Fig 13.1). This is significant as MDA-MB 231 cells lack these hormone receptors. An increase in these receptors would therefore sensitise these TNBC cells towards hormone targeted drugs, such as TAM, and as a result increased the efficacy of TAM in transfected MDA-MB 231 cells. Furthermore, there was an increase in Myc expression post *CETP* knock-down, possibly in response to the increased ER expression in MDA-MB 231 cells. This is possibly a compensatory mechanism of MDA-MB 231 cells to maintain its resistance.

Despite the advancement of cancer research and the development of numerous novel therapeutic strategies in overcoming cancer mortalities, MDR remains a major obstacle in long-

term drug effectiveness. One of the key contributors to MDR is the increased drug efflux pumps of the ABC-transporter protein family, which reduces intracellular drug accumulation and therefore reduces the drug-to-target interaction in initiating downstream apoptotic pathways (Jaramillo et al., 2018). P-gp, or also known as ABCB1, is one of the main drug exporters and an overexpression of P-gp have been found to confer to various tumour malignancies, including; breast, colon, kidney, liver and ovarian cancers (Jaramillo et al., 2018). Furthermore, P-gp knock-out mice showed an increased drug absorption as opposed to drug excretion and thus resulted in an increase in cytotoxicity (Jaramillo et al., 2018). In this study, we observed a decreased expression of drug efflux pumps upon *CETP* knock-down in MCF-7 cells and therefore overcoming drug resistance. In TNBC cells, however, the genes in these pathways remained unchanged or slightly increased post *CETP* knock-down. Once again this shows that TNBC cells are more resistant than ER+ BC cells and that the effects of *CETP* knock-down is very different between the two cell lines. However, we were still able to observe an increased drug efficacy and reduced drug resistance in TNBC cells upon *CETP* knock-down, even though the effects were greater in ER+ BC cells.

In summary, these arrays suggests that the effects of *CETP* knock-down is cell line dependent and that the reduction in resistance that we observed so far in both cell lines are due to a change in different pathways. In MCF-7 cells, *CETP* knock-down favoured a downregulation in genes involved in the cholesterol synthesis pathway, decreased surface hormone and growth factor receptor gene expressions, as well as a reduced gene expression of drug efflux pumps. While in MDA-MB 231 cells, *CETP* knock-down possibly sensitized these TNBC cells towards endocrine therapy by increased gene expressions of surface receptors and cholesterol efflux genes. Therefore, the difference in the affected pathways post *CETP* knock-down between these two cell lines is a good indication that the different subtypes of BC can reprogramme their metabolic pathways to adapt to various treatments. Therefore, it is vital to acknowledge these differences especially in the development of novel cholesterol-targeted therapies.

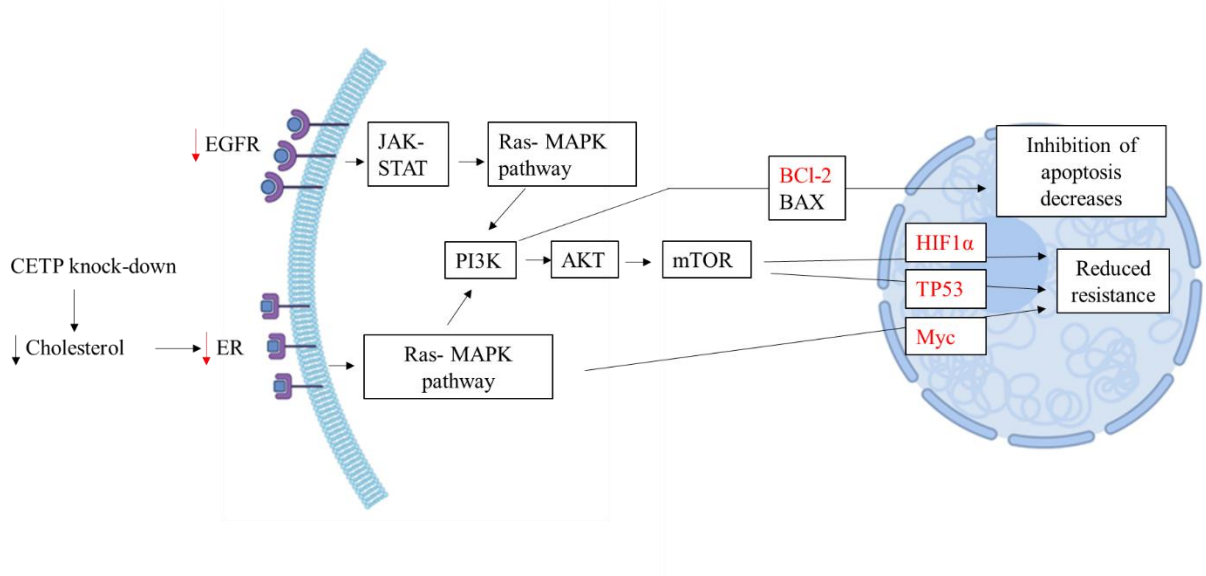

Figure 13.2: Cholesterol's involvement in various BC signalling pathways

The figure above summarizes the involvement of certain genes in difference BC signalling pathways. The activation of estrogen receptor through the binding of hormone estrogen activates several downstream pathways such as PI3K-AKT and MAPK pathways, which signals for cell proliferation. Similarly, the activation of EGFR results in JAK-STAT and MAPK pathways. However, CETP knock-down resulted in a decreased gene expression or hormone and growth factor receptors (ER and EGFR; gene suppression is indicated as red arrows). In addition, it also downregulated genes highlighted in red (BCl-2, HIF1α, Myc and TP53) and thereby reducing resistance and decrease inhibition of apoptosis in MCF-7 cells. These genes were not greatly affected in MDA-MB 231 cells post CETP knock-down. [Image created with BioRender.com]

The results from the study proved that CETP is involved in cancer resistance, as well as cell proliferation. Therefore, to further confirm these results, a mice xenograft study was conducted and as expected, tumour growth was reduced by 86.45% in transfected MDA-MB 231 cells, with no observable side effects and metastasis. Furthermore, survival plots depicted unfavourable result in patients expressing high levels of *CETP*. This, therefore, proves that targeting *CETP* could be a useful strategy in reducing cholesterol levels and resistance. However, as previously mentioned that CETP is a key regulator of both intracellular and extracellular cholesterol homeostasis and thus permanent inhibition, or removal of the gene could be fatal. In addition, previous CETP inhibitors showed off-target effects resulting in severe side effects. Therefore, further research is warranted for targeting CETP as a possible

chemotherapeutic strategy. However, this study showed that *CETP* could be an effective BC resistance marker and it can be useful in cancer prognosis.

14. Future Work

For future work, it would be interesting to see the effects of *CETP* knock-down on the drug efficacy in a non-cancerous cell line, such as HEK 293. Previously, I have performed an MTT assay on the effects of AP and TAM on cell growth in HEK 293 cells. Preliminary data showed TAM and AP treatments are less effective in non-cancerous cells, especially at 5 µM concentration (Supplementary Fig 17.1). However, the effects of *CETP* knock-down on the efficacy of these drugs are unknown. In addition, the protein expression profiles of several selected genes could be quantified using western blotting, as gene expression may not always correlate to protein expression profiles. Some of which have been performed in MCF-7 cells to observe if the effects of *CETP* knock-down would be the same on a protein level as opposed to mRNA expression (Supplementary Fig 17.2). In addition, the xenograft study could be expanded on, in which treatments of TAM and AP can be administered post tumour detection to observe the effects of treatments on stably transfected and non-transfected tumours. Stable knock-down has commenced (Supplementary Fig 17.3-17.5), however, *CETP* knock-down is yet to be confirmed using RT-qPCR and western blotting. It would also be interesting to look into encapsulating *CETP* siRNA for a more targeted and specific knock-down effect. Furthermore, RNA and protein could also be extracted from these tumours to compare the expressions *in vitro* vs *in vivo*. An overexpression study could be performed to see if the effects of proliferation and resistance would be reversed if *CETP* expression was enhanced. In addition, *CETP* levels can be measured in cancer patients, as well as non-cancer patients to compare *CETP* baseline levels.

15. Conclusion

In conclusion, *CETP* knock-down is effective in increasing TAM's efficacy in both ER+ and ER- BC cells. Furthermore, the effect of TAM was greatly increased with the combination of a cholesterol depleting agent such as AP post *CETP* knock-down through a decrease in CE levels, lipid rafts and free cholesterol. The arrays depicted the difference in mechanisms in MCF-7 and MDA-MB 231 cells point towards different cholesterol homeostasis mechanisms in these cell lines. In MCF-7 cells, *CETP* knock-down decreased cancer resistance through a decrease in cholesterol accumulation, as well as a decrease in hormone receptors and drug

efflux pumps. While *CETP* does not seem to affect most of the cholesterol mediated processes in MDA-MB 231 cells. However, in MDA-MB 231 cells, *CETP* knock-down showed an increased gene expressions involved in cholesterol efflux and upregulated *ER* expression, thus sensitised these cells to TAM. The mice xenograft study confirmed *CETP* as a cell survival gene, where tumour growth was reduced by 86.45% when *CETP* was knocked down. In addition, Kaplan-Meier survival Plots showed that patients with lower levels of *CETP* have a better chance of survival compared to patients with higher levels of *CETP*. Therefore, from this study, we concluded that *CETP* could be a promising drug resistance marker in predicting the effectiveness of cancer treatment and possibly a good target in reducing drug resistance through a decrease in excess cholesterol.

16. Reference List

Acconcia, F., Barnes, C.J., and Kumar, R. (2006). Estrogen and tamoxifen induce cytoskeletal remodeling and migration in endometrial cancer cells. Endocrinology *147*, 1203-1212.

Agerholm-Larsen, B., Nordestgaard, B.G., Steffensen, R., Jensen, G., and Tybjærg-Hansen, A. (2000). Elevated HDL cholesterol is a risk factor for ischemic heart disease in white women when caused by a common mutation in the cholesteryl ester transfer protein gene. Circulation *101*, 1907-1912.

Akram, M. (2013). Mini-review on glycolysis and cancer. Journal of Cancer Education *28*, 454-457.

Ali, S., Rasool, M., Chaoudhry, H., Pushparaj, P.N., Jha, P., Hafiz, A., Mahfooz, M., Sami, G.A., Kamal, M.A., and Bashir, S. (2016). Molecular mechanisms and mode of tamoxifen resistance in breast cancer. Bioinformation *12*, 135-139.

Alla, V.M., Agrawal, V., DeNazareth, A., Mohiuddin, S., Ravilla, S., and Rendell, M. (2013). A reappraisal of the risks and benefits of treating to target with cholesterol lowering drugs. Drugs *73*, 1025-1054.

Althuis, M.D., Fergenbaum, J.H., Garcia-Closas, M., Brinton, L.A., Madigan, M.P., and Sherman, M.E. (2004). Etiology of hormone receptor–defined breast cancer: a systematic review of the literature. Cancer Epidemiology and Prevention Biomarkers *13*, 1558-1568.

American Cancer Society, A. (2016). Breast Cancer.

Arakawa, R., Abe-Dohmae, S., Asai, M., Ito, J.-i., and Yokoyama, S. (2000). Involvement of caveolin-1 in cholesterol enrichment of high density lipoprotein during its assembly by apolipoprotein and THP-1 cells. Journal of lipid research *41*, 1952-1962.

Azimian, H., Dayyani, M., Toossi, M.T.B., and Mahmoudi, M. (2018). Bax/Bcl-2 expression ratio in prediction of response to breast cancer radiotherapy. Iranian journal of basic medical sciences *21*, 325-332.

Babina, I.S., and Turner, N.C. (2017). Advances and challenges in targeting FGFR signalling in cancer. Nature Reviews Cancer *17*, 318-332.

Bai, F., Yin, Y., Chen, T., Chen, J., Ge, M., Lu, Y., Xie, F., Zhang, J., Wu, K., and Liu, Y. (2018). Development of liposomal pemetrexed for enhanced therapy against multidrug resistance mediated by ABCC5 in breast cancer. International journal of nanomedicine *13*, 1327-1339.

Barter, P. (2000). CETP and atherosclerosis (Am Heart Assoc), pp. 2109-2122.

Barter, P.J., Caulfield, M., Eriksson, M., Grundy, S.M., Kastelein, J.J., Komajda, M., Lopez-Sendon, J., Mosca, L., Tardif, J.-C., and Waters, D.D. (2007). Effects of torcetrapib in patients at high risk for coronary events. New England journal of medicine *357*, 2109-2122.

Becatti, M., Prignano, F., Fiorillo, C., Pescitelli, L., Nassi, P., Lotti, T., and Taddei, N. (2010). The involvement of Smac/DIABLO, p53, NF-kB, and MAPK pathways in apoptosis of keratinocytes from perilesional vitiligo skin: Protective effects of curcumin and capsaicin. Antioxidants & redox signaling *13*, 1309-1321.

Bharti, A.C., and Aggarwal, B.B. (2002). Nuclear factor-kappa B and cancer: its role in prevention and therapy. Biochemical pharmacology *64*, 883-888.

Bhosale, P.B., Ha, S.E., Vetrivel, P., Kim, H.H., Kim, J.-A., Park, K.-I., Kim, S.M., and Kim, G.S. (2020). Flavonoid-induced apoptotic cell death in human cancer cells and its mechanisms. Journal of Biomedical and Translational Research *21*, 50-58.

Bisgaier, C., and Newton, R. (2001). Methods of treating alzheimer's disease (Google Patents).

Biswas, D.K., Cruz, A.P., Gansberger, E., and Pardee, A.B. (2000). Epidermal growth factor-induced nuclear factor κB activation: a major pathway of cell-cycle progression in estrogen-receptor negative breast cancer cells. Proceedings of the National Academy of Sciences *97*, 8542-8547.

Bland, J.M., and Altman, D.G. (2004). The logrank test. bmj *328*, 1073-1073.

Blank, N., Schiller, M., Krienke, S., Wabnitz, G., Ho, A.D., and Lorenz, H.M. (2007). Cholera toxin binds to lipid rafts but has a limited specificity for ganglioside GM1. Immunology and cell biology *85*, 378-382.

Boekholdt, S.M., Kuivenhoven, J.-A., Wareham, N.J., Peters, R.J., Jukema, J.W., Luben, R., Bingham, S.A., Day, N.E., Kastelein, J.J., and Khaw, K.-T. (2004). Plasma levels of cholesteryl ester transfer protein and the risk of future coronary artery disease in apparently healthy men and women: the prospective EPIC (European Prospective Investigation into Cancer and nutrition)–Norfolk population study. Circulation *110*, 1418-1423.

Bots, M.L., Visseren, F.L., Evans, G.W., Riley, W.A., Revkin, J.H., Tegeler, C.H., Shear, C.L., Duggan, W.T., Vicari, R.M., and Grobbee, D.E. (2007). Torcetrapib and carotid intima-media thickness in mixed dyslipidaemia (RADIANCE 2 study): a randomised, double-blind trial. The Lancet *370*, 153-160.

Bouwman, P., and Jonkers, J. (2012). The effects of deregulated DNA damage signalling on cancer chemotherapy response and resistance. Nature Reviews Cancer *12*, 587-598.

Bozgeyik, E. (2019). MicroRNA-17-5P targets expression of cancer-associated genes in breast cancer cells. Meta Gene, In press.

Bozza, P.T., and Viola, J.P. (2010). Lipid droplets in inflammation and cancer. Prostaglandins, Leukotrienes and Essential Fatty Acids (PLEFA) *82*, 243-250.

Breastcancer.org (2017a). Hormone Receptor Status.

Breastcancer.org (2017b). How to Read Hormone Receptor Test Results.

Brunelle, J.K., and Letai, A. (2009). Control of mitochondrial apoptosis by the Bcl-2 family. Journal of cell science *122*, 437-441.

Bubici, C., and Papa, S. (2019). The Warburg Effect Regulation Under Siege: the Intertwined Pathways in Health and Disease. Frontiers in cell and developmental biology *7*, 1-3.

Buchwald, H. (1992). Cholesterol inhibition, cancer, and chemotherapy. The Lancet *339*, 1154-1156.

Buhaescu, I., and Izzedine, H. (2007). Mevalonate pathway: a review of clinical and therapeutical implications. Clinical biochemistry *40*, 575-584.

CANSA, N.C.R. (2014). Cancer Fact Sheet. 1-9.

Cao, X., Hou, J., An, Q., Assaraf, Y.G., and Wang, X. (2020). Towards the overcoming of anticancer drug resistance mediated by p53 mutations. Drug Resistance Updates *49*, 1-10.

Cariou, B., Goronflot, T., Rimbert, A., Boullu, S., Le May, C., Moulin, P., Pichelin, M., Potier, L., Smati, S., and Sultan, A. (2021). Routine use of statins and increased COVID-19 related mortality in inpatients with type 2 diabetes: Results from the CORONADO study. Diabetes & metabolism *47*, 1-4.

Chae, Y.K., Yousaf, M., Malecek, M.-K., Carneiro, B., Chandra, S., Kaplan, J., Kalyan, A., Sassano, A., Platanias, L.C., and Giles, F. (2015). Statins as anti-cancer therapy; Can we translate preclinical and epidemiologic data into clinical benefit? Discovery medicine *20*, 413-427.

Chang, M. (2012). Tamoxifen resistance in breast cancer. Biomolecules & therapeutics *20*, 256-267.

Chang, T., Chang, C.C., and Cheng, D. (1997). Acyl-coenzyme A: cholesterol acyltransferase. Annual review of biochemistry *66*, 613-638.

Chen, Z., Shi, T., Zhang, L., Zhu, P., Deng, M., Huang, C., Hu, T., Jiang, L., and Li, J. (2016). Mammalian drug efflux transporters of the ATP binding cassette (ABC) family in multidrug resistance: A review of the past decade. Cancer letters *370*, 153-164.

Cheng, X., Li, J., and Guo, D. (2018). SCAP/SREBPs are central players in lipid metabolism and novel metabolic targets in cancer therapy. Current topics in medicinal chemistry *18*, 484-493.

Clark, R.W., Sutfin, T.A., Ruggeri, R.B., Willauer, A.T., Sugarman, E.D., Magnus-Aryitey, G., Cosgrove, P.G., Sand, T.M., Wester, R.T., and Williams, J.A. (2004). Raising high-density lipoprotein in humans through inhibition of cholesteryl ester transfer protein: an initial multidose study of torcetrapib. Arteriosclerosis, thrombosis, and vascular biology *24*, 490-497.

Cleator, S., Heller, W., and Coombes, R.C. (2007). Triple-negative breast cancer: therapeutic options. The lancet oncology *8*, 235-244.

Clemons, M., and Goss, P. (2001). Estrogen and the risk of breast cancer. New England journal of medicine *344*, 276-285.

Cooke, A.L., Morris, J., Melchior, J.T., Street, S.E., Jerome, W.G., Huang, R., Herr, A.B., Smith, L.E., Segrest, J.P., and Remaley, A.T. (2018). A thumbwheel mechanism for APOA1 activation of LCAT activity in HDL. Journal of lipid research *59*, 1244-1255.

Cotte, A.K., Aires, V., Fredon, M., Limagne, E., Derangère, V., Thibaudin, M., Humblin, E., Scagliarini, A., de Barros, J.-P.P., and Hillon, P. (2018). Lysophosphatidylcholine acyltransferase 2-mediated lipid droplet production supports colorectal cancer chemoresistance. Nature communications *9*, 1-16.

Coussens, L.M., and Werb, Z. (2002). Inflammation and cancer. Nature *420*, 860-867.

Cronin-Fenton, D.P., Damkier, P., and Lash, T.L. (2014). Metabolism and transport of tamoxifen in relation to its effectiveness: new perspectives on an ongoing controversy. Future Oncology *10*, 107-122.

Cruz, A.L., Barreto, E.d.A., Fazolini, N.P., Viola, J.P., and Bozza, P.T. (2020). Lipid droplets: platforms with multiple functions in cancer hallmarks. Cell death & disease *11*, 1-16.

Cruz, P.M., Mo, H., McConathy, W., Sabnis, N.A., and Lacko, A.G. (2013). The role of cholesterol metabolism and cholesterol transport in carcinogenesis: a review of scientific findings, relevant to future cancer therapeutics. Frontiers in pharmacology *4*, 1-7.

Cruzeiro, G.A., dos Reis, M.B., Silveira, V.S., Lira, R.C.P., Neder, L., Oliveira, R.S., Yunes, J.A., Brandalise, S.R., Aguiar, S., and Eterovic, A.K. (2018). HIF1A is overexpressed in medulloblastoma and its inhibition reduces proliferation and increases EPAS1 and ATG16L1 methylation. Current cancer drug targets *18*, 287-294.

de Gonzalo-Calvo, D., López-Vilaró, L., Nasarre, L., Perez-Olabarria, M., Vázquez, T., Escuin, D., Badimon, L., Barnadas, A., Lerma, E., and Llorente-Cortés, V. (2015). Intratumor cholesteryl ester accumulation is associated with human breast cancer proliferation and aggressive potential: a molecular and clinicopathological study. BMC cancer *15*, 1-14.

de Grooth, G.J., Klerkx, A.H., Stroes, E.S., Stalenhoef, A.F., Kastelein, J.J., and Kuivenhoven, J.A. (2004). A review of CETP and its relation to atherosclerosis. Journal of lipid research *45*, 1967-1974.

de Vries-van der Weij, J., Zadelaar, S., Toet, K., Havekes, L.M., Kooistra, T., and Rensen, P.C. (2009). Human CETP aggravates atherosclerosis by increasing VLDL-cholesterol rather than by decreasing HDL-cholesterol in APOE* 3-Leiden mice. Atherosclerosis *206*, 153-158.

DeBose-Boyd, R.A., and Ye, J. (2018). SREBPs in lipid metabolism, insulin signaling, and beyond. Trends in biochemical sciences *43*, 358-368.

Denko, N.C. (2008). Hypoxia, HIF1 and glucose metabolism in the solid tumour. Nature Reviews Cancer *8*, 705-713.

Di Pietro, G., Magno, L.A.V., and Rios-Santos, F. (2010). Glutathione S-transferases: an overview in cancer research. Expert opinion on drug metabolism & toxicology *6*, 153-170.

Ding, J., Zhao, J., Huan, L., Liu, Y., Qiao, Y., Wang, Z., Chen, Z., Huang, S., Zhao, Y., and He, X. (2020). Inflammation-Induced Long Intergenic Noncoding RNA (LINC00665) Increases Malignancy Through Activating the Double-Stranded RNA–Activated Protein Kinase/Nuclear Factor Kappa B Pathway in Hepatocellular Carcinoma. Hepatology *72*, 1666-1681.

Ding, Y., Zhang, W., Zhang, M., Fu, K., Chen, W., Ding, C., He, X., Zhang, X., Huang, L., and Yin, Z. (2015). Functional and association studies of the cholesteryl ester transfer protein (CETP) gene in a Wannan Black pig model. Animal genetics *46*, 702-706.

Doe, M.R., Ascano, J.M., Kaur, M., and Cole, M.D. (2012). Myc posttranscriptionally induces HIF1 protein and target gene expression in normal and cancer cells. Cancer research *72*, 949-957.

Dong, B., Singh, A.B., Fung, C., Kan, K., and Liu, J. (2014). CETP inhibitors downregulate hepatic LDL receptor and PCSK9 expression in vitro and in vivo through a SREBP2 dependent mechanism. Atherosclerosis *235*, 449-462.

dos Santos, C.R., Domingues, G., Matias, I., Matos, J., Fonseca, I., de Almeida, J.M., and Dias, S. (2014). LDL-cholesterol signaling induces breast cancer proliferation and invasion. Lipids in health and disease *13*, 1-9.

Dulak, J., and Józkowicz, A. (2005). Anti-angiogenic and anti-inflammatory effects of statins: relevance to anti-cancer therapy. Current cancer drug targets *5*, 579-594.

Englinger, B., Laemmerer, A., Moser, P., Kallus, S., Röhrl, C., Pirker, C., Baier, D., Mohr, T., Niederstaetter, L., and Meier-Menches, S.M. (2020). Lipid droplet-mediated scavenging as novel intrinsic and adaptive resistance factor against the multikinase inhibitor ponatinib. International journal of cancer *147*, 1680-1693.

Esau, L., Sagar, S., Bangarusamy, D., and Kaur, M. (2016). Identification of CETP as a molecular target for estrogen positive breast cancer cell death by cholesterol depleting agents. Genes & cancer *7*, 309-322.

Evans, R.M. (1988). The steroid and thyroid hormone receptor superfamily. Science *240*, 889-895.

FDA, f.a.d.a. (2018). FDA Drug Safety Communication: Important safety label changes to cholesterol-lowering statin drugs.

Fedele, P., Calvani, N., Marino, A., Orlando, L., Schiavone, P., Quaranta, A., and Cinieri, S. (2012). Targeted agents to reverse resistance to endocrine therapy in metastatic breast cancer: where are we now and where are we going? Critical reviews in oncology/hematology *84*, 243-251.

Fielding, C.J., and Fielding, P.E. (1995). Molecular physiology of reverse cholesterol transport. Journal of lipid research *36*, 211-228.

Forrest, M.J., Bloomfield, D., Briscoe, R.J., Brown, P., Cumiskey, A.M., Ehrhart, J., Hershey, J., Keller, W., Ma, X., and McPherson, H. (2008). Torcetrapib-induced blood pressure elevation is independent of CETP inhibition and is accompanied by increased circulating levels of aldosterone. British journal of pharmacology *154*, 1465-1473.

Foulkes, W.D., and Shuen, A.Y. (2013). In brief: BRCA1 and BRCA2. The Journal of pathology *230*, 347-349.

Frank-Kamenetsky, M., Grefhorst, A., Anderson, N.N., Racie, T.S., Bramlage, B., Akinc, A., Butler, D., Charisse, K., Dorkin, R., and Fan, Y. (2008). Therapeutic RNAi targeting PCSK9 acutely lowers plasma cholesterol in rodents and LDL cholesterol in nonhuman primates. Proceedings of the National Academy of Sciences *105*, 11915-11920.

Frank, P.G., Cheung, M.W.-C., Pavlides, S., Llaverias, G., Park, D.S., and Lisanti, M.P. (2006). Caveolin-1 and regulation of cellular cholesterol homeostasis. American Journal of Physiology-Heart and Circulatory Physiology *291*, H677-H686.

Frank, P.G., Galbiati, F., Volonte, D., Razani, B., Cohen, D.E., Marcel, Y.L., and Lisanti, M.P. (2001). Influence of caveolin-1 on cellular cholesterol efflux mediated by high-density lipoproteins. American Journal of Physiology-Cell Physiology *280*, C1204-C1214.

Frasor, J., Danes, J.M., Komm, B., Chang, K.C., Lyttle, C.R., and Katzenellenbogen, B.S. (2003). Profiling of estrogen up-and down-regulated gene expression in human breast cancer cells: insights into gene networks and pathways underlying estrogenic control of proliferation and cell phenotype. Endocrinology *144*, 4562-4574.

Fulda, S., and Debatin, K.-M. (2006). Extrinsic versus intrinsic apoptosis pathways in anticancer chemotherapy. Oncogene *25*, 4798 - 4811.

G Vallianou, N., Kostantinou, A., Kougias, M., and Kazazis, C. (2014). Statins and cancer. Anti-Cancer Agents in Medicinal Chemistry (Formerly Current Medicinal Chemistry-Anti-Cancer Agents) *14*, 706-712.

Galbraith, M.D., Allen, M.A., Bensard, C.L., Wang, X., Schwinn, M.K., Qin, B., Long, H.W., Daniels, D.L., Hahn, W.C., and Dowell, R.D. (2013). HIF1A employs CDK8-mediator to stimulate RNAPII elongation in response to hypoxia. cell *153*, 1327-1339.

Gao, Y., Zhao, Q., Mu, X., Zhu, H., Liu, B., Yao, B., Liu, X., Xue, W., Wang, B., and Liu, S. (2019). SREBP1 promotes 5-FU resistance in colorectal cancer cells by inhibiting the expression of caspase7. International journal of clinical and experimental pathology *12*, 1095-1100.

Gedvilaite, G., Vilkeviciute, A., Kriauciuniene, L., Asmoniene, V., and Liutkeviciene, R. (2019). Does CETP rs5882, rs708272, SIRT1 rs12778366, FGFR2 rs2981582, STAT3 rs744166, VEGFA rs833068, IL6 rs1800795 polymorphisms play a role in optic neuritis development? Ophthalmic genetics *40*, 219-226.

Ghasemi, F., Shafiee, M., Banikazemi, Z., Pourhanifeh, M.H., Khanbabaei, H., Shamshirian, A., Moghadam, S.A., ArefNezhad, R., Sahebkar, A., and Avan, A. (2019). Curcumin inhibits NF-kB and Wnt/β-catenin pathways in cervical cancer cells. Pathology-Research and Practice *215*, 1-6.

Ghayee, H.K., and Auchus, R.J. (2007). Basic concepts and recent developments in human steroid hormone biosynthesis. Reviews in Endocrine and Metabolic Disorders *8*, 289-300.

Giunchi, F., Fiorentino, M., and Loda, M. (2019). The metabolic landscape of prostate cancer. European urology oncology *2*, 28-36.

Golomb, B.A., and Evans, M.A. (2008). Statin adverse effects. American Journal of Cardiovascular Drugs *8*, 373-418.

Gould, S., and Scott, R.C. (2005). 2-Hydroxypropyl-β-cyclodextrin (HP-β-CD): a toxicology review. Food and Chemical Toxicology *43*, 1451-1459.

Green, D., and Kroemer, G. (1998). The central executioners of apoptosis: caspases or mitochondria? Trends in cell biology *8*, 267-271.

Greene, E.R., Huang, S., Serhan, C.N., and Panigrahy, D. (2011). Regulation of inflammation in cancer by eicosanoids. Prostaglandins & other lipid mediators *96*, 27-36.

Gu, L., Saha, S.T., Thomas, J., and Kaur, M. (2019). Targeting cellular cholesterol for anticancer therapy. The FEBS journal *286*, 4192-4208.

Győrffy, B. (2021). Survival analysis across the entire transcriptome identifies biomarkers with the highest prognostic power in breast cancer. Computational and structural biotechnology journal *19*, 4101-4109.

Györffy, B., Lanczky, A., Eklund, A.C., Denkert, C., Budczies, J., Li, Q., and Szallasi, Z. (2010). An online survival analysis tool to rapidly assess the effect of 22,277 genes on breast cancer prognosis using microarray data of 1,809 patients. Breast cancer research and treatment *123*, 725-731.

Haag, M.D., Hofman, A., Koudstaal, P.J., Stricker, B.H., and Breteler, M.M. (2009). Statins are associated with a reduced risk of Alzheimer disease regardless of lipophilicity. The Rotterdam Study. Journal of neurology, neurosurgery & psychiatry *80*, 13-17.

Hanahan, D. (2014). Rethinking the war on cancer. The Lancet *383*, 558-563.

Hanahan, D., and Weinberg, R.A. (2000). The hallmarks of cancer. cell *100*, 57-70.

Hanahan, D., and Weinberg, R.A. (2011). Hallmarks of cancer: the next generation. cell *144*, 646-674.

Hankinson, S.E., Willett, W.C., Manson, J.E., Colditz, G.A., Hunter, D.J., Spiegelman, D., Barbieri, R.L., and Speizer, F.E. (1998). Plasma sex steroid hormone levels and risk of breast cancer in postmenopausal women. JNCI: Journal of the National Cancer Institute *90*, 1292-1299.

Hazlehurst, L.A., and Dalton, W.S. (2006). De novo and acquired resistance to antitumor alkylating agents. In Cancer Drug Resistance (Springer), pp. 377-389.

He, M., Zhang, W., Dong, Y., Wang, L., Fang, T., Tang, W., Lv, B., Chen, G., Yang, B., and Huang, P. (2017). Pro-inflammation NF-κB signaling triggers a positive feedback via

enhancing cholesterol accumulation in liver cancer cells. Journal of Experimental & Clinical Cancer Research *36*, 1-13.

Helleday, T. (2010). Homologous recombination in cancer development, treatment and development of drug resistance. Carcinogenesis *31*, 955-960.

Hemann, M., and Lowe, S. (2006). The p53–Bcl-2 connection (Nature Publishing Group), pp. 1256–1259.

Hientz, K., Mohr, A., Bhakta-Guha, D., and Efferth, T. (2017). The role of p53 in cancer drug resistance and targeted chemotherapy. Oncotarget *8*, 8921-8946.

Hodges, L.C., Cook, J.D., Lobenhofer, E.K., Li, L., Bennett, L., Bushel, P.R., Aldaz, C.M., Afshari, C.A., and Walker, C.L. (2003). Tamoxifen Functions As a Molecular Agonist Inducing Cell Cycle-Associated Genes in Breast Cancer Cells1 1 National Institute of Environmental Health Sciences (ES98263 and ES07784) and the Women's American Legion Auxiliary Fellowship. 2 2 IMAGE clones were annotated according to the official gene names from the Human Gene Nomenclature Committee, when available. The official gene names for cyclin D1, cyclin A2, and fra-1 are CCND1, CCNA2, and FOSL1, respectively. Molecular Cancer Research *1*, 300-311.

Holohan, C., Van Schaeybroeck, S., Longley, D.B., and Johnston, P.G. (2013). Cancer drug resistance: an evolving paradigm. Nature Reviews Cancer *13*, 714-726.

Hong, F., Gao, Y., Li, Y., Zheng, L., Xu, F., and Li, X. (2020). Inhibition of HIF1A-AS1 promoted starvation-induced hepatocellular carcinoma cell apoptosis by reducing HIF-1α/mTOR-mediated autophagy. World journal of surgical oncology *18*, 1-8.

Hoque, A., Chen, H., and Xu, X.C. (2008). Statin induces apoptosis and cell growth arrest in prostate cancer cells. Cancer epidemiology, biomarkers & prevention : a publication of the American Association for Cancer Research, cosponsored by the American Society of Preventive Oncology *17*, 88-94.

Horton, J.D., Cohen, J.C., and Hobbs, H.H. (2007). Molecular biology of PCSK9: its role in LDL metabolism. Trends in biochemical sciences *32*, 71-77.

Housman, G., Byler, S., Heerboth, S., Lapinska, K., Longacre, M., Snyder, N., and Sarkar, S. (2014). Drug resistance in cancer: an overview. Cancers *6*, 1769-1792.

Howe, L.R. (2007). Inflammation and breast cancer. Cyclooxygenase/prostaglandin signaling and breast cancer. Breast cancer research *9*, 1-9.

Howe, V., Sharpe, L.J., Alexopoulos, S.J., Kunze, S.V., Chua, N.K., Li, D., and Brown, A.J. (2016). Cholesterol homeostasis: how do cells sense sterol excess? Chemistry and physics of lipids *199*, 170-178.

Hu, M.-H., Wu, T.-Y., Huang, Q., and Jin, G. (2019). New substituted quinoxalines inhibit triple-negative breast cancer by specifically downregulating the c-MYC transcription. Nucleic acids research *47*, 10529-10542.

Huang, J., Li, L., Lian, J., Schauer, S., Vesely, P.W., Kratky, D., Hoefler, G., and Lehner, R. (2016). Tumor-induced hyperlipidemia contributes to tumor growth. Cell reports *15*, 336-348.

Hultsch, S., Kankainen, M., Paavolainen, L., Kovanen, R.-M., Ikonen, E., Kangaspeska, S., Pietiäinen, V., and Kallioniemi, O. (2018). Association of tamoxifen resistance and lipid reprogramming in breast cancer. BMC cancer *18*, 1-14.

Humpton, T., and Vousden, K.H. (2019). Taking up the reins of power: metabolic functions of p53. Journal of molecular cell biology *11*, 610-614.

Hydbring, P., and Larsson, L.-G. (2010). Cdk2: a key regulator of the senescence control function of Myc. Aging (Albany NY) *2*, 244-250.

Ikonen, E. (2008). Cellular cholesterol trafficking and compartmentalization. Nature reviews Molecular cell biology *9*, 125-138.

Isaacsohn, J. (1992). The role of cholesterol. Yale University School of medicine heart book, 37-49.

Izem, L., Liu, Y., and Morton, R.E. (2020). Exon 9-deleted CETP inhibits full length-CETP synthesis and promotes cellular triglyceride storage. Journal of lipid research *61*, 422-431.

Jansen, R.S., Mahakena, S., de Haas, M., Borst, P., and van de Wetering, K. (2015). ATP-binding cassette subfamily C member 5 (ABCC5) functions as an efflux transporter of glutamate conjugates and analogs. Journal of Biological Chemistry *290*, 30429-30440.

Jaramillo, A.C., Saig, F.A., Cloos, J., Jansen, G., and Peters, G.J. (2018). How to overcome ATP-binding cassette drug efflux transporter-mediated drug resistance? Cancer Drug Resistance *1*, 6-29.

Kang, M.H., Zhang, L.-H., Wijesekara, N., de Haan, W., Butland, S., Bhattacharjee, A., and Hayden, M.R. (2013). Regulation of ABCA1 protein expression and function in hepatic and pancreatic islet cells by miR-145. Arterioscler Thromb Vasc Biol *33*, 2724-2732.

Kartal-Yandim, M., Adan-Gokbulut, A., and Baran, Y. (2016). Molecular mechanisms of drug resistance and its reversal in cancer. Critical reviews in biotechnology *36*, 716-726.

Kastan, M.B., and Bartek, J. (2004). Cell-cycle checkpoints and cancer. Nature *432*, 316-323.

Kaur, M., and Esau, L. (2015). Two-step protocol for preparing adherent cells for high-throughput flow cytometry. Biotechniques *59*, 119-126.

Khan, A.S., and Frigo, D.E. (2017). A spatiotemporal hypothesis for the regulation, role, and targeting of AMPK in prostate cancer. Nature Reviews Urology *14*, 164-180.

Kim, D.-A., Choi, H.S., Ryu, E.-S., Ko, J., Shin, H.-S., Lee, J.-M., Chung, H., Jun, E., Oh, E.-S., and Kang, D.-H. (2019). Tannic acid attenuates the formation of cancer stem cells by inhibiting NF-κB-mediated phenotype transition of breast cancer cells. American journal of cancer research *9*, 1664-1681.

Konishi, H., Mohseni, M., Tamaki, A., Garay, J.P., Croessmann, S., Karnan, S., Ota, A., Wong, H.Y., Konishi, Y., and Karakas, B. (2011). Mutation of a single allele of the cancer susceptibility gene BRCA1 leads to genomic instability in human breast epithelial cells. Proceedings of the National Academy of Sciences *108*, 17773-17778.

Krishna Vadlapatla, R., Dutt Vadlapudi, A., Pal, D., and K Mitra, A. (2013). Mechanisms of drug resistance in cancer chemotherapy: coordinated role and regulation of efflux transporters and metabolizing enzymes. Current pharmaceutical design *19*, 7126-7140.

Kuivenhoven, J., Pritchard, H., Hill, J., Frohlich, J., Assmann, G., and Kastelein, J. (1997). The molecular pathology of lecithin: cholesterol acyltransferase (LCAT) deficiency syndromes. Journal of lipid research *38*, 191-205.

Lagace, T.A. (2014). PCSK9 and LDLR degradation: regulatory mechanisms in circulation and in cells. Current opinion in lipidology *25*, 387-393.

Lagrost, L. (1994). Regulation of cholesteryl ester transfer protein (CETP) activity: review of in vitro and in vivo studies. Biochimica et Biophysica Acta (BBA)-Lipids and Lipid Metabolism *1215*, 209-236.

Lakomy, D., Rébé, C., Sberna, A.-L., Masson, D., Gautier, T., Chevriaux, A., Raveneau, M., Ogier, N., Nguyen, A.T., and Gambert, P. (2009). Liver X Receptor–Mediated Induction of Cholesteryl Ester Transfer Protein Expression Is Selectively Impaired in Inflammatory Macrophages. Arteriosclerosis, thrombosis, and vascular biology *29*, 1923-1929.

Lavie, Y., and Liscovitch, M. (2000). Changes in lipid and protein constituents of rafts and caveolae in multidrug resistant cancer cells and their functional consequences. Glycoconjugate journal *17*, 253-259.

Le Lay, S., Hajduch, E., Lindsay, M.R., Le Lièpvre, X., Thiele, C., Ferré, P., Parton, R.G., Kurzchalia, T., Simons, K., and Dugail, I. (2006). Cholesterol-induced caveolin targeting to lipid droplets in adipocytes: a role for caveolar endocytosis. Traffic *7*, 549-561.

Lee, H.-S., Kim, Y., and Park, T. (2018). New common and rare variants influencing metabolic syndrome and its individual components in a Korean population. Scientific reports *8*, 1-7.

Levens, D. (2013). Cellular MYCro economics: Balancing MYC function with MYC expression. Cold Spring Harbor perspectives in medicine *3*, 1-16.

Li, H., Zhang, Y., Chen, H.-H., Huang, E., Zhuang, H., Li, D., and Ni, F. (2019). Rosmarinic acid inhibits stem-like breast cancer through hedgehog and Bcl-2/Bax signaling pathways. Pharmacognosy Magazine *15*, 600-606.

Li, J., Qu, X., Tian, J., Zhang, J.-T., and Cheng, J.-X. (2018). Cholesterol esterification inhibition and gemcitabine synergistically suppress pancreatic ductal adenocarcinoma proliferation. PLoS One *13*, 1-11.

Li, Y.C., Park, M.J., Ye, S.-K., Kim, C.-W., and Kim, Y.-N. (2006a). Elevated levels of cholesterol-rich lipid rafts in cancer cells are correlated with apoptosis sensitivity induced by cholesterol-depleting agents. The American journal of pathology *168*, 1107-1118.

Li, Z., Mintzer, E., and Bittman, R. (2006b). First synthesis of free cholesterol− BODIPY conjugates. The Journal of organic chemistry *71*, 1718-1721.

Liang, J., and Shang, Y. (2013). Estrogen and cancer. Annual review of physiology *75*, 225-240.

Liscovitch, M., and Lavie, Y. (2000). Multidrug resistance: a role for cholesterol efflux pathways? Trends in biochemical sciences *25*, 530-534.

Liu, Q., Luo, Q., Halim, A., and Song, G. (2017). Targeting lipid metabolism of cancer cells: a promising therapeutic strategy for cancer. Cancer letters *401*, 39-45.

Liutkeviciene, R., Vilkeviciute, A., Kriauciuniene, L., Banevicius, M., Budiene, B., Stanislovaitiene, D., Zemaitiene, R., and Deltuva, V.P. (2020). Association of genetic variants at CETP, AGER, and CYP4F2 locus with the risk of atrophic age-related macular degeneration. Molecular Genetics & Genomic Medicine *8*, 1-10.

Livak, K.J., and Schmittgen, T.D. (2001). Analysis of relative gene expression data using real-time quantitative PCR and the 2− ΔΔCT method. methods *25*, 402-408.

Longley, D., and Johnston, P. (2005). Molecular mechanisms of drug resistance. The Journal of Pathology: A Journal of the Pathological Society of Great Britain and Ireland *205*, 275-292.

Longo, J., van Leeuwen, J.E., Elbaz, M., Branchard, E., and Penn, L.Z. (2020). Statins as anticancer agents in the era of precision medicine. Clinical Cancer Research *26*, 5791-5800.

Lopez, D. (2008). Inhibition of PCSK9 as a novel strategy for the treatment of hypercholesterolemia. Drug news & perspectives *21*, 323-330.

Lu, W.J., Desta, Z., and Flockhart, D.A. (2012). Tamoxifen metabolites as active inhibitors of aromatase in the treatment of breast cancer. Breast cancer research and treatment *131*, 473-481.

Luo, Q., Hu, K., Chen, F., Gan, F.-J., Leng, Y.-X., Chen, X.-M., and Sun, S.-H. (2019). Juglone Induces Michigan Cancer Foundation-7 Human Breast Cancer Cells Apoptosis through Bcl-2-Associated X protein/B-cell lymphoma/leukemia-2 Signal Way. Pharmacognosy Magazine *15*, 573-578.

Mahammad, S., and Parmryd, I. (2015). Cholesterol depletion using methyl-β-cyclodextrin. In Methods in Membrane Lipids (Springer), pp. 91-102.

Mansoori, B., Mohammadi, A., Davudian, S., Shirjang, S., and Baradaran, B. (2017). The different mechanisms of cancer drug resistance: a brief review. Advanced pharmaceutical bulletin *7*, 339-348.

Maron, D.J., Fazio, S., and Linton, M.F. (2000). Current perspectives on statins. Circulation *101*, 207-213.

Masson, D. (2009). Anacetrapib, a cholesterol ester transfer protein (CETP) inhibitor for the treatment of atherosclerosis. Current opinion in investigational drugs (London, England: 2000) *10*, 980-987.

Masterjohn, C. (2005). Cholesterol's importance to the cell membrane. 1-1.

Maughan, K.L., Lutterbie, M.A., and Ham, P.S. (2010). Treatment of breast cancer. Chemotherapy *81*, 1339-1346.

Mayengbam, S.S., Singh, A., Pillai, A.D., and Bhat, M.K. (2021). Influence of cholesterol on cancer progression and therapy. Translational Oncology *14*, 1-20.

Meek, D.W. (2004). The p53 response to DNA damage. DNA repair *3*, 1049-1056.

Miller, D.M., Thomas, S.D., Islam, A., Muench, D., and Sedoris, K. (2012). c-Myc and cancer metabolism (AACR), pp. 1-9.

Millwood, I.Y., Bennett, D.A., Holmes, M.V., Boxall, R., Guo, Y., Bian, Z., Yang, L., Sansome, S., Chen, Y., and Du, H. (2018). Association of CETP gene variants with risk for vascular and nonvascular diseases among Chinese adults. JAMA cardiology *3*, 34-43.

Mizutani, T., Masuda, M., Nakai, E., Furumiya, K., Togawa, H., Nakamura, Y., Kawai, Y., Nakahira, K., Shinkai, S., and Takahashi, K. (2008). Genuine functions of P-glycoprotein (ABCB1). Current drug metabolism *9*, 167-174.

Mor, A., and Philips, M.R. (2006). Compartmentalized ras/mapk signaling. Annu Rev Immunol *24*, 771-800.

Morton, R.E., and Izem, L. (2014). Cholesteryl ester transfer proteins from different species do not have equivalent activities. Journal of lipid research *55*, 258-265.

Morton, R.E., Liu, Y., and Izem, L. (2019). ApoF knockdown increases cholesteryl ester transfer to LDL and impairs cholesterol clearance in fat-fed hamsters. Journal of lipid research *60*, 1868-1879.

Mourits, M.J., De Vries, E.G., Willemse, P.H., Ten Hoor, K.A., Hollema, H., and Van der Zee, A.G. (2001). Tamoxifen treatment and gynecologic side effects: a review. Obstetrics & Gynecology *97*, 855-866.

Murata, M. (2018). Inflammation and cancer. Environmental health and preventive medicine *23*, 1-8.

Nair, P., Lu, M., Petersen, S., and Ashkenazi, A. (2014). Apoptosis initiation through the cell-extrinsic pathway. Methods in enzymology *544*, 99-128.

NCBI (2018). CETP cholesteryl ester transfer protein [Homo sapiens (human)].

Nefedova, Y., Landowski, T., and Dalton, W. (2003). Bone marrow stromal-derived soluble factors and direct cell contact contribute to de novo drug resistance of myeloma cells by distinct mechanisms. Leukemia *17*, 1175-1182.

Nelson, E.R., Chang, C.-y., and McDonnell, D.P. (2014). Cholesterol and breast cancer pathophysiology. Trends in Endocrinology & Metabolism *25*, 649-655.

Neuwirt, H., Bouchal, J., Kharaishvili, G., Ploner, C., Jöhrer, K., Pitterl, F., Weber, A., Klocker, H., and Eder, I.E. (2020). Cancer-associated fibroblasts promote prostate tumor growth and progression through upregulation of cholesterol and steroid biosynthesis. Cell Communication and Signaling *18*, 1-18.

Nguyen, T.T., Ung, T.T., Li, S., Lian, S., Xia, Y., Park, S.Y., and Do Jung, Y. (2019). Metformin inhibits lithocholic acid-induced interleukin 8 upregulation in colorectal cancer cells by suppressing ROS production and NF-kB activity. Scientific reports *9*, 1-13.

NIH, N.C.I. (2017). Hormone Therapy for Breast Cancer.

Nissen, S.E., Tardif, J.-C., Nicholls, S.J., Revkin, J.H., Shear, C.L., Duggan, W.T., Ruzyllo, W., Bachinsky, W.B., Lasala, G.P., and Tuzcu, E.M. (2007). Effect of torcetrapib on

the progression of coronary atherosclerosis. New England journal of medicine *356*, 1304-1316.

Norman, A., Demel, R., De Kruyff, B., and Van Deenen, L. (1972). Studies on the Biological Properties of Polyene Antibiotics EVIDENCE FOR THE DIRECT INTERACTION OF FILIPIN WITH CHOLESTEROL. Journal of Biological Chemistry *247*, 1918-1929.

Nowak, C., and Ärnlöv, J. (2018). A Mendelian randomization study of the effects of blood lipids on breast cancer risk. Nature communications *9*, 1-7.

O'Donovan, P.J., and Livingston, D.M. (2010). BRCA1 and BRCA2: breast/ovarian cancer susceptibility gene products and participants in DNA double-strand break repair. Carcinogenesis *31*, 961-967.

Ohashi, R., Mu, H., Wang, X., Yao, Q., and Chen, C. (2005). Reverse cholesterol transport and cholesterol efflux in atherosclerosis. Qjm *98*, 845-856.

Onodera, R., Motoyama, K., Okamatsu, A., Higashi, T., Kariya, R., Okada, S., and Arima, H. (2013). Involvement of cholesterol depletion from lipid rafts in apoptosis induced by methyl-β-cyclodextrin. International journal of pharmaceutics *452*, 116-123.

Osati, S., Ali, H., and van Lier, J.E. (2016). BODIPY–steroid conjugates: Syntheses and biological applications. Journal of Porphyrins and Phthalocyanines *20*, 61-75.

Pan, Y., Fei, Q., Xiong, P., Yang, J., Zhang, Z., Lin, X., Pan, M., Lu, F., and Huang, H. (2019). Synergistic inhibition of pancreatic cancer with anti-PD-L1 and c-Myc inhibitor JQ1. Oncoimmunology *8*, 1-12.

Payne, A.H., and Hales, D.B. (2004). Overview of steroidogenic enzymes in the pathway from cholesterol to active steroid hormones. Endocrine reviews *25*, 947-970.

Pearce, M.C., Satterthwait, A.C., Zhang, X.-k., and Kolluri, S.K. (2019). Cancer therapeutics based on BCL-2 functional conversion. Apoptosis *24*, 1-2.

Pearson, H. (2006). Why did a promising heart drug fail? (Nature Publishing Group).

Phillips, M.C. (2014). Molecular mechanisms of cellular cholesterol efflux. Journal of Biological Chemistry *289*, 24020-24029.

Podar, K., and Anderson, K.C. (2010). A therapeutic role for targeting c-Myc/Hif-1-dependent signaling pathways. Cell Cycle *9*, 1722-1728.

Porta, C., Paglino, C., and Mosca, A. (2014). Targeting PI3K/Akt/mTOR signaling in cancer. Frontiers in oncology *4*, 1-11.

Potischman, N., Swanson, C.A., Siiteri, P., and Hoover, R.N. (1996). Reversal of relation between body mass and endogenous estrogen concentrations with menopausal status. JNCI: Journal of the National Cancer Institute *88*, 756-758.

Prasad, G., Bandesh, K., Giri, A.K., Kauser, Y., Chanda, P., Parekatt, V., Mathur, S., Madhu, S.V., Venkatesh, P., and Bhansali, A. (2019). Genome-wide association study of metabolic syndrome reveals primary genetic variants at CETP locus in Indians. Biomolecules *9*, 321-337.

Pratt, A.J., and MacRae, I.J. (2009). The RNA-induced silencing complex: a versatile gene-silencing machine. Journal of Biological Chemistry *284*, 17897-17901.

Pritchard, A.L., and Hayward, N.K. (2013). Molecular pathways: mitogen-activated protein kinase pathway mutations and drug resistance. Clinical Cancer Research *19*, 2301-2309.

Ramsunder, N. (2015). Side effects of statins. South African Journal of Diabetes and Vascular Disease *12*, 48-50.

Randrianarisoa, E., Lehn-Stefan, A., Krier, J., Böhm, A., Heni, M., Hrabě de Angelis, M., Fritsche, A., Häring, H.-U., Stefan, N., and Staiger, H. (2019). AMPK subunits harbor largely non-overlapping genetic determinants for body fat mass, glucose-and cholesterol metabolism. The Journal of Clinical Endocrinology & Metabolism *105*, 14-25.

Rascio, F., Spadaccino, F., Rocchetti, M.T., Castellano, G., Stallone, G., Netti, G.S., and Ranieri, E. (2021). The Pathogenic Role of PI3K/AKT Pathway in Cancer Onset and Drug Resistance: An Updated Review. Cancers *13*, 1-15.

Rawlings, J.S., Rosler, K.M., and Harrison, D.A. (2004). The JAK/STAT signaling pathway. Journal of cell science *117*, 1281-1283.

Reers, M., Smiley, S.T., Mottola-Hartshorn, C., Chen, A., Lin, M., and Chen, L.B. (1995). [29] Mitochondrial membrane potential monitored by JC-1 dye. In Methods in enzymology (Elsevier), pp. 406-417.

Repa, J.J., and Mangelsdorf, D.J. (2002). The liver X receptor gene team: potential new players in atherosclerosis. Nature medicine *8*, 1243-1248.

Reynolds, A., Leake, D., Boese, Q., Scaringe, S., Marshall, W.S., and Khvorova, A. (2004). Rational siRNA design for RNA interference. Nature biotechnology *22*, 326-330.

Rick, W. (1974). Trypsin. In Methods of enzymatic analysis (Elsevier), pp. 1013-1024.

Ring, A., and Dowsett, M. (2004). Mechanisms of tamoxifen resistance. Endocrine-Related Cancer *11*, 643-658.

Rogers, M.A., Liu, J., Song, B.-L., Li, B.-L., Chang, C.C., and Chang, T.-Y. (2015). Acyl-CoA: cholesterol acyltransferases (ACATs/SOATs): enzymes with multiple sterols as substrates and as activators. The Journal of steroid biochemistry and molecular biology *151*, 102-107.

Rosenson, R.S. (2004). Statins in atherosclerosis: lipid-lowering agents with antioxidant capabilities. Atherosclerosis *173*, 1-12.

Rosenson, R.S., Brewer, H.B., Davidson, W.S., Fayad, Z.A., Fuster, V., Goldstein, J., Hellerstein, M., Jiang, X.-C., Phillips, M.C., and Rader, D.J. (2012). Cholesterol efflux and atheroprotection. Circulation *125*, 1905-1919.

Sagar, S., Esau, L., Moosa, B., Khashab, N.M., Bajic, V.B., and Kaur, M. (2014). Cytotoxicity and apoptosis induced by a plumbagin derivative in estrogen positive MCF-7 breast cancer cells. Anti-Cancer Agents in Medicinal Chemistry (Formerly Current Medicinal Chemistry-Anti-Cancer Agents) *14*, 170-180.

Sakao, K., Fujii, M., and Hou, D.X. (2009). Acetyl derivate of quercetin increases the sensitivity of human leukemia cells toward apoptosis. Biofactors *35*, 399-405.

Sancar, A., Lindsey-Boltz, L.A., Ünsal-Kaçmaz, K., and Linn, S. (2004). Molecular mechanisms of mammalian DNA repair and the DNA damage checkpoints. Annual review of biochemistry *73*, 39-85.

Sandur, S.K., Ichikawa, H., Sethi, G., Ahn, K.S., and Aggarwal, B.B. (2006). Plumbagin (5-hydroxy-2-methyl-1, 4-naphthoquinone) suppresses NF-κB activation and NF-κB-regulated gene products through modulation of p65 and IκBα kinase activation, leading to potentiation of apoptosis induced by cytokine and chemotherapeutic agents. Journal of Biological Chemistry *281*, 17023-17033.

Santarpia, L., Lippman, S.M., and El-Naggar, A.K. (2012). Targeting the MAPK–RAS–RAF signaling pathway in cancer therapy. Expert opinion on therapeutic targets *16*, 103-119.

Sato, R. (2010). Sterol metabolism and SREBP activation. Archives of biochemistry and biophysics *501*, 177-181.

Schlacher, K. (2018). A new road to cancer-drug resistance (Nature Publishing Group), pp. 478-480.

Schmidt, A.F., Hunt, N.B., Gordillo-Marañón, M., Charoen, P., Drenos, F., Kivimaki, M., Lawlor, D.A., Giambartolomei, C., Papacosta, O., and Chaturvedi, N. (2021). Cholesteryl ester transfer protein (CETP) as a drug target for cardiovascular disease. Nature communications *12*, 1-10.

Schneider, C.A., Rasband, W.S., and Eliceiri, K.W. (2012). NIH Image to ImageJ: 25 years of image analysis. Nature methods *9*, 671-675.

Schroepfer Jr, G.J. (2000). Oxysterols: modulators of cholesterol metabolism and other processes. Physiological reviews *80*, 361-554.

Schulz, R., Schlüter, K.-D., and Laufs, U. (2015). Molecular and cellular function of the proprotein convertase subtilisin/kexin type 9 (PCSK9). Basic research in cardiology *110*, 1-19.

Scientific American, and Moyo, M.W. (2014). Cholesterol might be linked to breast cancer.

Shain, K.H., Landowski, T.H., and Dalton, W.S. (2000). The tumor microenvironment as a determinant of cancer cell survival: a possible mechanism for de novo drug resistance. Current opinion in oncology *12*, 557-563.

Shannon, P., Markiel, A., Ozier, O., Baliga, N.S., Wang, J.T., Ramage, D., Amin, N., Schwikowski, B., and Ideker, T. (2003). Cytoscape: a software environment for integrated models of biomolecular interaction networks. Genome research *13*, 2498-2504.

Sharp, A., and Harper-Wynne, C. (2014). Treatment of advanced breast cancer (ABC): the expanding landscape of targeted therapies. J Cancer Biol Res *2*, 1036-1040.

Shen, X.-B., Huang, L., Zhang, S.-H., Wang, D.-P., Wu, Y.-L., Chen, W.-N., Xu, S.-H., and Lin, X. (2015). Transcriptional regulation of the apolipoprotein F (ApoF) gene by ETS and C/EBPα in hepatoma cells. Biochimie *112*, 1-9.

Shim, S.H., Sur, S., Steele, R., Albert, C.J., Huang, C., Ford, D.A., and Ray, R.B. (2018). Disrupting cholesterol esterification by bitter melon suppresses triple-negative breast cancer cell growth. Molecular carcinogenesis *57*, 1599-1607.

Shinkai, H. (2012). Cholesteryl ester transfer-protein modulator and inhibitors and their potential for the treatment of cardiovascular diseases. Vascular health and risk management *8*, 323-331.

Sidaraite, A., Liutkeviciene, R., Glebauskiene, B., Vilkeviciute, A., and Kriauciuniene, L. (2020). Associations of cholesteryl ester transfer protein (CETP) gene variants with pituitary adenoma. Biomedical Papers of the Medical Faculty of Palacky University in Olomouc *164*, 1-7.

Simms, D., Cizdziel, P.E., and Chomczynski, P. (1993). TRIzol: A new reagent for optimal single-step isolation of RNA. Focus *15*, 532-535.

Simões, A.E., Pereira, D.M., Amaral, J.D., Nunes, A.F., Gomes, S.E., Rodrigues, P.M., Lo, A.C., D'Hooge, R., Steer, C.J., and Thibodeau, S.N. (2013). Efficient recovery of

proteins from multiple source samples after trizol® or trizol® LS RNA extraction and long-term storage. BMC genomics *14*, 1-14.

Simoes, I.C., Morciano, G., Lebiedzinska-Arciszewska, M., Aguiari, G., Pinton, P., Potes, Y., and Wieckowski, M.R. (2020). The mystery of mitochondria-ER contact sites in physiology and pathology: A cancer perspective. Biochimica et Biophysica Acta (BBA)-Molecular Basis of Disease *1866*, 1-16.

Singh, M.S., Francis, P.A., and Michael, M. (2011). Tamoxifen, cytochrome P450 genes and breast cancer clinical outcomes. The Breast *20*, 111-118.

Sinzinger, H., Wolfram, R., and Peskar, B.A. (2002). Muscular side effects of statins. Journal of cardiovascular pharmacology *40*, 163-171.

Smart, E.J., Graf, G.A., McNiven, M.A., Sessa, W.C., Engelman, J.A., Scherer, P.E., Okamoto, T., and Lisanti, M.P. (1999). Caveolins, liquid-ordered domains, and signal transduction. Molecular and cellular biology *19*, 7289-7304.

Smith, P.e., Krohn, R.I., Hermanson, G., Mallia, A., Gartner, F., Provenzano, M., Fujimoto, E., Goeke, N., Olson, B., and Klenk, D. (1985). Measurement of protein using bicinchoninic acid. Analytical biochemistry *150*, 76-85.

Snejdrlova, M., Altschmiedova, T., Vrablik, M., Stulc, T., Lastuvka, J., Lanska, V., and Ceska, R. (2020). Statin intolerance in clinical practice. Current atherosclerosis reports *22*, 1-8.

Sohn, J., Lin, H., Fritch, M.R., and Tuan, R.S. (2018). Influence of cholesterol/caveolin-1/caveolae homeostasis on membrane properties and substrate adhesion characteristics of adult human mesenchymal stem cells. Stem cell research & therapy *9*, 1-15.

Spruance, S.L., Reid, J.E., Grace, M., and Samore, M. (2004). Hazard ratio in clinical trials. Antimicrobial agents and chemotherapy *48*, 2787-2792.

Srinivas, P., Gopinath, G., Banerji, A., Dinakar, A., and Srinivas, G. (2004). Plumbagin induces reactive oxygen species, which mediate apoptosis in human cervical cancer cells. Molecular carcinogenesis *40*, 201-211.

Stancu, C., and Sima, A. (2001). Statins: mechanism of action and effects. Journal of cellular and molecular medicine *5*, 378-387.

Stroes, E.S., Thompson, P.D., Corsini, A., Vladutiu, G.D., Raal, F.J., Ray, K.K., Roden, M., Stein, E., Tokgözoğlu, L., and Nordestgaard, B.G. (2015). Statin-associated muscle symptoms: impact on statin therapy—European Atherosclerosis Society consensus panel statement on assessment, aetiology and management. European heart journal *36*, 1012-1022.

Strom, B.L., Schinnar, R., Karlawish, J., Hennessy, S., Teal, V., and Bilker, W.B. (2015). Statin therapy and risk of acute memory impairment. JAMA internal medicine *175*, 1399-1405.

Stuhlmiller, T.J., Miller, S.M., Zawistowski, J.S., Nakamura, K., Beltran, A.S., Duncan, J.S., Angus, S.P., Collins, K.A., Granger, D.A., and Reuther, R.A. (2015). Inhibition of lapatinib-induced kinome reprogramming in ERBB2-positive breast cancer by targeting BET family bromodomains. Cell reports *11*, 390-404.

Su, Z., Yang, Z., Xu, Y., Chen, Y., and Yu, Q. (2015). Apoptosis, autophagy, necroptosis, and cancer metastasis. Molecular cancer *14*, 1-14.

Suhaili, S.H., Karimian, H., Stellato, M., Lee, T.-H., and Aguilar, M.-I. (2017). Mitochondrial outer membrane permeabilization: a focus on the role of mitochondrial membrane structural organization. Biophysical reviews *9*, 443-457.

Suhy, A., Hartmann, K., Newman, L., Papp, A., Toneff, T., Hook, V., and Sadee, W. (2014). Genetic variants affecting alternative splicing of human cholesteryl ester transfer protein. Biochemical and biophysical research communications *443*, 1270-1274.

Sultan, S., D'Souza, A., Zabetakis, I., Lordan, R., Tsoupras, A., Kavanagh, E.P., and Hynes, N. (2019). Statins: rationale, mode of action, and side effects. In The Impact of Nutrition and Statins on Cardiovascular Diseases (Elsevier), pp. 171-200.

Sung, H., Ferlay, J., Siegel, R.L., Laversanne, M., Soerjomataram, I., Jemal, A., and Bray, F. (2021). Global cancer statistics 2020: GLOBOCAN estimates of incidence and mortality worldwide for 36 cancers in 185 countries. CA: a cancer journal for clinicians *71*, 209-249.

Supino, R. (1995). MTT assays. In In vitro toxicity testing protocols (Springer), pp. 137-149.

Tabas, I. (2002). Consequences of cellular cholesterol accumulation: basic concepts and physiological implications. The Journal of clinical investigation *110*, 905-911.

Takahashi, K., Jiang, X.-c., Sakai, N., Yamashita, S., Hirano, K., Bujo, H., Yamazaki, H., Kusunoki, J., Miura, T., and Kussie, P. (1993). A missense mutation in the cholesteryl ester transfer protein gene with possible dominant effects on plasma high density lipoproteins. The Journal of clinical investigation *92*, 2060-2064.

Tall, A.R., Yvan-Charvet, L., Terasaka, N., Pagler, T., and Wang, N. (2008). HDL, ABC transporters, and cholesterol efflux: implications for the treatment of atherosclerosis. Cell metabolism *7*, 365-375.

Taylor, F., Ward, K., Moore, T.H., Burke, M., Smith, G.D., Casas, J.P., and Ebrahim, S. (2011). Statins for the primary prevention of cardiovascular disease. The Cochrane database of systematic reviews *1*, 1-76.

Thavarajah, R., Mudimbaimannar, V.K., Elizabeth, J., Rao, U.K., and Ranganathan, K. (2012). Chemical and physical basics of routine formaldehyde fixation. Journal of oral and maxillofacial pathology: JOMFP *16*, 400-405.

Tilborghs, S., Corthouts, J., Verhoeven, Y., Arias, D., Rolfo, C., Trinh, X.B., and van Dam, P.A. (2017). The role of nuclear factor-kappa B signaling in human cervical cancer. Critical reviews in oncology/hematology *120*, 141-150.

Tirinato, L., Pagliari, F., Di Franco, S., Sogne, E., Marafioti, M.G., Jansen, J., Falqui, A., Todaro, M., Candeloro, P., and Liberale, C. (2020). ROS and Lipid Droplet accumulation induced by high glucose exposure in healthy colon and Colorectal Cancer Stem Cells. Genes & diseases *7*, 620-635.

Tosi, M.R., and Tugnoli, V. (2005). Cholesteryl esters in malignancy. Clinica chimica acta *359*, 27-45.

Townsend, D.M., and Tew, K.D. (2003). The role of glutathione-S-transferase in anti-cancer drug resistance. Oncogene *22*, 7369-7375.

Trajkovska, K.T., and Topuzovska, S. (2017). High-density lipoprotein metabolism and reverse cholesterol transport: strategies for raising HDL cholesterol. Anatolian journal of cardiology *18*, 149-154.

Ulloth, J.E., Almaguel, F.G., Padilla, A., Bu, L., Liu, J.-W., and De Leon, M. (2007). Characterization of methyl-β-cyclodextrin toxicity in NGF-differentiated PC12 cell death. Neurotoxicology *28*, 613-621.

van der Schoor, L.W., Verkade, H.J., Kuipers, F., and Jonker, J.W. (2015). New insights in the biology of ABC transporters ABCC2 and ABCC3: impact on drug disposition. Expert opinion on drug metabolism & toxicology *11*, 273-293.

Vaupel, P., Schmidberger, H., and Mayer, A. (2019). The Warburg effect: essential part of metabolic reprogramming and central contributor to cancer progression. International journal of radiation biology *95*, 912-919.

Walker, J.M. (2009). The bicinchoninic acid (BCA) assay for protein quantitation. In The protein protocols handbook (Springer), pp. 11-15.

Wang, C., Mayer, J.A., Mazumdar, A., Fertuck, K., Kim, H., Brown, M., and Brown, P.H. (2011). Estrogen induces c-myc gene expression via an upstream enhancer activated by

the estrogen receptor and the AP-1 transcription factor. Molecular Endocrinology *25*, 1527-1538.

Wang, C.C., Chiang, Y.-M., Sung, S.-C., Hsu, Y.-L., Chang, J.-K., and Kuo, P.-L. (2008). Plumbagin induces cell cycle arrest and apoptosis through reactive oxygen species/c-Jun N-terminal kinase pathways in human melanoma A375. S2 cells. Cancer letters *259*, 82-98.

Wang, L., Smith, J., Breton, C., Clark, P., Zhang, J., Ying, L., Che, Y., Lape, J., Bell, P., and Calcedo, R. (2018). Meganuclease targeting of PCSK9 in macaque liver leads to stable reduction in serum cholesterol. Nature biotechnology *36*, 717-725.

Wang, N., Silver, D.L., Thiele, C., and Tall, A.R. (2001). ATP-binding cassette transporter A1 (ABCA1) functions as a cholesterol efflux regulatory protein. Journal of Biological Chemistry *276*, 23742-23747.

Wang, R., He, W., Li, Z., Chang, W., Xin, Y., and Huang, T. (2014). Caveolin-1 functions as a key regulator of 17β-estradiol-mediated autophagy and apoptosis in BT474 breast cancer cells. International journal of molecular medicine *34*, 822-827.

Ward, C., Langdon, S.P., Mullen, P., Harris, A.L., Harrison, D.J., Supuran, C.T., and Kunkler, I.H. (2013). New strategies for targeting the hypoxic tumour microenvironment in breast cancer. Cancer treatment reviews *39*, 171-179.

Webb, P., Lopez, G.N., Uht, R.M., and Kushner, P.J. (1995). Tamoxifen activation of the estrogen receptor/AP-1 pathway: potential origin for the cell-specific estrogen-like effects of antiestrogens. Molecular Endocrinology *9*, 443-456.

Whitfield, G.B., Brock, T.D., Ammann, A., Gottlieb, D., and Carter, H.E. (1955). Filipin, an antifungal antibiotic: isolation and properties. Journal of the American Chemical Society *77*, 4799-4801.

WHO, W.H.O. (2018). Breast cancer statistics.

Wilhelm, L.P., Voilquin, L., Kobayashi, T., Tomasetto, C., and Alpy, F. (2019). Intracellular and Plasma Membrane Cholesterol Labeling and Quantification Using Filipin and GFP-D4. In Intracellular Lipid Transport (Springer), pp. 137-152.

Wu, J.e., Ding, J., Yang, J., Guo, X., and Zheng, Y. (2018). MicroRNA roles in the nuclear factor kappa B signaling pathway in cancer. Frontiers in immunology *9*, 1-9.

Wu, Q., Yang, Z., Nie, Y., Shi, Y., and Fan, D. (2014). Multi-drug resistance in cancer chemotherapeutics: mechanisms and lab approaches. Cancer letters *347*, 159-166.

Xu, C., Zhang, L., Wang, D., Jiang, S., Cao, D., Zhao, Z., Huang, M., and Jin, J. (2021). Lipidomics reveals that sustained SREBP-1-dependent lipogenesis is a key mediator of

gefitinib-acquired resistance in EGFR-mutant lung cancer. Cell Death Discovery *7*, 1-9.

Ye, J., and DeBose-Boyd, R.A. (2011). Regulation of cholesterol and fatty acid synthesis. Cold Spring Harbor perspectives in biology *3*, 7.

Yebyo, H.G., Aschmann, H.E., Kaufmann, M., and Puhan, M.A. (2019). Comparative effectiveness and safety of statins as a class and of specific statins for primary prevention of cardiovascular disease: A systematic review, meta-analysis, and network meta-analysis of randomized trials with 94,283 participants. American heart journal *210*, 18-28.

Yin, F., Feng, F., Wang, L., Wang, X., Li, Z., and Cao, Y. (2019). SREBP-1 inhibitor Betulin enhances the antitumor effect of Sorafenib on hepatocellular carcinoma via restricting cellular glycolytic activity. Cell death & disease *10*, 1-12.

Yogosawa, S., and Yoshida, K. (2018). Tumor suppressive role for kinases phosphorylating p53 in DNA damage-induced apoptosis. Cancer science *109*, 3376-3382.

Yokoo, M., Kubota, Y., Motoyama, K., Higashi, T., Taniyoshi, M., Tokumaru, H., Nishiyama, R., Tabe, Y., Mochinaga, S., and Sato, A. (2015). 2-Hydroxypropyl-β-cyclodextrin acts as a novel anticancer agent. PLoS One *10*, 1-20.

Yu, P., Zhang, C., Gao, C.-Y., Ma, T., Zhang, H., Zhou, M.-M., Yang, Y.-W., Yang, L., and Kong, L.-Y. (2017). Anti-proliferation of triple-negative breast cancer cells with physagulide P: ROS/JNK signaling pathway induces apoptosis and autophagic cell death. Oncotarget *8*, 64032-64049.

Yue, S., Li, J., Lee, S.-Y., Lee, H.J., Shao, T., Song, B., Cheng, L., Masterson, T.A., Liu, X., and Ratliff, T.L. (2014). Cholesteryl ester accumulation induced by PTEN loss and PI3K/AKT activation underlies human prostate cancer aggressiveness. Cell metabolism *19*, 393-406.

Yvan-Charvet, L., Wang, N., and Tall, A.R. (2010). Role of HDL, ABCA1, and ABCG1 transporters in cholesterol efflux and immune responses. Arteriosclerosis, thrombosis, and vascular biology *30*, 139-143.

Zhang, J.-H., Chung, T.D., and Oldenburg, K.R. (1999). A simple statistical parameter for use in evaluation and validation of high throughput screening assays. Journal of biomolecular screening *4*, 67-73.

Zhang, N., Zhang, H., Liu, Y., Su, P., Zhang, J., Wang, X., Sun, M., Chen, B., Zhao, W., and Wang, L. (2019). SREBP1, targeted by miR-18a-5p, modulates epithelial-

mesenchymal transition in breast cancer via forming a co-repressor complex with Snail and HDAC1/2. Cell Death & Differentiation *26*, 843-859.

Zhao, C., and Dahlman-Wright, K. (2010). Liver X receptor in cholesterol metabolism. Journal of Endocrinology *204*, 233-240.

Zhou, G., and Xia, J. (2018). Using OmicsNet for Network Integration and 3D Visualization. Current Protocols in Bioinformatics *65*, 1-26.

Zhou, M., Gu, L., Zhu, N., Woods, W.G., and Findley, H.W. (2003). Transfection of a dominant-negative mutant NF-kB inhibitor (IkBm) represses p53-dependent apoptosis in acute lymphoblastic leukemia cells: interaction of IkBm and p53. Oncogene *22*, 8137-8144.

Zidovetzki, R., and Levitan, I. (2007). Use of cyclodextrins to manipulate plasma membrane cholesterol content: evidence, misconceptions and control strategies. Biochimica et Biophysica Acta (BBA)-Biomembranes *1768*, 1311-1324.

17. Supplementary data

17.1 The effects of TAM and AP on non-cancerous cells

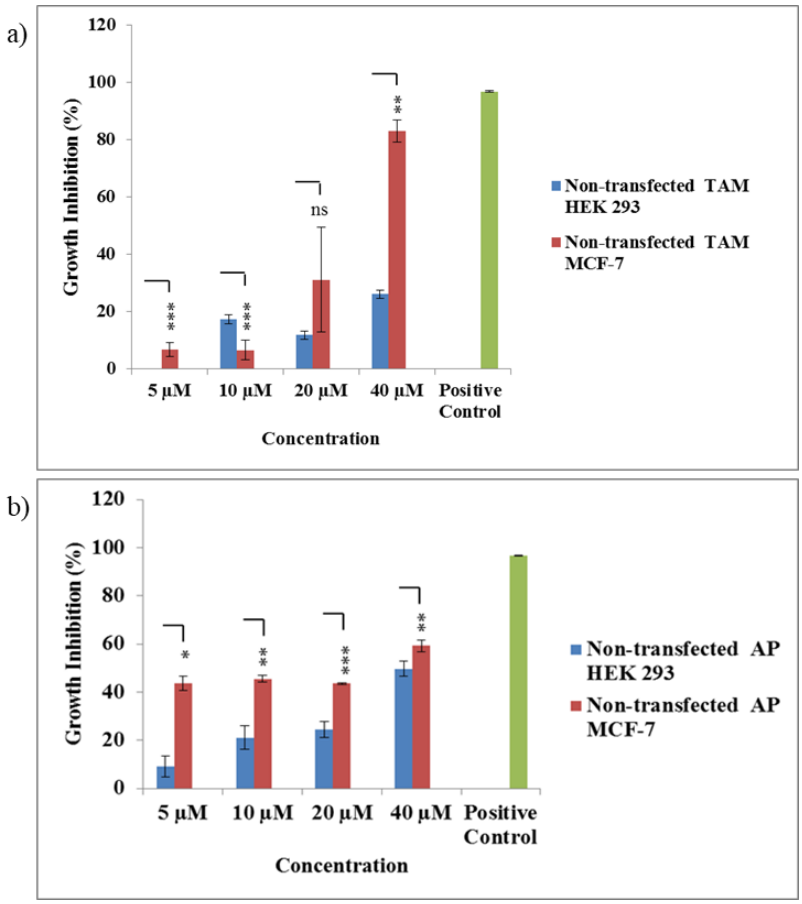

Figure 17.1: The effects of TAM and AP on HEK 293 cells

TAM and AP treatment on HEK 293 cells were not as toxic as compared to MCF-7 cells, especially at 5 µM (a and b). On average, growth inhibition in HEK 293 cells were less than 40% for both treatments, as opposed to 50 to 70% in MCF-7 cells. This could mean that using a cholesterol depleter to treat cancer by depleting excess cholesterol could be promising with reduced side effects.

17.2 CETP knock-down on protein expression in MCF-7 cells

a)

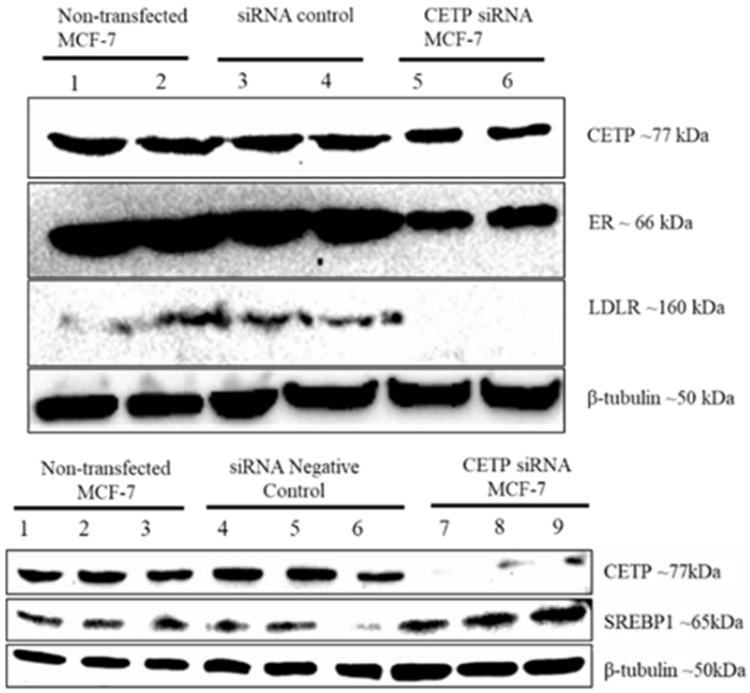

b)

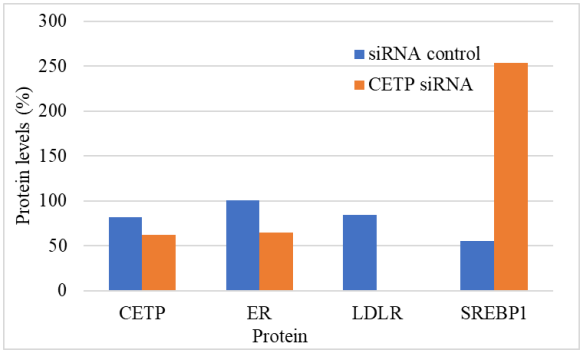

Figure 17.2: The effects of *CETP* knock-down on various proteins in MCF-7 cells

Successful CETP knock-down in MCF-7 cells (by 38% (b)) have been consistently proven and this also resulted in the reduced expression of ER and LDLR in MCF-7 cells (by 64% and 84% respectively (b)). This correlated to the ER and LDLR gene expression profile post CETP knock-down. Thus, confirming that resistance in MCF-7 cells could have been reduced due to a decreased expression of surface receptors involved in cholesterol and estrogen influx. However, CETP knock-down increased SREBP *protein expression (by 153% (b)), while SREBF-1 gene was downregulated as observed from the array.*

17.3 CETP stable transfection/knock-down

The establishment of a stable *CETP* knocked down cell line was performed, which can be used for future mice xenograft study (full study as opposed to a pilot study).

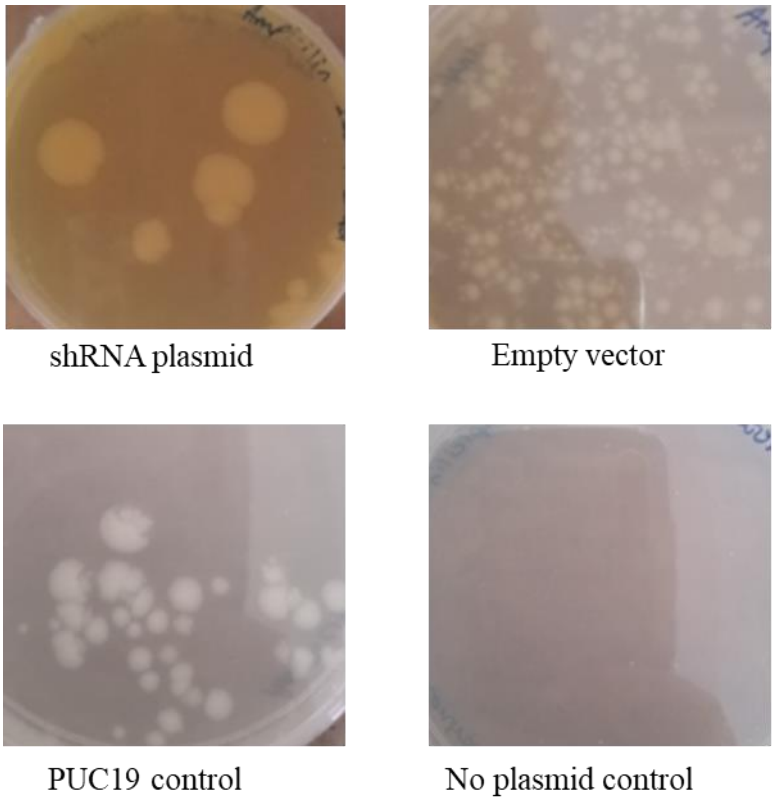

Figure 17.3: Bacterial transformation with CETP shRNA plasmid

CETP shRNA plasmid (Mission® shRNA plasmid; pLKO.1-puro, containing the puromycin human selectable marker) (Sigma Aldrich, UK)) was transformed in Subcloning Efficiency™ DH5α competent cells (Thermo Fisher Scientific, USA). The bacteria were grown on ampicillin-treated agar plates. Successfully transformed bacteria cells, containing the plasmid, were resistant to the ampicillin and thereby forming colonies. The colonies were then selected to extract the plasmid.

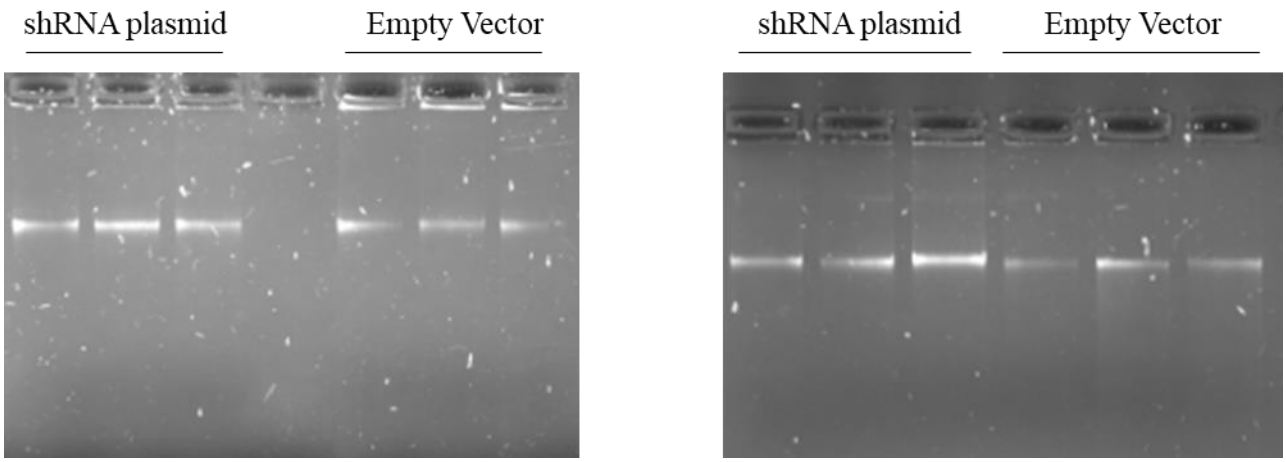

Figure 17.4: Plasmid extraction and purification

The extracted plasmid from the bacterial cells were then purified and electrophoresed on a 1% agarose gel to confirm successful plasmid extraction. The figure above depicted a successful shRNA plasmid extraction.

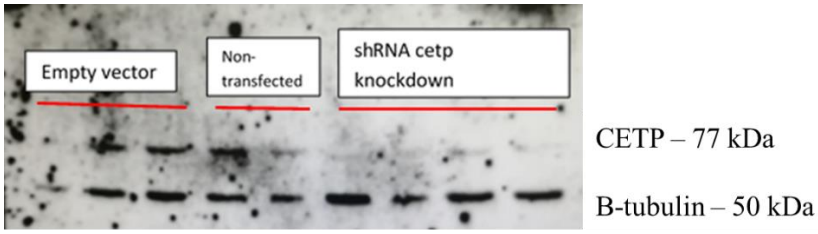

Figure 17.5: Western blotting to confirm successful *CETP* stable knock-down

MCF-7 cells were transfected with the extracted plasmid, for long-term CETP knock-down. The Xfect™ transfection reagent (Takara, Separations, SA) was used to stably transfect BC cells. The Xfect™ transfection reagent forms biodegradable nanoparticles for efficient transportation of plasmid DNA into cells. Protein extraction was performed and the lysate was used in western blotting to confirm successful CETP stable knock-down. The blot above showed that there was successful knock-down.

Table 17.1: Table with the full descriptions of the genes in the arrays

Gene	Description
APOB	Apolipoprotein B (including Ag(x) antigen)
APOC3	Apolipoprotein C-III
APOD	Apolipoprotein D
APOE	Apolipoprotein E
APOF	Apolipoprotein F
APOL1	Apolipoprotein L, 1
APOL2	Apolipoprotein L, 2
APOL5	Apolipoprotein L, 5
CDH13	Cadherin 13, H-cadherin (heart)
CEL	Carboxyl ester lipase (bile salt-stimulated lipase)
CELA3A	Chymotrypsin-like elastase family, member 3A
CELA3B	Chymotrypsin-like elastase family, member 3B
CETP	Cholesteryl ester transfer protein, plasma
CNBP	CCHC-type zinc finger, nucleic acid binding protein
COLEC12	Collectin sub-family member 12
CXCL16	Chemokine (C-X-C motif) ligand 16
CYB5R3	Cytochrome b5 reductase 3
CYP11A1	Cytochrome P450, family 11, subfamily A, polypeptide 1
CYP39A1	Cytochrome P450, family 39, subfamily A, polypeptide 1
CYP46A1	Cytochrome P450, family 46, subfamily A, polypeptide 1

CYP51A1	Cytochrome P450, family 51, subfamily A, polypeptide 1
CYP7A1	Cytochrome P450, family 7, subfamily A, polypeptide 1
CYP7B1	Cytochrome P450, family 7, subfamily B, polypeptide 1
DHCR24	24-dehydrocholesterol reductase
DHCR7	7-dehydrocholesterol reductase
FDFT1	Farnesyl-diphosphate farnesyltransferase 1
FDPS	Farnesyl diphosphate synthase
HDLBP	High density lipoprotein binding protein
HMGCR	3-hydroxy-3-methylglutaryl-CoA reductase
HMGCS1	3-hydroxy-3-methylglutaryl-CoA synthase 1 (soluble)
HMGCS2	3-hydroxy-3-methylglutaryl-CoA synthase 2 (mitochondrial)
IDI1	Isopentenyl-diphosphate delta isomerase 1
IDI2	Isopentenyl-diphosphate delta isomerase 2
IL4	Interleukin 4
INSIG1	Insulin induced gene 1
INSIG2	Insulin induced gene 2
LCAT	Lecithin-cholesterol acyltransferase
LDLR	Low density lipoprotein receptor
LDLRAP1	Low density lipoprotein receptor adaptor protein 1
LEP	Leptin
LIPE	Lipase, hormone-sensitive
LRP10	Low density lipoprotein receptor-related protein 10

LRP12	Low density lipoprotein receptor-related protein 12
LRP1B	Low density lipoprotein receptor-related protein 1B
LRP6	Low density lipoprotein receptor-related protein 6
LRPAP1	Low density lipoprotein receptor-related protein associated protein 1
MBTPS1	Membrane-bound transcription factor peptidase, site 1
MVD	Mevalonate (diphospho) decarboxylase
MVK	Mevalonate kinase
NPC1L1	NPC1 (Niemann-Pick disease, type C1, gene)-like 1
NR0B2	Nuclear receptor subfamily 0, group B, member 2
NR1H4	Nuclear receptor subfamily 1, group H, member 4
NSDHL	NAD(P) dependent steroid dehydrogenase-like
OLR1	Oxidized low density lipoprotein (lectin-like) receptor 1
OSBPL1A	Oxysterol binding protein-like 1A
OSBPL5	Oxysterol binding protein-like 5
PCSK9	Proprotein convertase subtilisin/kexin type 9
PMVK	Phosphomevalonate kinase
PPARD	Peroxisome proliferator-activated receptor delta
PRKAA1	Protein kinase, AMP-activated, alpha 1 catalytic subunit
PRKAA2	Protein kinase, AMP-activated, alpha 2 catalytic subunit
PRKAG2	Protein kinase, AMP-activated, gamma 2 non-catalytic subunit
SCAP	SREBF chaperone
SCARF1	Scavenger receptor class F, member 1

SNX17	Sorting nexin 17
SOAT1	Sterol O-acyltransferase 1
SORL1	Sortilin-related receptor, L(DLR class) A repeats containing
SREBF1	Sterol regulatory element binding transcription factor 1
SREBF2	Sterol regulatory element binding transcription factor 2
STAB1	Stabilin 1
STAB2	Stabilin 2
STARD3	StAR-related lipid transfer (START) domain containing 3
TM7SF2	Transmembrane 7 superfamily member 2
TRERF1	Transcriptional regulating factor 1
VLDLR	Very low density lipoprotein receptor
ABCB1	ATP-binding cassette, sub-family B (MDR/TAP), member 1
ABCC1	ATP-binding cassette, sub-family C (CFTR/MRP), member 1
ABCC2	ATP-binding cassette, sub-family C (CFTR/MRP), member 2
ABCC3	ATP-binding cassette, sub-family C (CFTR/MRP), member 3
ABCC5	ATP-binding cassette, sub-family C (CFTR/MRP), member 5
ABCG2	ATP-binding cassette, sub-family G (WHITE), member 2
AHR	Aryl hydrocarbon receptor
AP1S1	Adaptor-related protein complex 1, sigma 1 subunit
APC	Adenomatous polyposis coli
AR	Androgen receptor
ARNT	Aryl hydrocarbon receptor nuclear translocator

ATM	Ataxia telangiectasia mutated
BAX	BCL2-associated X protein
BCL2	B-cell CLL/lymphoma 2
BCL2L1	BCL2-like 1
BLMH	Bleomycin hydrolase
BRCA1	Breast cancer 1, early onset
BRCA2	Breast cancer 2, early onset
CCND1	Cyclin D1
CCNE1	Cyclin E1
CDK2	Cyclin-dependent kinase 2
CDK4	Cyclin-dependent kinase 4
CDKN1A	Cyclin-dependent kinase inhibitor 1A (p21, Cip1)
CDKN1B	Cyclin-dependent kinase inhibitor 1B (p27, Kip1)
CDKN2A	Cyclin-dependent kinase inhibitor 2A (melanoma, p16, inhibits CDK4)
CDKN2D	Cyclin-dependent kinase inhibitor 2D (p19, inhibits CDK4)
CLPTM1L	CLPTM1-like
CYP1A1	Cytochrome P450, family 1, subfamily A, polypeptide 1
CYP1A2	Cytochrome P450, family 1, subfamily A, polypeptide 2
CYP2B6	Cytochrome P450, family 2, subfamily B, polypeptide 6
CYP2C19	Cytochrome P450, family 2, subfamily C, polypeptide 19
CYP2C8	Cytochrome P450, family 2, subfamily C, polypeptide 8
CYP2C9	Cytochrome P450, family 2, subfamily C, polypeptide 9

CYP2D6	Cytochrome P450, family 2, subfamily D, polypeptide 6
CYP2E1	Cytochrome P450, family 2, subfamily E, polypeptide 1
CYP3A4	Cytochrome P450, family 3, subfamily A, polypeptide 4
CYP3A5	Cytochrome P450, family 3, subfamily A, polypeptide 5
DHFR	Dihydrofolate reductase
EGFR	Epidermal growth factor receptor
ELK1	ELK1, member of ETS oncogene family
EPHX1	Epoxide hydrolase 1, microsomal (xenobiotic)
ERBB2	V-erb-b2 erythroblastic leukemia viral oncogene homolog 2, neuro/glioblastoma derived oncogene homolog (avian)
ERBB3	V-erb-b2 erythroblastic leukemia viral oncogene homolog 3 (avian)
ERBB4	V-erb-a erythroblastic leukemia viral oncogene homolog 4 (avian)
ERCC3	Excision repair cross-complementing rodent repair deficiency, complementation group 3 (xeroderma pigmentosum group B complementing)
ESR1	Estrogen receptor 1
ESR2	Estrogen receptor 2 (ER beta)
FGF2	Fibroblast growth factor 2 (basic)
FOS	FBJ murine osteosarcoma viral oncogene homolog
GSK3A	Glycogen synthase kinase 3 alpha
GSTP1	Glutathione S-transferase pi 1
HIF1A	Hypoxia inducible factor 1, alpha subunit (basic helix-loop-helix transcription factor)

IGF1R	Insulin-like growth factor 1 receptor
IGF2R	Insulin-like growth factor 2 receptor
MET	Met proto-oncogene (hepatocyte growth factor receptor)
MSH2	MutS homolog 2, colon cancer, nonpolyposis type 1 (E. coli)
MVP	Major vault protein
MYC	V-myc myelocytomatosis viral oncogene homolog (avian)
NAT2	N-acetyltransferase 2 (arylamine N-acetyltransferase)
NFKB1	Nuclear factor of kappa light polypeptide gene enhancer in B-cells 1
NFKB2	Nuclear factor of kappa light polypeptide gene enhancer in B-cells 2 (p49/p100)
NFKBIB	Nuclear factor of kappa light polypeptide gene enhancer in B-cells inhibitor, beta
NFKBIE	Nuclear factor of kappa light polypeptide gene enhancer in B-cells inhibitor, epsilon
PPARA	Peroxisome proliferator-activated receptor alpha
PPARD	Peroxisome proliferator-activated receptor delta
PPARG	Peroxisome proliferator-activated receptor gamma
RARA	Retinoic acid receptor, alpha
RARB	Retinoic acid receptor, beta
RARG	Retinoic acid receptor, gamma
RB1	Retinoblastoma 1
RELB	V-rel reticuloendotheliosis viral oncogene homolog B
RXRA	Retinoid X receptor, alpha

RXRB	Retinoid X receptor, beta
SOD1	Superoxide dismutase 1, soluble
SULT1E1	Sulfotransferase family 1E, estrogen-preferring, member 1
TNFRSF11A	Tumor necrosis factor receptor superfamily, member 11a, NFKB activator
TOP1	Topoisomerase (DNA) I
TOP2A	Topoisomerase (DNA) II alpha 170kDa
TOP2B	Topoisomerase (DNA) II beta 180kDa
TP53	Tumor protein p53
TPMT	Thiopurine S-methyltransferase
UGCG	UDP-glucose ceramide glucosyltransferase
XPA	Xeroderma pigmentosum, complementation group A
XPC	Xeroderma pigmentosum, complementation group C